THE CHARACTERIZATION OF LYSINE SPECIFIC DEMETHYLASE 2 (LSD2), A NOVEL HISTONE DEMETHYASE

By

MICHAEL S. RUTENBERG

A DISSERTATION PRESENTED TO THE GRADUATE SCHOOL
OF THE UNIVERSITY OF FLORIDA IN PARTIAL FULFILLMENT
OF THE REQUIREMENTS FOR THE DEGREE OF
DOCTOR OF PHILOSOPHY

UNIVERSITY OF FLORIDA

2007

I dedicate this to God. You da man!

ACKNOWLEDGMENTS

I thank my mentor, Dr. Naohiro Terada, for his unending support and enthusiasm during my research education. I also thank Dr. Yujiang Shi at Brigham and Women's Hospital/Harvard Medical School for allowing me the opportunity to work with him and conduct my dissertation research in his lab. I thank the members of the Shi lab for assisting with the research contained within this dissertation, most notably Drs. Rui Fang, Pinchou Mei, and Fumiko Shimizu, as well as Thiago Leonor.

TABLE OF CONTENTS

page

LIST OF TABLES

LIST OF FIGURES

Abstract of Dissertation Presented to the Graduate School
of the University of Florida in Partial Fulfillment of the
Requirements for the Degree of Doctor of Philosophy

THE CHARACTERIZATION OF LYSINE SPECIFIC DEMETHYLASE 2 (LSD2), A NOVEL HISTONE DEMETHYLASE

By

Michael S. Rutenberg

December 2007

Chair: Naohiro Terada
Major: Medical Sciences--Molecular Cell Biology

Covalent modification of histones plays an important role in chromatin structure and genome function. In particular, the role of methylation of Lysine 4 on histone H3 is well established in gene regulation. We report a novel function of the dynamic regulation of H3K4 demethylation in the maintenance of constitutive heterochromatin. We show that LSD2, a homologue of LSD1, demethylates mono- and di-methyl K4H3 and is essential for maintaining the stability of pericentric heterochromatin. We also identify n-PAC, an LSD2 interacting protein, which recruits LSD2 to chromatin and enhances its demethylase activity *in vitro* and *in vivo*. LSD2 alone associates weakly with chromatin, however, when coexpressed with n-PAC, the two proteins associate closely with chromatin and induce a global demethylation and chromatin condensation. The induction of chromatin condensation requires the catalytic activity of LSD2 and its interaction with n-PAC. We also show that LSD2 knockdown results in precocious sister chromatid separation during mitosis, a hallmark of pericentric heterochromatin disruption. These data reveal a novel function for the dynamic regulation of H3K4 methylation in formation/maintenance of heterochromatin. We present data showing that LSD2, while sharing substrate specificity with its homologue, LSD1, does not share its role in gene transcription, but rather functions as a regulator of genomic structure.

CHAPTER 1
INTRODUCTION

Epigenetics

The term “epigenetics” was originally used in the 1940’s to describe the unknown and somewhat mysterious events underlying the transition from genotype to its phenotype. The evolutionary and developmental biologist, Conrad Waddington, is credited with coining the term. He defined epigenetics as “the interaction of genes with their environment, which bring the phenotype into being” and described the “epigenetic landscape” as a metaphor to explain the cell fate decisions made during cellular and tissue differentiation during development (29). Waddington described an epigenetic landscape, in which numerous marbles (representing cells) beginning in valleys and ridges travel via various possible trajectories from an elevated point of undifferentiation to a stable position of differentiation. At that time, hereditary elements were known as genes, however, the role of DNA as the heart of genetics had not been established. Epigenetics sought to describe the mechanisms by which macromolecules, including protein, RNA, and DNA mediated “gene” function at the cellular, tissue, and organismal level.

Since its original description, the evolution of the concept of epigenetics has been dramatic and extensive. From H.J. Muller’s investigation of “position effect variegation” in Drosophila in the 1930’s to Barbara McClintock’s study of transposable elements and variable mutability in maize and Mary Lyon’s hypothesis of X-chromosome inactivation in female mammals, epigenetics became the domain of anomolous and unpredictable hereditary phenomena. However, with major advances in genetics, molecular biology, developmental biology, and proteomics, many of these epigenetic mysteries began to be solved, and the concept itself, as well as the burgeoning field of epigenetics, became more narrowly defined. The overarching theme of contemporary epigenetics is the investigation of heritable phenotypes that can be

changed in the absence of changes in the underlying genotype. Holliday recently defined epigenetics as "the sum of the alterations to the chromatin template that collectively establish and propogate different patterns of gene expression (transcription) and silencing from the same genome" (40). More broadly, we can describe epigenetics as the mechanisms underlying the capacity for cells with identical genotypes to give rise to varied differentiated cells, tissues, and organs.

As biological advances continue to be made, ever more mysterious and seemingly impossible phenomena are discovered that fall within the realm of epigenetics. These now include heritable phenotypes due to prions, the phenomenon of repeat induced point mutation (RIP), and the phenomenon of wild-type gene reversion observed in the Arabidopsis HOTHEAD gene. An important observation regarding the development of this field is the apparent conservation of many forms of epigenetics throughout evolution (e.g. position effect variegation and genomic imprinting/dosage compensation), suggesting an important role of these phenomena in the evolution and survival of these organisms

Many of the underlying mechanisms for the epigenetic phenomena studied to date (e.g. PEV, X-inactivaation, genomic imprinting) appear to lie in the covalent modification of chromatin. This includes DNA methylation and a variety of covalent modifications added to histone proteins. There is intense focus on the origin of these "epigenetic" marks, the means of their faithful duplication from mother to daughter cell, and their mechanism of action in inducing phenotypic variability in the context of a static genotype. For the remainder of this discussion, I will largely focus on the details of histone modifications as "epigenetic marks", with particular emphasis on histone methylation and demethylation and their roles in genome metabolism.

Chromatin and the Nucleosome

The mammalian genome is massive in both size and complexity. The human genome contains ~ 3 X 10^9 base pairs and ~25,000 genes, the length of which is about 2m in its extended form. This presents the cell with the challenge of compacting the entire genome into the minute volume of a nucleus (~10,000 fold compaction), while maintaining an organization that supports the function, accessibility, and dynamics of active metabolism. Peterson and Laniel made the analogy of "…trying to stuff about 10,000 miles of spaghetti inside a basketball. Then, if that was not difficult enough, attempt to find a unique one inch segment of pasta from the middle of this mess, or try to duplicate, untangle and separate individual strings to opposite ends" .(78)The cell's solution to this challenge lies in the assembly of chromatin; the higher ordered organization of the genome into a structural and functional DNA/protein polymer. Chromatin consists of DNA, histone proteins, and non-histone DNA associated proteins, which are assembled into repeating units. These units can be further arranged into multiple levels of higher organization.

The most basic unit of chromatin is the nucleosome, which consists of a nucleosome core particle (NCP) comprised of 147bp of double-stranded DNA wrapped ~1.7 times around an octamer of core histones. The core histones are a group of small, highly conserved, basic proteins. The four basic core histones are H2A, H2B, H3, and H4. Additionally, the linker histone, H1, is not a component of the NCP, but instead contributes to higher-order chromatin organization and compaction.

The core histones (H2A, H2B, H3, and H4) all share structural features that enable them to contribute structurally and functionally to the nucleosome. They each consist of a globular domain, comprised of alpha helices, and an unstructured N-terminal "histone tail" domain. The globular domains of the histones are responsible for polymerizing with one another and

interacting with the DNA duplex that wraps around the histone core. The NCP consists of a central heterotypic tetramer of H3 and H4, flanked by two heterodimers of H2A and H2B. The N-terminal histone tails of each histone subunit (~25 amino acids) and the carboxy-terminus of H4 protrude beyond the globular core of the NCP as unstructured, flexible appendages extending outside of the encircling DNA. These histone tails accessible to other nuclear proteins, yet maintain close contact with the DNA.

Chromatin was initially identified and characterized cytologically(41). It was categorized as either "heterochromatin", which was condensed throughout the cell cycle and prominently stained with basic dyes; or "euchromatin", which was decondensed and weakly stained during interphase (58). Heterochromatin was proposed to be condensed and metabolically inactive (repressive for transcription and recombination) with DNA that is relatively inaccessible to cis-acting factors. Euchromatin, on the other hand, was thought to be "relaxed", transcriptionally active (or at least permissive), and contained DNA that is accessible to cis-acting factors. Since these initial descriptions, functional differences between different forms of chromatin have been described, as well as progress made into their molecular characterization.

Heterochromatin

Mammalian heterochromatin is now divided into two categories based on structural and functional features. "Constitutive heterochromatin" contains highly repetitive DNA sequences, is gene poor, and is maintained independent of cell cycle and developmental stage. Pericentromeric and telomeric heterochromatin are examples of constitutive heterochromatin that are conserved from yeast to humans. Pericentromeric heterochromatin flanks the highly repetitive centromere sequences of each chromosome and contributes to the formation of the kinetechore, providing structural integrity of the mitotic chromosome and spindle apparatus.

Telomeric heterochromatin acts as a transcriptionally inert cap at each chrmomome end, and ensures genomic stability during replication and nuclear division.

Much of the work characterizing constitutive heterochromatin has been done in yeast, although the basic structure and function of these domains appear to be largely conserved. Studies in the fission yeast, S. pombe, show that genes inserted into these genomic regions undergo gene silencing and are subject to specific histone modifications that are characteristic of heterochromatin(3, 32, 70, 84). These modifications include hypoacetylation of histones H3 and H4, methylation of lysines 9 and 27 on H3 and lysine 20 on H4, and a corresponding absence of lysine 4 methylation of histone H3(13). Additonally, non-histone proteins are associated with the presence of these heterochromatin specific histone modifications (e.g. Swi6/HP1). Loss of these specific histone modifications, the enzymes responsible for generating them, or the proteins associated with them, prevents the proper formation/maintenance and function of heterochromatin (31, 33, 72).

"Facultative heterochromatin" is the other major classification of heterochromatin found in mammals. Similar to constitutive heterochromatin, it is compacted and transcriptionally repressive. However, facultative heterochromatin is in gene rich regions, developmentally regulated, and can be reversible. Metazoan facultative heterochromatin can also be more variable from cell to cell within an organism than constitutive heterochromatin, which is typically identical from chromosome to chromosome between different differentiated cell and tissue types. The best-studied examples of facultative heterochromatin are genomic imprinting and X-chromosome inactivation. These are both methods of gene dosage compensation, which are proposed to ensure that chromosome differences between the sexes do not result in gross differences in gene expression levels.

Genomic imprinting is a cis-acting epigenetic mechanism for regulating expression of alleles based on the parental source of genetic material. There are numerous mammalian genes that have been identified that undergo genomic imprinting, the best studied is the H19/Igf2 locus. Imprinted genes display mono-allelic expression that is determined by epigenetic modifications (i.e. DNA methylation) transmitted from the parental gametes to the zygote. Genomic imprinting persists in the soma of the developing zygote, however, developing germ cells erase their parental imprints and regenerate their own for transmission to successive generations.

X-chromosome inactivation is another example of facultative heterochromatin, which functions to balance the gene expression between sexes with different sex chromosomes. X-inactivation operates by silencing nearly the entirety of every X-chromosome (Xi) in excess of 1. In every somatic cell, the silencing occurs randomly and is characterized by DNA and histone modifications unique to the Xi. These modifications include DNA methylation, hypoacetylation on histones H3 and H4, and histone lysine methylation patters similar to those of constitutive heterochromatin. An additional feature of the Xi is the incorporation of the core histone variant macroH2A.

Euchromatin

Euchromatin is cytologically less dense than heterochromatin and occupies the majority of the 4% of coding DNA of the mammalian genome. It is less condensed than heterochromatin and associated with transcriptional activity or permissivity. Correlative with its ability for gene activity, recent evidence suggests characteristic patterns of euchromatic chromatin modifications. These include DNA hypomethylation, hyperacteylation of histones H3 and H4, methylation of lysines 4, 36, and 79 of histone H3, and a relative absence of methylation on lysines 9 and 27 of histone H3(8, 80, 109).

Histone Modificatons

It has been known for decades that histones can be posttranslationally methylated and acetylated (2). The list of histone modifications has grown substantially since then, and now includes phosphorylation, ubiquitination, sumoylation, biotinylation and ADP-ribosylation. The most common target of these modifications is the N-terminal tail of the core histones (especially H3 and H4), however, recent findings show modifications of residues further into the globular domains of histones and even on carboxy-terminal domains (61). For each of these covalent histone modifications, there are enzymes responsible for the opposing activities that either add or remove the particular chemical group. The identity of these enzymes, their substrate specificities, modification specificities, and biological significance are of major interest in the field of epigenetics.

Histone acetylation

The addition of acetyl groups to histones has been known for over forty years and for nearly as long has been suspected to play a role in transcriptional activity (2). Studies correlated histone lysine acetylation to active gene transcription, but it took over thirty years for a direct mechanistic link to be made between active histone acetylation and transcriptional activation. This came in 1996, with the identification that p55, the Tetrahymena homolog of a well-studied yeast transcriptional activator, Gcn5p, was a nuclear histone acetyltransferase (HAT). These findings also provided evidence that the bromodomain of HAT proteins was responsible for their targeting to chromatin and led to the hypothesis that HATs associate with other known chromatin associated proteins (e.g. SWI/SNF), as well as basal transcriptional machinery, to regulate gene expression (11). Following this discovery, numerous other known transcriptional co-activators were shown to have intrinsic HAT activity, including CBP/p300 and Tip60.

The role of histone lysine acetylation in transcription regulation from yeast to humans is now well established. There is an extensive list of proteins containing nuclear HAT activity, each with substrate specificity for a particular residue(s) along one or several histones. For example, TAF1 acetyltransferase activity is known only to target lysine 14 on histone H3, while p300/CBP has activity for K5 on H2A and K12 and K15 on H2B (78).

At nearly the same time as the identification of HATs as transcriptional co-activators, a transcriptional co-repressor was shown to possess histone deacetylase activity (HDAC). Rpd3 (mammalian HDAC1) was the first known transcriptional co-repressor shown to remove acetyl groups from histones, and its deacetylase activity was proven to be required for gene repression and PEV (18, 104).

There are now several families described for both HATs and HDACs with varied substrate specificities and various biological functions. While the N-terminal tails of the core histones H3 and H4 are the most decorated by lysine acetylation (6 residues on H3, 5 residues on H4), all histones are subject to these modifications. Many of the enzymes responsible for these modifications (both "writing" and "erasing") are found in large protein complexes containing other chromatin associated proteins, many of which contain additional enzymatic activities. These large protein complexes are recruited to gene regions where they catalyze histone acetylation or deacetylation reactions to up- or down-regulate transcription, respectively (76, 98).

Histone Phosphorylation

Phosphorylation is another well-studied post-translational histone modification. Phosphates can be added to both serine and threonine residues in each of the core histones and H1. There are a number of residues phosphorylated on each histone, found in both the N- and carboxy-termini. Numerous kinases have been identified that are responsible for mediation of this modification and their mechanisms of regulation and biological roles are of great interest.

One of the early reports of histone phosphorylation showed a relationship between the histone modification and chromosome condensation during mitosis and meiosis (35). It has since been shown that phosphorylation of serine 10 on H3 is required for the initiation of condensation in Tetrahymena and mammalian cells (110, 114). Members of the aurora kinase family are known to mediate this Ser 10 phosphorylation in many organisms (including humans). Threonine 3 and 11 on histone H3 are also specifically phosphorylated during chromatin condensation in mitosis, however, their spatio-temporal patterns are somewhat distinct from Ser 10 phosphorylation (81). DAP kinase family members are known to mediate these modifications, however, like Ser 10, the role of threonine phosphorylation in chromatin condensation is not yet understood.

Mahadevan et al. were the first to identify a possible role for histone phosphorylation in the induction of transcriptional activation of immediate-early genes following stimulation of cell proliferation (57). They showed a conversion of MAP kinase pathways on the aurora B family members MSK1 and MSK2 to induce Ser 10 phosphorylation. However, the role of histone phosphorylation in gene activation is unclear.

Protein phophatases have been identified that reverse the phosphorylation mediated by histone kinases. Type 1 protein phoshpatases (PP1) are responsible for removing the phosphates from Ser 10 H3 associated with mitosis (73). There is also evidence that protein phosphatase type 2A (PP2A) activity is responsible for dephosphorylating histones involved in transcription regulation (74).

There are overlapping substrate specificities for many of the known histone kinases and phosphatases. For example, in human there are at least 4 kinases capable of phosphorylating Ser 10 H3. The activities of these kinases are cell cycle dependent and appear to mediate different biological functions attributed to this modification. The dynamic balance between the enzymes

responsible for adding and removing histone phosphates is likely critical to their function in transcription regulation, chromosome condensation, and other physiological processes.

Histone Methylation

The addition of methyl groups to the ε-amino group of lysines on histones was first described by Murray in 1964 (67). That same year, evidence was presented that supported histone methylation as an active posttranslational modification (2). In addition to lysine methylation, it has been shown that histone arginine residues are subject to methylation on their η-guanidino group. Histone methylation provides an immensely complex network of modifications. Histones H3 and H4 are the primary targets of methylation. H3 can be methylated on 8 residues (K4, K9, K14, K27, K36, K79, R2, R17, R26), while H4 can be methylated on 3 residues (K20, K59, R3). Lysine methylation can also occur to varying degrees, either mono-, di-, or tri-methylation; while arginine methylation can be either mono- or dimethylated, with dimethylation occurring in either a symmetric or asymmetric configuration. The variety of methylation sites and their varying degrees of methylation results in the potential for an enourmous array of methylated histone combinations. Certain methyl-histone combinations correlate with specific genomic activities (e.g. transcriptional regulation, heterochromatin formation) and are likely integral to these processes.

Histone Lysine Methyltransferases

It took over thirty years after the discovery that histones are methylated for the first enzyme with histone lysine methyltransferase activity to be identified. Suv39h1 was identified by Thomas Jenuwein's group in 2000 as a histone methyltransferase with specificity towards lysine 9 on H3 (83). Suv39h1 is the human orthologue of Drosophila Su(var)3-9, a protein that was already known to be involved in position effect variegation (107).

The discovery of HMTase activity by Suv39h1 led to the identification of the conserved SET domain as the catalytic component of this group of enzymes. There are now numerous SET domain containing histone methyltransferses that have been characterized (e.g. Ezh2, M11, Nsd1) and nearly 50 predicted in the mammalian genome based on SET-domain analyses. Each of the known HMTases has strict histone and residue specificity. They also have specific degrees of processivity. Certain HMTases are capable of adding a single methyl group to a specific unmodified residue (e.g. PR-Set7 converts H4K20 to H4K20me), while others add multiple methyl groups to an unmodified residue (e.g. G9a converts H3K9 to H3K9dime). Others can generate any variety of methylation states to an unmodified residue (e.g. Ezh2 converts H3K27 to mono-, di-, or tri-methyl K27). And still others only catalyze methyltransferase reactions on residues already methylated (e.g. Suv39h1 converts H3K9me to di- or tri-methyl H3K9) (45) Furthermore, HMTases can have specificity for free cellular histones or nucleosomal histones.

Each of the SET containing HMTases uses S-adenosyl-L-methionine (SAM) as a cofactor, which provides the methyl group for the methyltransferase reaction. Dot1 is the only identified non-SET containing histone lysine methyltransferase (111). It is responsible for methylating lysine 79 on H3. In addition to the absence of a SET domain, Dot1p is unique in targeting a lysine residue located within the H3 globular domain (K79), as opposed to the location of the other lysine targets of H3 and H4 in the N-terminal tails.

Histone Arginine Methyltransferases

The protein arginine methyltransferase (PRMT) family of enzymes is responsible for methylating histone and non-histone proteins. Despite the highly conserved catalytic core of members of the PRMT family, these proteins have a wide range of substrate specificities. Like the lysine methyltransferases, these enzymes require SAM as a methyl group donor.

CARM1 was the first of these proteins reported to contain histone methyltransferase activity. CARM1 specifically methylates H3 Arg 17, in association with nuclear hormone receptors and p160 transcriptional co-activators involved in transcription regulation (15). PRMT1 was later identified as another histone arginine methyltransferase that also associates with nuclear hormone receptors as well as the p300 histone acetyltransferase (55, 112). Generally, PRMT histone methyltransferase activity is correlated with gene activation.

Histone Methyl Binding Proteins

The biological relevance of histone methylation ultimately depends on its effect on genomic metabolism. One mechanism for these effects is the specific recruitment of factors to methylated histones. Effector molecules can be targeted to genomic regions based on the methylation patterns of histones/nucleosomes. The specificity of these proteins depends on the particular histone, amino acid residue, and the extent of methylation. Several of the known histone methyl binding proteins contain conserved protein domains that mediate their specificity (e.g. chromodomain,WD40 repeats) (see below). These effector proteins are responsible for mediating the resulting changes in genome function, often through the coordination of factors that regulate chromatin modification, transcriptional activity, DNA damage repair, and chromosome condensation.

Heterochromatin protein 1 (HP1) is a well-studied histone methyl binding protein. It was identified in a Drosophila screen for proteins tightly bound to DNA and was shown to specifically associate with heterochromatin (44). It was later shown to play an essential role in position effect variegation, suggesting a role for HP1 in heterochromatin formation (21). HP1 is well conserved from fission yeast (Swi6) to humans. Mammalian HP1 is expressed as three isoforms: HP1α, HP1β, and HP1γ. While the functional differences between the isoforms aren't

known, there are differences in nuclear localization. HP1α is primarily localized to pericentromeric heterochromatin. HP1β localizes to pericentromeric heterochromatin, but is also found to some extent in euchromatic regions, while HP1γ more generously localizes to euchromatic regions (64).

HP1 contains a highly conserved chromodomain (CD) in its N-terminal region, which is found in numerous chromatin associated proteins and is responsible for its association with methylated lysine 9 on H3 (69). HP1 binds both di- and tri-methylated lys 9 H3 via its chromodomain, but it has a higher affinity for trimethylated K9 (5, 23, 49). The chromoshadow domain is found in the carboxy-terminus of HP1. The chromoshadow domain is a dimerization module, allowing interactions between HP1 molecules (both homo- and heterotypic), and facilitating interactions with other proteins containing chromoshadow domains. These interacting proteins include DNA methyltransferases (DNMT1, DNMT3a) and the histone methyltransferase Su(var)3-9 (and its mammalian orthologues) (24). These interactions provide a mechanism for heterochromatin formation (and therefore upregulation of PEV) in which HP1 is recruited to initiation sites of di- or tri-methylated K9 H3, which are then subject to further lysine methylation by associated Su(var)3-9 to propagate a heterochromatin epigenetic signature.

The polycomb group (PcG) is a class of proteins with members that associate with specific methylated histone motifs. Originally identified in Drosophila screens investigating homeotic gene derepression, they are now known to maintain the spatio-temporal silencing of homeotic genes (HOX) during development. The PcG proteins are found in complexes that are conserved from Drosophila to mammals, and contain proteins with chromatin association domains (e.g. chromodomain, zinc finger, and WD40) and histone modifying enzymatic domains (e.g. SET). There are two well-characterized PcG complexes (PRC1 and PRC2) and a third that has recently

been identified (PhoRC). The core protein components of human PRC1 are: HPC1-3, HPH1-3, Bmi1, and Ring1A (in Drosophila Polycomb (Pc), Polyhomeotic (Ph), Posterior sex combs (Psc), and dRing, respectively). The PRC2 complex contains the four core components: EZH2, EED, SUZ12, and RbAp46/48d (in Drosophila E(z) Enhancer of zeste, Esc (Extra sex combs), Su(z)12, and Nurf55, respectively). PRC1 and 2 appear to act in concert to recognize and then propagate the methylation of Lys27 on H3 in the repression of HOX gene expression.

The E(z) component of PRC2 contains a SET domain with methyltransferase activity towards H3K27 (14). It has been proposed that trimethylation of H3K27 by PRC2 leads to recruitment of PRC1 via the chromodomain of the Pc protein, which binds specifically to methylated Lys 27 of H3 (14). This model suggests recruitment of the PRC2 complex at sites targeted for gene repression, and subsequent binding of the PRC1 complex. While a role for PcG protein mediated gene repression is firmly established, the precise mechanism for PRC1/2 and H3K27 methylation in mediating gene repression is unclear.

In addition to the effector pr(82)oteins that recognize methylated histones in the context of gene repression, recent studies have provided examples of histone methyl binding proteins that recognize gene-activation associated methylated histones. The first of these effectors identified was ChD1, a chromodomain containing protein that is found the in yeast SAGA and SLIK histone acetyltransferase coactivator complexes. ChD1 contains two chromodomains (CD1 and CD2). CD2 was shown to preferentially recognize di- and tri-methylated Lys 4 H3 peptides in vitro, and SLIK complexes containing ChD1 with a mutation in CD2 lack histone acetyltransferase activity on methyated diMeK4H3 substrates compared to wild-type ChD1 containing complexes (17, 82).

The BPTF protein (bromodomain and PHD finger transcription factor) was also recently shown to contain binding affinity for methylated Lys 4 H3 (115). BPTF is the largest subunit of the NURF nucleosomal remodeling complex that is clearly implicated in transcription activation (66). As indicated by the name, BPTF contains a bromodomain (which recognizes acetylated histone tails), and a PHD finger, which is commonly found in chromatin-associated proteins (9, 19). The PHD finger was confirmed to be necessary and sufficient for preferential binding of BPTF to trimethylated K4 H3, and suggests a mechanism for recruitment of NURF to sites of gene activation. The PhD finger of the ING2 (inhibitor of growth) protein, a component of the mSin3A-HDAC1 gene repression complex, was also shown to mediate preferential binding to triMeK4 H3 in response to DNA damage induced growth suppression (92). These implicate the PHD finger as a specialized lysine-methyl binding domain, and further advance the role of histone methylation as a regulator of genome metabolism.

Histone Demethylation

Each of the previously discussed histone modifications (acetylation, phosphorylation, ubiquitination, etc.) is mediated by enzymes with opposing functions (e.g. histone acetyltransferases and histone deacetylases), enabling their reversibility and providing a dynamic system of regulation. Histone methylation, on the other hand, was long presumed to be a stable epigenetic mark, lacking the dynamic regulation observed with other modifications. Support for this came largely from the thermodynamic stability of amino-methyl bonds (especially methyl-lysine) relative to acetyl and phosphoryl groups; lack of evidence for dynamic changes in histone methylation during the cell cycle as was observed for other modifications (e.g. phosphorylation of Ser 10 H3 during mitosis); and an inability to identify factors responsible for the active removal of these marks (106). It was proposed that erasure of histone methylation relied on either passive dilution during replication, replacement of histone core subunits, or proteolytic

cleavage of modified histone N-terminal tails (1, 46, 106). At this time, the PAD family of enzymes (protein arginine deiminase) had been identified. These enzymes are capable of removing mono-methylated arginines from histones, but their activity results in the conversion of methylated arginine to the altered amino acid citrulline. PAD proteins are limited to mono-methylated arginines, and they don't represent a true reversal of arginine methylation. As a result, idea of the histone methylation as a permanent epigenetic mark persisted.

This changed in 2004, with the discovery that LSD1 (lysine specific demethylase 1), a nuclear amine oxidase, possessed intrinsic histone demethylase activity (93). LSD1 was a previously identified component of several chromatin associated complexes, including CoREST transcriptional repressor complexes and nuclear hormone receptor complexes (37, 42, 94). It was shown to remove di- and mono-methyl marks from Lys 4 of H3, however is unable to catalyze the reaction on trimethylated Lys 4 H3.

Lysine Specifie Demethylase 1 (LSD1)

LSD1 is a nuclear homolog of the amine oxidase family of proteins and the first identified histone demethylase. It is the 92kD protein product of the *Aof2* gene with domain conservation from yeast to human. LSD1 contains an N-terminal SWIRM domain commonly found in chromatin-associated proteins. The catalytic activity resides in the carboxy-terminal amine oxidase domain, which contains a binding site for FAD, a required cofactor for catalysis. Mammalian LSD1 contains a "spacer" region contained within the amine oxidase domain, although it not completely conserved in other species. Structural studies determined that the spacer region contributes to a "tower" domain, which is involved in allosteric regulation of LSD1 (97).

LSD1 catalyzes a demethylation reaction converting mono- or di-methylated Lys 4 H3 to an unmodified lysine residue. These activities are confirmed by *in vivo* and *in vitro* studies,

which also confirm an inability of LSD1 to act on trimethylated Lys 4 H3. The LSD1 mediated demethylation reaction involves a two-electron oxidation step via an aminium cation. Hydrolysis of the aminium generates a carbinolamine, which readily breaks down to generate formaldehyde and lysine. Two successive rounds of this reaction are required to generate unmodified lysine from its dimethyl form. FAD is required as the electron acceptor and must be regenerated by oxidation of FADH2 for repeated rounds of catalysis (93, 97). Structural and binding studies indicate that the substrate binding pocket of LSD1 is incapable of discriminating between different degrees of Lys 4 methylation (unmodified, mono-, di-, or tri-methyl), and therefore, the chemical mechanism of the demethylation reaction provides the constraints to mono- and di-methyl Lys 4 (97). The requirement of a free electron pair on the methylated lysine in the two-electron oxidation reaction further supports the structural, binding, and functional data in predicting LSD1 activity.

LSD1 is a component of several protein complexes involved in transcription regulation, including CtBP and CoREST corepressor complexes (94, 95, 105). HDAC1/2 and other chromatin-associated proteins are also components of these complexes. The coordination of LSD1 mediated Lys 4 H3 demethylation and HDAC mediated H3 and H4 deacetylation helps orchestrate their corepressor activities. CtBP/CoREST corepressor complexes are responsible for silencing neuron specific genes in non-neural tissues. Experiments replacing wild-type LSD1 with a catalytic inactive mutant resulted in the derepression of the previously silenced genes in non-neural cell lines (93). Subsequent studies showed that CoREST directly interacts with LSD1 as a positive regulator, facilitating its demethylase activity and preventing its proteosomal degradation *in vivo* (51, 95). CoREST, via its two SANT domains, directly mediates bridging

between LSD1 and nucleosomal substrates, and is required for the activity of LSD1 on nucleosomal subtrates in contrast to bulk histones (51, 95, 116).

Other LSD1 associated proteins are likely involved in its gene regulation activity. Indeed, it has been shown that in certain contexts, the substrate specificity of LSD1 can even be changed. Metzger et al. showed that LSD1 interacts with the androgen receptor in testes and in prostate cell lines (62). They showed that in a cell and tissue-specific context, LSD1 is capable of demethylating mono- and di-methyl Lys 9 H3, which mediates gene activation of the *PSA* (prostate serum antigen) gene. Another report shows that LSD1 has varied roles in cell lineage specific differentiation during pituitary organogenesis (113). This study showed LSD1 involvement in the activation of certain subsets of genes and the repression of others. They also found that LSD1 plays a role in both gene activation and repression of the *Gh* (growth hormone) gene during pituitary organogenesis. The opposing functions of LSD1 on a single gene are determined by its association with co-activator or co-repressor complexes, which are dependant on differentiation stage and cell lineage (113). Consistent with these data, it was shown in an estrogen receptor (ER) positive mammary adenocarcinoma line (MCF7) that LSD1 was enriched at the promoters of at least 22% (4212 out of 20045 total) of the genes surveyed following stimulation by an ER ligand. It was shown that LSD1 is required for activation of many of these genes, while it functions as a co-repressor for others (25). These data underscore the significance of LSD1 in gene regulation, and indicate the importance of LSD1 associated proteins in determining its role in co-activation and co-repression.

Recent studies of LSD1 homologs in lower organisms suggest additional roles for the nuclear amine oxidase family in genome regulation. S. Pombe contains two LSD1 homologs, spLSD1 and spLSD2, that have been shown to interact with one another (30, 50, 68). spLSD1

possesses Lys 9 H3 demethylase activity *in vitro* and *in vivo*. SpLSD1/spLSD2 colocalize to promoter regions across the yeast genome. In addition to a role in gene activation, the elimination of these proteins leads to dysregulation of constitutive heterochromatin in S. pombe. spLSD1/2 colocalize to heterochromatin boundaries (telomeric and pericentromeric) and inactivation of spLSD1 or reduction of expression of spLSD1/spLSD2 led to heterochromatin spreading effects. Altogether, these data support a role for spLSD1/spLSD2 beyond that of gene expression regulation, implicating their function in the maintenance of heterochromatin boundaries (30, 50).

The Drosophila LSD1 ortholog is also implicated in gene regulation as well as heterochromatin formation. However, dLSD1 appears to function mechanistically very differently from the S. pombe demethylases. In contrast to spLSD1/2, which have K9 H3 demethylase activity, dLSD1 demethylates mono- and di-methyl K4 H3 (20, 87). dLSD1 localizes to sites of heterochromatin formation during embryonic development, and its absence results in the spreading of euchromatin histone patterns into heterochromatin regions (contrasting with the spreading of heterochromatin in spLSD1 null organisms). Loss of dLSD1 also suppresses PEV, another indication of disruption in heterochromatin. It is proposed that dLSD1 demethylates K4 H3 in conjuction with Su(var)3-9 methylation of K9 H3 and HP1 to establish characteristic epigenetic fingerprint of heterochromatin (87).

Biology of Histone Methylation

Since the initial discovery of histone methylation, a role in transcription regulation has been suggested (2). Recent evidence indicates specific individual histone methylation patterns determine gene activity. Generally, methylation of lysines 4, 36, and 79 of H3 correlate with euchromatin and gene activity; while methylation of lysine 9 and 27 on H3 and lysine 20 of H4 correlate with gene repression. Histone arginine methylation is typically associated with gene

activation. The role of these modifications in transcription regulation is generally well conserved (7, 53, 71, 100). But this picture is complicated by several observations: 1) the function of specific methylated residues depends on their location within a gene region (i.e. promoter versus intragenic); 2) the degree of methylation (mono-, di-, or tri-methylation) on a single residue is implicated in different physiological outputs; and 3) coordination of cis and trans-histone modifications impact each other and the physiological output.

While the role of histone methylation in gene transcription has been by far the most extensively studied, histone methylation is implicated in several other biological pathways. It has long been known that H3K9 methylation is important in heterochromatin formation, and many of the methyltransferases inv(52)olved are known (e.g. yeast- Set4, drosophila- Su(var)3-9). Importantly, a role for histone demethylation in constitutive heterochromatin maintenance/formation has also recently been identified (see LSD1 above).

Lysine 9 methylation on histone H3 is widely correlated with gene repression (53, 71). However, gene inactivity associated with K9H3 methylation is restricted to the promoter regions of genes and, in contrast, H3K9 methylation in intergenic regions correlates with gene activity (108, 109). Conversely, while trimethylated Lys 4 H3 is generally indicative of active gene transcription, this mark is largely confined to the promoter region and transcription start site, and isn't maintained within intragenic regions (52, 109). The significance of the specificities of the patterns of these epigenetics marks is largely unknown.

The biological significance of histone methylation not only depends on the residue modified or the location within a gene region, but also depends on the degree of methylation. Methylation of lysine 4 H3 strongly correlates to euchromatic regions of the genome (8, 80, 100). However, whether a promoter region is di- or tri-methylated determines if the gene is

poised for transcription ("transcriptionally competent") or actively transcribed, respectively (88, 91). These results suggest a model in which promoters enriched for dimethyl K4H3 are poised for gene activation (or perhaps basally expressed) and are converted to a trimethyl K4H3 upon full activation.

Perhaps one of the more complex and least understood mechanisms of control for histone methylation is the coordination and interdependence of many of the modifications. "Cis-histone" regulation is defined by modifications on a histone influencing other modifications of distinct residues on the same histone (e.g. H3K4 methylation precludes H3K9 methylation, but often overlaps with H3K9 acetylation). Additionally, "trans-histone" regulation has been shown, in which modifications on one core histone can regulate subsequent modifications to the other histones within a nucleosome. Trans-histone regulation is best described in *S. cerevesiae*, in which monoubiquitination of histone H2B at Lys 123 regulates the methylation of Lys 4 and 79 on H3 (10, 102).

Histone methylation is also implicated in chromosome dynamics during mitosis. Methylation of Lys 9 H3 is required for maintenance of constitutive heterochromatin, which comprises an essential component of the centromere for kinetochore formation and sister chromatid cohesion during mitosis (59, 77). Without pericentromeric heterochromatin, the cohesin complex, which is responsible for maintaining cohesion between sister chromatids, cannot be loaded properly and cohesion is lost (6, 72).

Coordination of Chromatin Modifications

It is now becoming evident just how complex these systems of epigenetic modifications are. Based on global patterns of chromatin modifications that are related to specific physiological events, a "histone code" has been proposed (46, 99). The histone code proposes a system of chromatin modifying proteins ("writers") and a system of effector proteins ("readers")

that respond to specific patterns of chromatin modifications to mediate genomic metabolism. At the center of the histone code hypothesis is the coordination of the various chromatin modifications. Large multi-subunit protein complexes have been identified that contain a variety of chromatin associated proteins, including: histone modifying proteins, histone and DNA binding proteins, nucleosome remodeling proteins, DNA methyltransferases, and transcription factors. Such complexes have been identified that are involved in gene regulation, chromatin condensation, sister chromatid cohesion, DNA replication, etc. (26, 36, 86, 94). These complexes orchestrate the chromatin changes that are responsible for mediating specific physiological events.

Centromere Stucture and Organization

The centromere is a specialized region on the eukaryotic chromosome that provides the platform for the formation of the mitotic kinetechore, chromosome condensation, maintenance of sister chromatid cohesion, and mediates the metaphase spindle checkpoint. Its structure and function are essential to the faithful segregation of chromosomes during mitosis. Human centomeres consist of α-satellite repeats organized into repeating higher-order tandem arrays, with chromosome-specific α-satellites and overall lengths (from <200kb to 5Mb). Each centromere is flanked by pericentromeric heterochromatin, consisting of clusters of α-satellite repeats interrupted by interspersed elements (SINES, LINES, and LTRs). The structure and function of the centromeric region is dependent on the unique genetic and epigenetic compositions. In addition to the centromere-specific arrangement of repetitive genetic elements, the centromere incorporates a unique histone variant, CENP-A. CENP-A is a centromere specific homolog of histone H3. Its periodic incorporation into the centromere region contributes to the characteristic constriction observed at the centromere of each chromosome.

Contromere Epigenetics

The epigenetic signatures of the human centromere and pericentric heterochromatin are unlike any other characterized regions of the genome. It is believed that the epigenetic imprint of the region is largely responsible for its maintenance during cell divisions. The centromere specifically contains CENP-A nucleosomes (containing tetramers of CENP-A/H4 flanked by H2A/H2B dimers), which alternate with normal nucleosomes containing H3. Centromeric H3 is enriched for di-methylation on Lys 4, however, unlike typical euchromatin, centromeric nucleosomes are hypoacetylated. The centromere is depleted of methyled Lys 9 on H3. Unlike H3, CENP-A does not appear to be modified.

The boundary region between the centromere and pericentromere is marked by an abrupt change in epigenetic status. First, CENP-A is absent from pericentric heterochromatin. Futhermore, pericentromeric heterochromatin is enriched for di- and tri-methylated Lys 9 H3 and trimethylated Lys20 H4. Lysine 4 H3, on the other hand, is unmethylated in this region. The enrichment of methylated K9 H3 recruits HP1 to pericentric heterochromatin, which is a defining feature of the region. Flanking the distal boundaries of pericentric heterochromatin are regions enriched for trimethylated Lys 4 H3 (13, 101). As might be predicted by its epigenetic composition, heterochromatin is transcriptionally silent and refractory to recombination (48). Recent work indicates a requirement for microRNAs and the RNAi pathway (Dicer, RISC, RITS etc.) for the induction and maintenance of pericentric heterochromatin (12, 13)(HP Cam, Nat Gen 2005; SM Buker, Nat Struct Bio, 2007). Changes in either the centromere or pericentric domains can be induced by changes in the expression of proteins characteristic of these domains. In Drosophila, overexpression of the K9H3 HMT, Su(var)3-9, or HP1 can induce the spreading of heterochromatin outward from the centromere, inducing PEV into surrounding regions. Overexpression of CENP-A induces centromere domain spreading into flanking heterochromatin

regions (12). While some of mediators responsible for the epigenetic profile of heterochromatin are known (e.g. Suv39h H3K9 HMT), there is much yet to be learned about the means by which this unique and highly specialized structure is organized and maintained.

The Function of Pericentric Heterochromatin

Pericentric heterochromatin is an essential component of the functional centromere. While the exact details of its function aren't completely understood, its importance is well appreciated. One important function of pericentric heterochromatin is the maintenance of sister chromatid cohesion during metaphase of mitosis. The cohesin complex is responsible for maintaining sister chromatid cohesion during mitosis. Cohesin is a highly conserved multiprotein complex consisting of four components, including two core structural maintenance of chromosome proteins (SMC1 and SMC3) and two accessory subunits (Rad21/Scc1 and SA1/SA2) (54). The SMC components of cohesin form a hinged clamp-like structure with an ATP-binding cassette domain at one end. Cohesin is proposed to form a ring around newly replicated DNA and maintain its cohesion until sister chromatid segregation during anaphase of mitosis. At metaphase, the cohesin complex is removed from the chromosome arms, and remains only at the centromeres (38). This centromere cohesion is required until each chromatid pair is aligned along the metaphase plate and anaphase begins (85). HP1 association with cohesin subunits has been clearly demonstrated in yeast, and loss of the epigenetic marks responsible for recruitment of HP1 (di- and tri-MeK9 H3), or HP1 itself, results in the premature separation of sister chromatids (4, 22, 77).

CHAPTER 2
MATERIALS AND METHODS

Cell Culture

Cells were grown in DMEM (High Glucose, w/o L-Glutamine, w/ sodium-pyruvate)(Gibco) supplemented with 10% FBS, Penicillin (100U/ml), Streptomycin (100ug/ml), and L-Glutamine (2mM). Transfections were done in 6-well plates on glass coverslips (12mm X 12mm). 2ug/well of DNA was transfected using Fugene (Roche) at 3:1 Fugene:DNA. Media was changed 24 hours post transfection.

DNA Vectors

Aof1 and *n-PAC* cDNAs were cloned from HeLa cells and inserted into the pOZ-FH-N tandem affinity purification vector at the XhoI and Not restriction sites. LSD2 and n-PAC GFP fusion proteins were inserted into XhoI and HindIII sites of pCDNA3.

Immunoblotting

Adherent cells were washed 2X in cold PBS, collected using a cell scraper, and centrifuged at 750g. The cell pellet was resuspened in 10X pellet volume of RIPA buffer [1% NP-40; 1% sodium deoxycholate; 0.1% SDS; 0.15M NaCl; 0.01M sodium phosphate, pH 7.2; 2mM EDTA; 50mM sodium fluoride; protease inhibitors (1X Roche complete mini-EDTA free PI tablets); and 0.2mM sodium vanadate] and kept on ice for at least 30' with vigorous vortexing every 5'. Lysed cells were spun at 4°C, 12,000rpm, for 10 minutes. The supernatant was collected, protein sample buffer was added, and samples were boiled for 10 minutes. Proteins were transferred onto 0.45um nitrocellulose (0.2um was used for histone samples in *in vitro* demethylase assays) with a Bio-Rad transfer apparatus (300mA/6 hours or 125mA/o/n) at 4°C. The membrane was blocked in 3.5% non-fat milk in PBST at room temperature for 1 hour. Membranes were incubated in primary antibody (diluted in PBST/milk) at room temperature for 1 hour (or o/n at

4°C), followed by two quick rinses and 3X 10’ washes in PBST/milk. Membranes were incubated in secondary antibodies diluted 1:5000 [goat anti-mouse or goat anti-rabbit conjugated to horseradish peroxidase (Sigma)] for 30 minutes at room temperature, followed by 2X quick rinses, 3X 10’ mintues washes in PBST/milk, and 1X quick rinse in PBS. The membrane was treated with Pierce ECL Western Blotting Substrate and developed using Kodak X-OMAT Blue or X-OMAT HS.

Pheonix Retroviral Production

Pheonix A (amphotropic) cells were plated in a 10cm dish 1 day prior to tranfection to reach ~70% confluence on the day of transfection. 5 minutes prior to DNA transfection, chloroquine was added to the cells at a final concentration of 25uM. The retroviral DNA construct was transfected using the following calcium phosphate precipitation method: 1) 20ug retroviral plasmid DNA was added to a 15ml conical tube; 2) ddH20 was added (a volume appropriate to bring the total volume of DNA, ddH2O, CaCl2 mixture to 500ul); 3) 50ul 2.5M CaCl2 was added to the tube and mixed by flicking; 4) 500ul 2X HBS pH 7.05 (HEPES buffered saline; 50mM HEPES, pH 7.05; 10 mM KCl; 12 mM Dextrose; 280 mM NaCl; 1.5 mM Na2HPO4) was added dropwise to the DNA/CaCl2 mixture and bubbled vigorously for 8-10 sec. The mixture was then added dropwise to the 10cm dish of Pheonix cells. The media was changed 12-18 h after transfection and the cells were placed in a 32°C incubator with 5% CO2. 30-36h after the media change, the Pheonix cell supernatant was harvested and syringe filtered (0.45um). Polybrene (final conc. 4ug/ml) was added to the viral supernatant before it was applied to target cells for transduction. Cells in flasks were transduced overnight by incubation in the viral supernatant. Cells in 6-well dishes were “spinoculated” by adding viral supernatant to each transduced well, followed by centrifugation of the plate at 2000rpm at RT for 90 minutes,

and placed in a 32°C incubator o/n. After o/n incubation fresh 10%FBS/DMEM was added to the transduced cells. For drug selected cells, antibiotics were added 48h post transduction.

Tandem Affinity Purification

Generation of pOZ-LSD2 HeLa Suspension Cells

Pheonix amphotropic retrovirus containing pOZ-FH-N-LSD2 was produced as described above. 12ml of viral supernatant was applied to ~1X10^7 HeLa suspension (HeLa S) cells in a 75mm2 cell culture flasks (grown in 10%FBS/DMEM—see above). Polybrene was added to the virus at a final concentration of 4ug/ml. HeLa cells were incubated with virus overnight. HeLa cells were harvested and virus media was replaced with 40mL fresh 10%FBS/DMEM and replated in 175mm2 flask.

Cells were selected 36 hours after replating the transduced HeLa S cells. 3mls medium containing 8ul anti-IL2R was added to the HeLa cells in culture. The flask was gently swirled every 30 minutes for 6 hours. Media was removed (unattached cells collected) and the flask was gently washed with PBS. Cells were briefly trypsinized (~4 minutes) and divided into two T25 flasks, each filled with 50mls cells+media. Flasks were placed in a magnetic "sandwhich" and gently rocked/rotated every 5' for 30'. While still on magnetic plates, the T25 flasks were placed vertically and the media was carefully removed (and replated in a new T75 flask until assurance of selection results). The selected cells were gently washed (in T25 still sandwiched between the magnets) with 50ml fresh media. 20ml of media was added to each T25 and the flasks were removed from the magnets. All selected cells were collected in the fresh media and replated in T75. Cells were grown for 2 days before selecting again.

Large Scale HeLa Suspension (HeLa S) Cultures

After selecting the HeLa S-pOZ-LSD2 (HeLa-SD2) cells twice, expression of the TAP-tagged *Aof1* construct was confirmed by immunoblot and immunofluorescence. HeLa-LSD2

cells were expanded to four 150mm2 tissue culture flasks. At ~70% confluence, the HeLa-LSD2 cells were transferred to 2 liters of Minimum Essential Medium Eagle-Joklik Modification (Sigma-M0518) (12g/L plus 3g/L sodium bicarbonate, 100U/ml penicillin, 100ug/ml Streptomycin, 2mM L-Glutamine, 10% Newborn Calf Serum) and grown in a 3L Bellco spinner flask. The spinner flasks were grown in a non-humidified incubator at 37°C in the absence of supplemental CO2. Prior to cell density reaching 5X10^5 cells/ml (3 days), the cells were split (1 L each) into two 3L spinner flasks and 2L fresh media was added to each. After 1 day (prior to cell densities reaching 5X10^5 cells/ml), the culture from each 3L flask was split into two 8L spinner flasks (1.5L each) and 1.5L fresh Joklik media (see above) was added to each (giving a total of 3L in each of four 8L spinner flasks). 48 hours later, 5 liters of fresh Joklik media was added to each 8L flask. 48 hours later, cells were harvested and processed according to the tandem affinity purification protocol.

Tandem Affinity Purification (TAP)

All of the following steps were conducted at 4°C or on ice. Cells were collected from the 8L flasks into 1 Liter polypropyline tubes and centrifuged at 3400rpm for 10'. Pelleted cells were washed 1X with cold PBS. The volume of the cell pellet was determined, and cells were resuspended in 5.5X the pellet volume with Hypotonic Buffer (HB-10mM Tris pH7.9, 10mM KCL, 1.5mM MgCl2, plus fresh 200uM PMSF and 10mM B-mercaptoethanol). Cells were incubated in HB on ice for 10'. After cells swelled in HB, they were spun down at 2500rpm for 10 minutes. The swollen pellet volume was determined and the cell pellet was resuspended in HB (+PMSF, B-ME, and PIs) equal to the pellet volume and then applied to a dounce homogenizer (Type A pestle). Cells were dounced until cell membrane lysis was nearly 100% (~20-25 strokes). The cell lysate was centrifuged at 4000 rpm for 15'. After centrifugation, the

top lipid layer was discarded and the remaining supernatant (cytoplasmic extract) was collected and snap-frozen in liquid nitrogen. The volume of the nuclear pellet was estimated and resuspend in ½ volume with Low salt buffer (LSB- 20mM Tris, pH 7.9; 20mM KCl; 1.5mM MgCl2; 0.2mM EDTA; 25% Glycerol; plus fresh 200uM PMSF and 10mM B-ME). The nuclear pellet was stirred gently in a beaker, while an equal volume of High salt buffer (HSB- 20mM Tris, pH 7.9; 1.2M KCl; 1.5mM; 0.2mM EDTA; 25% glycerol; plus fresh 200uM PMSF and 10mmM B-ME) was gravity dripped slowly into the stirring nuclear homogenate. The nuclear extract was stirred for 40 minutes after the HSB was completely added. The nuclear extract was centrifuged at 15,000rpm for 40 minutes at 4°C. Following centrifugation, the top lipid layer was discarded and the nuclear extract was collected.

The nuclear extract was dialyzed (SpectroPor, MWCO 8,000KDa, 32mm) twice in 6L of dialysis buffer (20mM Tris pH 7.9; 100mM KCl;. 20% glycerol; 0.2mM EDTA; plus fresh 0.2mM PMSF and 10mM B-ME), for lengths of 3.5 hours and 12 hours. The dialysate was centrifuged at 15,000rpm, for 40' at 4°C.

800ul of anti-FLAG antibody conjugated agarose beads (Sigma) were added to 42.5mls of the dialyzed nuclear extract, and gently rotated at 4°C for 20 hours. Following incubation, the mixture was centrifuged at 1200rpm for 5min at 4°C. The supernatant ("flow through") was collected and snap frozen. The beads were washed 3 times in 4ml wash buffer (WB- 50mM Tris, pH7.9; 10% glycerol; 100mM KCl; 0.2mM EDTA; 5mM MgCl2; 10mM B-ME; 0.1% NP-40) and added to a centrifuge filter tube (Bio-Rad) for elution. The FLAG purified sample was eluted twice using 850ul of FLAG elution buffer (wash buffer+Tris pH7.9 to 200mM; 0.4mg/ml FLAG peptide; protease inhibitors) for each. These samples constitute the FLAG E1 (FgE1) and

FLAG E2 (FgE2) elutions. A final elution using 0.1M Glycine pH2.7 was performed (FLAG E3).

250ul anti-HA antibody conjugated to agarose beads (Sigma) was added to 600ul of FLAG-E1 and rotated gently at 4°C for 6 hours. The sample was centrifuged, flow through was collected, and the sample was washed 6 times in wash buffer. The HA samples were eluted (HA-E1 and HA-E2) using 400ul HA elution buffer (wash buffer+Tris pH7.9 to 200mM, 0.4mg/ml HA peptide, protease inhibitors), followed by 400ul 0.1M Glycine pH2.7 elution for HA-E3. All samples were aliquoted and snap frozen using liquid nitrogen.

Mass Spectrometry

Flag–HA double-purified material was separated by 4–20% NuPAGE (Invitrogen) gradient SDS–polyacrylamide-gel electrophoresis (SDS–PAGE) and stained with Coomassie blue. The various protein bands were excised and analysed by mass spectrometry at the Harvard Medical School Taplin Biological Mass Spectrometry Facility.

In Vitro Demethylation Assay

Bulk histones, nucleosomes, or histone peptides were incubated with recombinant LSD2 protein or tandem affinity purified LSD2 in histone demethylase buffer (50mM Hepes, pH8.0, 80mM NaCl, 0.1 Units formaldehyde dehydrogenase (FDH), and 1mM NAD+) at 32°C for 2 hours to overnight. A typical reaction used 6ug of either nucleosomes (extracted from HeLa) or bulk histones from calf thymus (Sigma), or 0.25-1ug histone peptides in 100ul total reaction volume. The reaction mixture was analyzed by SDS-PAGE and immunoblotting using histone modification specific antibodies, or MALDI-TOF mass spectrometry.

Immunofluorescence

Cells were plated on glass coverslips in six well dishes. Following any specific experimental treatment/conditions, cells were washed 2X with PBS and fixed with 3%

paraformaldehyde/PBS for 10 minutes at room temperature (RT). Cells were rinsed 3X with PBS and permeabilized with 0.5% Triton/PBS for 10 minutes at RT. Cells were washed in PBS 2X and blocked for 1 hour at RT in 1% BSA/PBS. Primary antibodies were diluted in 0.1%BSA/PBS and incubated for 1 hour at RT. The coverslips were washed 3X for 5'. Secondary antibodies (1:1000) and DAPI (final concentration 500nM) was diluted in 1%BSA/PBS and incubated for 1 hour. Coverslips were washed 3X for 5', followed by a quick ddH20 rinse and mounted (Southern Biotechnology mounting reagent).

Live Cell Imaging

U2OS cells were plated onto glass bottom tissue culture dishes (MatTek Corp.) at ~40% confluence. Transfections were conducted using Fugene as described above. The transfection media was changed after 12 hours. Cells were imaged using an Olympus DSU (63X objective) with an enclosed humidified environmental chamber perfused with 5% CO2. Cells appeared healthy and viable under these conditions. GFP was visualized using the FITC-3540B filter set. Images were captured approximately every hour. Differential interference contrast (DIC) images were taken at the beginning and end of each set of images in order to visualize whole cells, including those not transfected with GFP constructs.

Reverse-Transcriptase Real Time Polymerase Chain Reaction (Real Time RT-PCR)

Total RNA was isolated using the Trizol Reagent (Invitrogen). 2ug of RNA was used as a template for reverse transcription reactions (RT) using Superscript Synthesis for First Strand Synthesis Kit (Invitrogen) with random hexamer primers. Real time PCR was done in 15ul total reactions, which included: 40-100ng RNA equivalent of first strand cDNA, 0.25nM forward primer, 0.25nM reverse primer, 7.5ul 2X SYBR Green Supermix (Bio-Rad). Samples were run in duplicate on 96 well plates using the Bio-Rad iQ5 Real-Time PCR Detection System. Using the cycle number required to meet the sample threshold for each sample (Ct), quantitative

comparisons between samples for specific mRNAs of interest were made using the following equation: (2^(WTg-Tg))/(2^(WTc-Tc)): where WTg= wild-type sample- gene of interest; Tg=experimental sample- gene of interest; WTc= wild-type sample- loading control; Tc=experimental sample- loading control.

For non-quantitative PCR, the following conditions were used: 20ng RNA equivalent of cDNA, 10uM forward primer, 10uM reverse primer, 22ul PCR Supermix (Invitrogen). Primers for each gene target are as follows: P1- ccaagacttatcgatgcggtatg; P2- gtattcctcacatcatcgtccg; P3- gaggagctcagattgtcaatgg; P4- gaccacactctgctaactcc; LSD2f- gtgctttgcaagtgcttctg; LSD2r- tgaagaaacctcgcggaaag

Metaphase Chromosome Spreading

HeLa-S cells were grown 10%FBS/DMEM media in non-treated Petri dishes to prevent attachment. Cells were treated in 100ng/ml of Colcemid for 2-3 hours. Cells were removed from colcemid, washed with PBS, and resuspended in hypotonic solution (0.0375 M KCl, 0.4% sodium butyrate) for 15 min at a concentration of 5 X 10^5 cells/ml. 90ul of the cells in hypotonic solution was spun onto glass coverslips by centrifugation at 1,900 rpm 10 min in a cytocentrifuge (Cytopro 7620; Wescor). The coverslips were then incubated in KCM buffer (120mM KCl; 20mM NaCl; 10mM Tris-HCl, pH7.7; 0.1% Triton X-100) for 10 min at RT and fixed in 3% paraformaldehyde for 10 min at RT. The samples were blocked and processed for immunofluorescence as described above.

Luciferase Assay

A Gal4-TK-Luciferase construct was used as a reporter for gene transcription activity. The construct contains five tandem Gal4 binding sites attached to the HSV thymidine kinase (TK) basal promoter upstream of the luciferase gene. U2OS or HEK293 cells were plated in 12-well dishes 1 day prior to tansfection for growth to ~70% confluence at the time of transfection.

Gal4-Luc, wild-type or mutant LSD2 fused to Gal4-DBD, a B-galactosidase expression construct, and pCDNA3.1 using Fugene (3:1 Fugene:DNA ratio). 36 hours after transfection, cell extracts were harvested using Promega Reporter Lysis Buffer(plus PIs and PMSF). Cell extracts were centrifuged at 15K rpm, for 10 min at 4°C. The supernatant was collected. 30ul of cell extract was added to 300ul of luciferase assay buffer (25 mM Glycine-Glycine; 15 mM MgSO4; 15 mM KPO4, pH 7.8; 4 mM EDTA; 1 mM DTT; 1mM ATP). 100ul luciferin was added and each sample was analyzed for relative luciferase units (RLU) on a luminometer. The β-galactosidase activity assay was used for each sample to determine the relative transfection efficiency. 30ul of each sample of cell lysate was added to β-gal assay buffer (0.3µl 1 M MgCl2; 0.9µl B-ME; 66µl ONPG (4 mg/ml ONPG in 0.1 M sodium phosphate, pH 7.5); 203µl 0.1 M sodium phosphate, pH 7.5). β-gal reactions were run until a faint yellow color developed. 200µl of 1 M Na2CO3 was added to stop each reaction. Optical density was determined at 420 nm and used to determine relative transfection efficiency for each reaction.

MALDI-TOF Mass Spectrometry

Two microliters of the 100µl demethylation reaction mixture was desalted by passing through a C_{18} ZipTip (Millipore). Prior to desalting, the ZipTips were activated and equilibrated using 10µl of 50% acetonitrile/0.1% TFA (2×), followed by 10µl of 0.1% trifluoroacetic acid (TFA) (3×). The reaction mixture was then loaded onto the activated ZipTips. The ZipTips were washed with 10µl of 0.1% TFA (5×), and the bound material was eluted from the ZipTip using 2 µl of 70% acetonitrile containing 1 mg/ml α-cyano-4-hydroxycinnamic acid MALDI matrix and 0.1% TFA. The eluates were spotted onto a circle of open MALDI target areas to allow solvent evaporation and peptide/matrix cocrystallization. The samples were analysed by a MALDI-TOF

MS (PerSeptive Biosystems Voyager-DE STR Bioscpectrometry Workstation) at the Dana Farber Cancer Institute Molecular Biology Core Facilities.

Nuclear Matrix Preparation

Cells were transfected on glass coverslips as described above. Nuclear matrices were prepared as originally described by Kantidze et al. (47) as follows: coverslips were rinsed twice with TM buffer (50 mM Tris-HCl), pH 7.5; 3mM MgCl2), followed by a 10' incubation on ice in permeabilization buffer (10 mM PIPES, pH 7.8; 0.5% Triton X-100; 100 mM NaCl; 0.3 M sucrose; 0.2 mM PMSF; 3 mM MgCl2). Cells were washed three times with TM buffer and treated with either RNase-free DNase I (182U/ml) (Invitrogen); 1ug/ml RNase A (Qiagen); or no nuclease treatment, for 30 min at 37°C in TM buffer. The buffer was replaced by TM buffer supplemented with 0.5 M NaCl and the coverslips were incubated for 30 min on ice. The coverslips were then washed twice with TM buffer, fixed with 3% pararformaldehyde for 10 min at RT, and blocked and immunostained as described above.

TUNEL Staining

TUNEL staining was performed according to the manufacturer's instructions for the *In Situ* Cell Death Detection Kit, TMR red (Roche).

Fluorescence Microscopy

Fluorescent imaging was done using a Nikon Eclipse 90I upright microscope with a Z-motor, and the following features: Plan Apo 63X and 100X objectives; Plan Fluor 40X and 10X objectives; Photometrics Coolsnap ES CCD Monochrome camera; and Nikon's NIS-Elements Basic Research software.

siRNA Knockdown

ON-TARGETplus SMARTpool siRNAs (Dharmacon) targeting human AOF1 transcripts were transfected into HeLa cells using Lipofectamine transfection reagent (Invitrogen). Either

25 picomoles (final concentration of 12.5nM) or 100 picomoles (50nM) of double-stranded RNA was used for each transfection. Cells were transfected two times, 12 hours apart. RNA was harvested 72 hours after the second siRNA transfection.

Co-Immunoprecipitation

Cells were washed in culture dishes 2X with cold PBS. Cells were scraped from the dishes using PBS+0.2mM PMSF. Cells were spun at 4°C at 1500rpm for 6 minutes. The cell pellet was resuspended in 2.5 times the pellet volume of IP Buffer II (50mM Tris, pH 7.4; 5mM EDTA; 0.1% NP-40; 300mM NaCl; 0.2mM PMSF; protease inhibitors). Cells were incubated on ice for 30 minutes and mixed every 5 min. IP Buffer 0 (50mM Tris, pH 7.4; 5mM EDTA; 0.1% NP-40) was added at an equal volume to Buffer II. The solution was mixed and spun at 4,200 rpm for 15 minutes at 4°C. The supernatant was collected and anti-HA agarose beads (Sigma) was added to the solution and rotated overnight at 4°C. The bead solution was spun at 1000 rpm for 2 minutes at 4°C and the supernatant (flow through) was collected. The beads were washed 3X at 4°C in wash buffer (50mM Tris-HCL, pH 7.9; 10% glycerol; 100mM KCl; 0.2mM EDTA; 5mM MgCl2; 10mM β-mercaptoethanol; 0.1% NP-40) and SDS-PAGE sample buffer was added directly to the beads and prepared for immunoblotting.

CHAPTER 3
RESULTS

Introduction

The German cell biologist Albrecht Kossol first identified histone proteins over a century ago. For most of the period since their discovery, histones were appreciated only for their role in packaging and organizing the eukaryotic genome. During the course of their study, it was discovered that histones were subject to covalent modification by addition of methyl or acetyl groups, which were suspected of playing a role in transcription regulation. However, it wasn't until 112 years after their discovery that a direct link was made between histone modifications and gene regulation (11). These and other findings in epigenetic research provide the framework for the study of epigenomics, and have led to the proposal of a "histone code", in which the genome is regulated by coordinated histone modifications and effector molecules that translate the modifications into biological responses (46, 99).

A role for histone modifications in genome metabolism is now firmly established. Processes ranging from gene transcription to DNA repair and chromosome condensation are now characterized by specific histone modifications. At the heart of genome metabolism are the mediators of these covalent modifications and their role in the dynamic regulation of histone modifications. Since the original identification of acetylated and methylated histones, numerous other histone modifications have been identified (e.g. phosphorylation, ubiquitination, sumoylation), along with enzymes of opposing functions that mediate the "writing" and "erasing" of these epigenetic marks (e.g. histone acetyltransferases/histone deacetylases; kinases/phosphatases).

Despite being one of the first histone modifications identified, histone methylation was only recently shown to undergo dynamic regulation. The recent identification of LSD1 as a bona

fide histone demethlyase ended the longstanding debate over the reversibility of histone methylation (93). While histone methyltransferases (HMTs) had been well characterized, prior to the discovery of LSD1 lysine 4 H3 demethylase acitivity, histone methylation was the only known histone modification whose active removal hadn't been proven. As a result, histone methylation was often regarded as a stable and permanent epigenetic mark; an error that led to many miscalculations of the role of histone methylation in genome physiology.

Since its histone demethylase activity was discovered, the role of LSD1 in transcription regulation has been an area of intense research. Its participation in the neuron-specific gene repression of a CtBP/CoREST corepressor complex in non-neuronal cells is well documented. Other work describing a role for LSD1 demethylation in association with androgen receptor mediated gene activation and estrogen receptor mediated gene activation and/or repression illustrates the significance of LSD1 and histone demethylation in the dynamic regulation of gene activity.

The nuclear amine oxidase family of proteins, of which LSD1 is a member, is well conserved from yeast to humans. It can be divided phylogenically into two subfamilies, one containing orthologs of LSD1, and a second containing orthologs of the human Aof1 protein (LSD2) (Figure 3-1). The focus of the work described here includes the biochemical and biological characterization of the human LSD1 homologue, LSD2, in an effort to advance our understanding of nuclear amine oxidases and histone demethylation in human cellular physiology.

LSD2 Sequence and Domain Analysis

The full length *Aof1* transcript (~ 2.5 kb) coding for LSD2 was cloned from a HeLa cDNA library. It encodes an 822 amino acid protein containing several conserved domains, including a zinc-finger domain, a SWIRM domain, and a C-terminal amine-oxidase domain (Figure 3-2).

The SWIRM domain and amine oxidase domain share homology with LSD1, in which they mediate chromatin targeting and enzyme catalysis, respectively. LSD2 noticeably lacks the spacer region within the LSD1 amine oxidase domain, while the LSD2 N-terminal zinc finger domain is absent in LSD1 (Figure 3-2).

Genomic database searches indicated another *Aof1* transcript identified by EST screens that encodes a 590aa protein (NP_694587), which we refer to as LSD2.1 (Figure 3-3A). LSD2 and LSD2.1 share N-terminal and C-terminal domains, however, LSD2.1 has large deletions across two coding regions, including the SWIRM domain and the amine oxidase domain (Figure 3-3B). To confirm the transcription of both LSD2 and LSD2.1, we used the reverse-transcription polymerase chain reaction (RT-PCR) to amplify fragments unique to either LSD2 or LSD2.1. Using primers targeting sequences common to LSD2 and LSD2.1, but flanking the LSD2.1 deletion sites, we were able to amplify two bands in each PCR reaction. The upper band was amplified from full length LSD2, and the lower band was amplified from LSD2.1 (Figure 3-3C). With each primer set, the upper band (LSD2) was far more intense than the lower band (LSD2.1), suggesting greater abundance of the full-length transcript over LSD2.1. Despite the presence of LSD2.1 transcripts, the deletion in the SWIRM domain and the amine oxidase domain suggest an unlikelihood that LSD2.1 possesses catalytic activity.

In Vitro Demethylase Activity

Based on its conserved SWIRM domain and the FAD-dependent amine oxidase domain, LSD2 was predicted to catalyze a two-electron oxidation reaction similar to LSD1. Using baculovirus generated recombinant GST-LSD2 and bacteria generated His-LSD2 and His-LSD2.1, we tested their enzymatic activities using an *in vitro* demethylase assay with bulk histone substrates. Immunoblotting the demethylase reactions with a panel of modification specific anti-histone antibodies revealed full-length LSD2 demethylase activity for mono- and

di-methylated lysine 4 on histone H3, confirming similar substrate specificities to LSD1 (3-5 A&B). No demethylase activity was observed with recombinant LSD2 on dimethyl- H3K9, H3K27, H3K36, H3K79, or H4K20 (Figure 3-4A and data not shown). Heat-treated LSD2 was catalytically inactive, suggesting a conformational requirement for LSD2 enzymatic activity. LSD2.1, on the other hand, had no detectable demethylase activity on H3K4 or any of the other residues tested (Figure 3-4C and data not shown). Recombinant LSD2 demethylase activity and substrate specificity Lys 4 H3 were further confirmed using the *in vitro* assay on nucleosomal substrates (Figure 3-4C). Neither LSD2.1 nor LSD2.2 recombinant protein showed demethylase activity on bulk histones or nuclesomes (Figure 3-4C).

Recombinant LSD2 demethylation activity *in vitro* was also measured using N-terminal histone peptide fragments with specific residue modifications. The demethylase activity on the peptide substrates was determined using MALDI-TOF mass spectrometry analysis, in which loss of a single methyl group results in a decrease of 14 daltons from the overall mass of the peptide substrate. As expected, LSD2 had demethylase activity only on Lys 4 methylated H3 peptides (Figure 3-D). Interestingly, however, dimethyl K4H3 peptide was reduced only to monomethyl K4H3, but was not reduced to the unmodified K4 H3 peptide, indicating incomplete demethylation of the peptide substrate. This is in contrast to the complete demethylation of bulk histone and nucleosomal dimethyl K4 to its unmodified form. The reason for the limited demethylation of peptide substrates is unclear.

These data confirm the *in vitro* demethylase activity of LSD2 and reveal its specificity for mono- and dimethyl-K4 H3 substrates. Because we were unable to detect demethylase activity in the LSD2 variants (LSD2.1 and LSD2.2), the remainder of our focus is on the study of full length LSD2.

Luciferase Assays for Transcriptional Repression Activity

Because of its identical substrate specificity to LSD1 and the known role of lysine 4 H3 methylation in transcription regulation, we suspected a role for LSD2 in gene repression. We conducted luciferase assays to determine the effect of LSD2 on gene transcription, using a luciferase construct driven by the herpes virus TK promoter and 5 tandem Gal4 binding sites upstream of the promoter (Gal4-Luc). Gal4-Luc was transiently cotransfected with Gal4-DBD-LSD1, Gal4-DBD-LSD2, or Gal4-DBD, and a B-galactosidase contruct (as a control for transfection efficiency). The effect of each Gal4-DBD construct on transcription was determined at different DNA transfection amounts. As previously shown, LSD1 had a strong dose-dependent repressive effect on Gal4-Luc expression compared to Gal4-DBD alone (Figure 3-6A). LSD2, on the other hand, had very little repression activity (Figure 3-6A). Because these were transient transfections, we wondered if a reporter system that was fully integrated into a nucleosomal/chromatin framework would better approximate the physiological context for LSD2 activity. We repeated the luciferase experiments using a HEK293 cell line with Gal4-Luc stably transfected. These experiments reproduced results similar to the previous luciferase assays, suggesting a limited role for LSD2 in transcription repression (Figure 3-6B).

Tandem Affinity Purification (TAP) of LSD2

To gain insight into the physiologic role of LSD2, we tandem affinity purified LSD2 and identified associating proteins using tandem mass spectrometry. This was accomplished using an N-terminal TAP (Flag:HA) tagged LSD2 expression construct (pOZ-LSD2). pOZ-LSD2 expresses very low levels of TAP tagged LSD2 from the pOZ retroviral promoter. This more closely approximates the physiological levels (compared to conventional overexpression) of LSD2, which helps eliminate overexpression effects on protein-protein interactions. pOZ-LSD2 was stably transduced into Hela suspension cells, which were grown to 48 liters and harvested

for tandem affinity purification. Following the TAP protocol for LSD2, half of the purified sample was submitted to the Taplin Biological Mass Spectrometry Facility at Harvard Medical School (Figure 3-7).

The results for the LSD2 tandem affinity purification have been grouped according to known function or associations (Table 3-1). It includes proteins involved in DNA damage repair (e.g. DNA-PKcs, Rad50, PARP1), nucleosome remodeling (BAP1, Snf2h), mitotic chromosome structure (e.g. SMC1 (structural maintenance of chromosme 1), SMC2) and chromatin modification (e.g. NSD3, EHMT1 EHMT2), as well as other less well-studied proteins.

Western blots using LSD2 TAP products were used to confirm the identities of many of the proteins identified by mass spec analysis. All of the proteins tested were confirmed by immunoblot, including: LSD2, SMC1, SMC2, Snf2h, NSD3, and NOT1 (data not shown).

TAP Identification of n-PAC and *In Vitro* Binding with LSD2

Of particular interest from the LSD2 TAP mass spec analysis was the identification of the uncharacterized protein, n-PAC (NP60) (protein ID: AAQ57265). N-PAC is 553 amino acids with a predicted molecular weight of 61 kDa. The n-PAC sequence reveals several interesting protein domains with significance to the study of LSD2 function (Figure 3-8A). These include two nuclear localization sequences, a PWWP (Pro-Trp-Trp-Pro) motif, an AT-hook, and an NAD-binding dehydrogenase domain. The PWWP domain is commonly found in chromatin associated proteins and mediates protein-protein interactions. The AT-hook is a zinc finger domain, which functions in DNA binding. The NAD-binding dehydrogenase domain is striking because of its likeness to the CtBP dehydrogenase domain, an LSD1 associated corepressor whose function has yet to be determined.

Because of its interesting domain features and the high incidence of n-PAC peptides in the LSD2 TAP mass spec analysis, we pursued the n-PAC interaction with LSD2. To confirm an

LSD2/n-PAC interaction we performed *in vitro* protein binding assays. Recombinant GST-LSD2 was mixed with nuclear lysate from HeLa cells stably expressing Fg-HA-nPAC. Immunoprecipitation with α-GST antibodies, followed by immunoblotting for n-PAC using α-HA antibodies, show n-PAC immunoprecipitates with GST-LSD2 but not with GST alone (Figure 3-8B). The reciprocal experiment was also done using GST-nPAC and several n-PAC deletion mutants. GST-tagged full-length n-PAC, GST-tagged PWWP deleted n-PAC (ΔPWWP), or GST-tagged-PWWP were mixed with nuclear extract from Fg-HA-LSD2 expressing HeLa cells. Fg-HA-LSD2 immunoprecipitated with all of the GST-nPAC constructs, whereas GST alone did not (Figure 3-8C). These data show an *in vitro* interaction between LSD2 and n-PAC and support our mass spec data from the LSD2 TAP.

TAP LSD2 *In Vitro* Activity

The biological activity of chromatin/histone modifying proteins is often dependent on their protein-protein interactions. They are usually found in association with regulatory proteins, chromatin-binding and recruiting proteins, and other enzymes that act in concert to mediate physiological functions. Changes in proteins associations can also provide varying contexts in which a single protein can execute different functions. In no better place is this exemplified than the function of LSD1. LSD1 interacts with CoREST, a positive regulator of demethylase activity in corepressor complexes, and BHC80, a negative regulator of LSD1 acitivity (51, 95). It was also shown that LSD1, in association with the androgen receptor, demethylates Lys 9 H3 (instead of Lys 4 H3) and can function as a transcriptional co-activator (62).

To determine the *in vitro* activity of LSD2 in the context of its associated proteins, we used TAP LSD2 products for *in vitro* demethylase assays using bulk histones and nucleosomes. The assays confirmed the specificity of LSD2 demethylase activity for K4 H3 using bulk histones,

however, TAP LSD2 activity on nucleosomes was very weak (Figure 3-9 top). With the addition of recombinant n-PAC, however, we were able to dramatically increase the LSD2 demethylase activity towards mono- and di-methyl K4H3 on nucleosomes (Figure 3-9 top). Using recombinant purified His-LSD2, we show a dose dependency on the n-PAC mediated enhancement of dimeK4H3 demethylase activity on nucleosomes (3-10A). Interestingly, the effect of n-PAC on LSD2 activity was exclusive to nucleosomal substrates, as TAP LSD2 alone (without the addition of recombinant n-PAC) very efficiently demethylated diMeK4H3 on bulk histones and the addition of n-PAC had no obvious impact on LSD2 demethylase activity (3-9 bottom and 3-10B).

N-PAC Associates with Nucleosomes

To further explore the effect of n-PAC on LSD2 activity on nucleosomes, we investigated the n-PAC association with chromatin *in vivo.* We separated the soluble and insoluble nuclear fractions from HeLa cells stably expressing Fg-HA-nPAC, and determined the amount of n-PAC in the soluble fraction using α-HA antibodies. These samples showed little detectable soluble nuclear n-PAC. However, with the addition of increasing amounts of Micrococcal Nuclease to digest the chromatin into polynucleosomes, and then further into oligonucleosomes, we were able to release soluble n-PAC from the insoluble chromatin fraction. Increasing digestion of the chromatin into smaller oligonucleosomes resulted in increasing levels of n-PAC found in the soluble fraction (data not shown). This suggests an association of n-PAC with intact chromatin that is disrupted by nucleosome digestion. Interestingly, LSD2 overexpressed in the absence of n-PAC is found almost entirely in the soluble nuclear fraction, in contrast to overexpressed n-PAC (data not shown).

Additionally, we performed pulldown assays using recombinant full-length His-nPAC or n-PAC deletion mutants incubated with purified oligonucleosomes. Using anti-His beads to pull

down n-PAC, we were able to show that n-PAC pulls down histone H3 protein (data not shown). These data combined with previous data showing *in vitro* LSD2 interactions with n-PAC suggest a model in which n-PAC, via its association with chromatin, may recruit LSD2 to its nucleosomal substrate.

LSD2 Activity *In Vivo*

We next turned to an *in vivo* system with which to study LSD2. Using a variety of LSD2 expression constructs (TAP-tagged, HA-tagged, GFP-fused LSD2), we overexpressed LSD2 in U2OS cells. LSD2 localized exclusively to the nucleus and displayed a diffuse nuclear staining pattern (Figure 3-11a & d). Using a variety of modification specific antibodies, we observed a moderate to strong decrease in diMeK4 H3 staining in LSD2 transfected cells compared to untransfected (Figure 3-11a-f). Monomethyl K4 H3 was the only other modification that had any obvious change in LSD2 ovexpression cells (although, only in high LSD2 expressing cells) (Figure 3-11s-u and data not shown). No change in staining was observed for triMeK4 H3, mono- or di-methyl K9 H3, diMeK36 H3, and diMeK79 H3 (Figure 3-12). Interestingly, the demethylation of diMeK4 by wild-type LSD2 was limited to interphase cells, whereas mitotic cells with overexpressed LSD2 were refractory to demethylation and maintained their intense diMeK4 staining pattern. In mitotic cells, LSD2 was excluded from the condensed chromatin and was confined to the chromatin periphery (Figure 3-13).

In order to show a requirement for LSD2 enzymatic activity for the observed K4 demethylation *in vivo*, we generated several LSD2 point mutants. The LSD2-M1 mutant has a point mutation in a conserved glutamine in the FAD binding domain (E412A), which abrogates FAD+ binding (unpublished data) (Figure 3-2). FAD+ is a required cofactor for the amine oxidase activity of LSD2, without which it is incapable of catalysis (unpublished data). GFP-M1 fusion constructs were transfected into U2OS cells, which showed no change in the diMeK4 H3

levels, confirming the requirement for the FAD+ cofactor for amine oxidase mediated demethylation (3-12j-l). The LSD2-M2 mutant is a point mutant of a conserved lysine in the amine oxidase domain (Figure 3-2). We mutated the lysine to alanine (K661A) and destroyed the demethylase acitivty of LSD2, as shown in transfected U2OS cells (3-12m-o). GFP-LSD2.1 *in vivo* demethylase activity was similarly measured, confirming the inactivity observed *in vitro* (3-12p-r). These observations were confirmed in several other cell lines, including HeLa, MCF7, and WI-38 (not shown).

LSD2 and n-PAC Interactions *In Vivo*

Because of the interaction between n-PAC and LSD2, and the dramatic effect of n-PAC on LSD2 activity on nucleosomes *in vitro*, we investigated their *in vivo* interactions. Using HeLa cells stably transduced with pOZ-n-PAC, reciprocal immunoprecipitations were done using α-HA beads to pull down tagged n-PAC, followed by immunoblotting using a custom antibody against LSD2. Endogenous LSD2 was efficiently pulled down with tagged n-PAC, but not in mock transfected cells (empty pOZ vector) (Figure 3-14). This provided strong supporting evidence for our mass spec and *in vitro* data showing n-PAC and LSD2 interactions.

We next used *in vivo* overexpression to investigate the biology of n-PAC and LSD2. Fg-HA-nPAC transiently transfected into U2OS cells displayed an interesting pattern of n-PAC staining. N-PAC localization was entirely nuclear and interphase cells displayed a punctate staining pattern throughout the nucleus (Figure 3-15). The size of the n-PAC dots varied somewhat from cell to cell, ranging from fine dots to larger foci like spots. In mitotic cells, n-PAC staining colocalized with the chromatin, showing complete overlap with DAPI staining throughout all stages of nuclear division (Figure 3-15). N-PAC overexpression itself had no effect on the K4H3 methylation patterns (Figure 3-15).

Next, we transiently cotransfected LSD2 with n-PAC into U2OS cells. N-PAC induced a striking change in the LSD2 nuclear staining pattern in many cotransfected cells. LSD2 no longer diffusely stained the nucleus, but adopted the punctate nuclear staining characteristic of n-PAC. In these cells, LSD2 and n-PAC colocalized perfectly (Figure 3-16). Cells cotransfected with LSD2 and n-PAC also showed a more pronounced diMeK4H3 demethylation than LSD2 transfected alone, a result consistent with our *in vitro* data (data not shown). LSD2/n-PAC cotransfected cells also showed a significant reduction in monoMeK4H3 staining compared to LSD2 transfected alone, which only showed monoMeK4 demethylation in cells with high LSD2 expression. Similar to LSD2 alone, LSD2 cotransfected with n-PAC retained specificity for mono- and di-methyl K4 H3 and showed no demethylase activity for other histone modifications tested, including K9, K36, and K79 H3 methylation (data not shown).

In LSD2/n-PAC cotransfected cells, we observed LSD2 colocalization with n-PAC on the condensed chromatin of mitotic cells (3-16). This was in striking contrast to the exclusion of LSD2 from condensed mitotic chromatin, when it was transfected alone. Interestingly, despite the localization of LSD2/n-PAC on these mitotic chromosomes, the chromatin maintained its methylated K4H3 staining, showing no evidence of LSD2 demethylase activity (3-17). The reason for this apparent inactivity of LSD2 demethylation on mitotic chromatin is not clear.

NPAC Association With Chromatin *In Vivo*

Thus far we provided solid evidence of an interaction between n-PAC and LSD2 *in vitro* and *in vivo*, as well as shown an association between n-PAC and chromatin. While the n-PAC staining pattern during mitosis clearly indicates an association between mitotic chromatin and n-PAC, the interphase staining pattern is less clear. To pursue this association further, we performed nuclear matrix preparations on transfected cells, followed by immunofuorescent staining. U2OS cells transfected with either n-PAC alone or LSD2 and n-PAC were treated with

RNAse, DNAse, or no nuclease treatment, followed by 0.5M NaCl extraction. The results indicate that RNAse treatement and salt extraction or salt extraction alone have little impact on the n-PAC staining pattern (Figure 3-18). However, DNase treatment and salt extraction resulted in loss of much of the n-PAC staining, leaving little residual nuclear n-PAC (Figure 3-18). It is likely that under these experimental conditions, n-PAC's association with chromatin was disrupted by DNAse treatment, resulting in its solubilization and extraction. These results confirm the n-PAC association with chromatin persists throughout the cell cycle.

Nuclear matrix preparations on cells cotransfected with n-PAC and LSD2 showed results similar to the experiments with n-PAC alone. RNAse treatment and extraction or extraction alone had little effect on the n-PAC staining pattern (Figure 3-19). LSD2 also colocalized normally with n-PAC in these cells (Figure 3-19). DNAse treated and salt extracted cells, on the other hand, lost much of their n-PAC and LSD2 staining (Figure 3-19).

With good evidence for n-PAC binding and recruitment of LSD2 to chromatin, we sought to determine if n-PAC binds preferentially to certain chromosomal loci. HeLa-pOZ-n-PAC cells were treated with colcemid and metaphase chromosome spreads were made. Immunofluorescence was performed for n-PAC localization along with other chromatin markers. The chromosome spreads revealed widespread n-PAC staining along metaphase chromosomes (Figures 3-20 & 3-21). While we were unable to determine a pattern of binding for n-PAC among the different chromosomes, there was striking symmetry in n-PAC binding between sister chromatids, suggesting non-random binding of n-PAC to specific regions along the individual chromosomes (Figures 3-20 & 3-21). Metaphase spreads stained for n-PAC and the centromere marker, CENP-A, generally showed an absence of n-PAC staining in the centromeres of metaphase chromosomes, although there were rare exceptions (Figure 3-21). Staining for the

telomere specific protein, Pin2, showed an absence of n-PAC in the telomeres of metaphase chromosomes (data not shown). Interestingly, metaphase spreads costained for n-PAC and dimethyl K4H3 showed a strong correlation between n-PAC staining and enriched diMeK4 H3 (3-20).

In order to further characterize n-PAC *in vivo*, we used Gfp-fused n-PAC deletion mutants to determine the critical domains for its interactions with LSD2 and chromatin (Figures 3-8A & 3-22C). The full length Gfp-n-PAC protein showed the characteristic n-PAC punctate nuclear staining (3-22A). In contrast, n-PAC with its N-terminal PWWP domain deleted (n-PAC-ΔPWWP) had a strikingly different pattern from wild-type n-PAC. The PWWP deletion mutant formed large nuclear foci in chromatin deficient regions of the nucleus (Figure 3-22A). Transfected cells immunostained for nucleolin and sp35, showed the n-PAC-del PWWP foci were distinct from nucleolar and spliceosome regions, respectively (data not shown). Interestingly, despite the loss of chromatin localization in the n-PAC PWWP deletion mutant, it retained its ability to interact with LSD2, as cotransfected LSD2 was recruited to the PWWP deletion mutant foci (Figure 3-22B). Not surprisingly, these results confirm the importance of the PWWP domain in mediating the specific pattern of n-PAC interaction with chromatin. They also show the PWWP domain isn't required for n-PAC interaction with LSD2.

We also expressed a GFP fusion construct containing only the n-PAC PWWP domain. This construct showed a diffuse nuclear staining pattern, with loss of the punctate pattern of wild-type n-PAC (3-22A). These n-PAC deletion mutants suggest a necessity, but insufficiency, of the PWWP domain for n-PAC localization to the chromatin, and implicate the carboxy-terminal domains of n-PAC in LSD2 interactions.

LSD2 and N-PAC Coexpression Induces a Mitosis Independent Chromatin Condensation

In addition to the change in LSD2 localization and the dramatic demethylation induced by the coexpression of LSD2 and n-PAC, we observed another striking phenotype. In U2OS cells transiently transfected with LSD2 and n-PAC, we noticed an unusually high number of cells displaying condensed chromatin characteristic of prophase of mitosis. Mitosis can be followed in U2OS cells by the microscopic analysis of their condensed chromatin pattern. Each stage of mitosis is readily visualized by a characteristic DAPI pattern (Figure 3-23A). In LSD2/n-PAC cotransfected cells, a prophase nuclear phenotype was observed in as many as 30% of the cells, compared to 1-2% of normally growing U2OS cell cultures. A dramatic reduction in dimethylK4 H3 staining was observed in these cells compared to untransfected cells with a similar DAPI pattern (3-23B). We did not observe an abnormal increase in prophase appearing cells in U2OS cells individually transfected with LSD2 or n-PAC. Although many n-PAC transfected cells did have observable changes in chromatin topology, it was not to the extent of LSD2/n-PAC transfeccted cells.

We reasoned that the prophase phenotype in LSD2/n-PAC cells was likely due to one of two possibilities: 1) forced entry into prophase induced by coexpression of LSD2/n-PAC or 2) prophase arrest induced by LSD2/n-PAC. To begin to investigate these possibilities, we immunostained LSD2/n-PAC cotransfected cells with various cell cycle markers.

Cyclin B1 is a well-studied marker for prophase of mitosis. Its expression is induced late in interphase, where it localizes to the cytoplasm. The transition from late G2 of interphase to prophase is marked by the phosphorylation of cyclin B1, resulting in its translocation to the nucleus prior to the breakdown of the nuclear envelope. Cyclin B1 protein levels peak at metaphase and gradually decrease during anaphase (79)(J Pines, Cell 1991). Immunofluorescent

analysis allows visualization of the transition from interphase to mitosis based on the expression level and localization of cyclin B1, coupled with the DAPI staining pattern.

U2OS cells transiently cotransfected with Gfp-LSD2/n-PAC were immunostained for cyclin B1. Using the DAPI staining pattern to identify cells with prophase-like condensed chromatin, we analyzed cells for the presence of LSD2/n-PAC and observed their cyclin B1 staining. Unexpectedly, we found almost no cotransfected prophase cells (as determined by DAPI) that displayed the characteristic prophase cyclin B1 staining pattern (Figure 3-24A). Many of the cotransfected cells with prophase-like condensed chromatin had some cytoplasmic cyclin B1, while others were cyclinB1 negative (3-24A). Very few were found that had typical cyclin B1 staining accompanying a prophase-like DAPI pattern.

Because cyclin B1 is a hallmark for prophase, its absence in LSD2/n-PAC cotransfected cells with prophase-like chromosome condensation was alarming. To determine the cell cycle stage of the LSD2/n-PAC cotransfected cells, we did immunostaining for several other cell cycle markers. Phosphorylation of Serine 10 on histone H3 (pS10 H3) is another mitosis marker (73). Ser 10 becomes phosphorylated in late G2 of interphase, as the cell is entering prophase and chromsome condensation begins. This histone modification is critical to proper chromosome condensation during mitosis, and persists through anaphase before it is removed during telophase (110, 114). Remarkably, nearly every LSD2/n-PAC cell with the prophase-like phenotype was negative for pS10 H3 staining (Figure 3-24B).

Phosphorylated threonine 3 on histone H3 (pT3 H3) is another chromatin marker for mitosis (81). pT3 H3 staining was also absent in the LSD2/n-PAC prophase-like cells (Figure 3-24C). These data provide convincing evidence that while these cells display condensed

chromatin characteristic of prophase, they are clearly not in prophase, nor does it appear that they are in mitosis.

Cell Cycle Analysis of Prophase-Like LSD2/n-PAC Transfected Cells

The absence of prophase/mitotic nuclear and chromatin markers in the presence of prophase-like condensed chromatin led us to propose three probable explanations for the phenotype. The first is that cells cotransfected with LSD2/n-PAC were undergoing apoptosis, and we were observing the chromatin condensation associated with programmed cell death. To explore this possibility, TUNEL staining for apoptotic cells was performed on cotransfected U2OS cells. LSD2/n-PAC transfected cells with the condensed chromatin phenotype were TUNEL negative, suggesting that apoptosis is not responsible for the condensation phenotype (Figure 3-24D).

The other likely explanations for a prophase-like chromosome condensation in the absence of other prophase markers include: 1) LSD2/n-PAC induction of premature chromosome condensation in the absence of cellular mitotic signals (i.e. during interphase), and 2) LSD2/n-PAC mediated impairment of chromosome decondensation at the exit of mitosis and cell division. To address these possibilities, we turned to live cell imaging. Live imaging allowed us to observe cotransfected cells during the cell cycle and monitor the chromatin condensation state before, during, and after cell division. U2OS cells were cotransfected with GFP-LSD2 and Fg-HA-nPAC and observed using time-lapse fluorescent microscopy in an enclosed environmental chamber (humidified and perfused with 5% CO2). We visualized the nuclei of transfected cells using the FITC channel to monitor GFP-LSD2. As early as 16 hours after transfection, many transfected cells displayed a prophase-like phenotype. Our live imaging experiments revealed a step-wise process of chromosome condensation in transfected cells in the absence of nuclear or cell division. We observed cells with an interphase LSD2/n-PAC staining pattern undergo a

progressive condensation; from diffuse nuclear LSD2 staining, to the characteristic LSD2/n-PAC punctate staining, to an increasingly dense prophase-like chromatin condensation (Figure 3-26A). The prophase-like condensed state persisted for many hours in the cotransfected cells, which contrasts with the typical prophase duration of only minutes (Figure 3-25B). In normally cycling U2OS cells, the entirety of mitosis occurs in 1-2 hours, whereas LSD2/n-PAC cotransfected cells maintained condensed chromatin and never underwent nuclear division. All of the cotransfected cells observed in our study underwent apparent nuclear compaction and cell death (as determined by DIC microscopic visualization) (Figure 3-25A). Consistent with our negative TUNEL staining in LSD2/n-PAC cells, the condensation observed by live cell imaging is uncharacteristic of the normally rapid apoptotic condensation. Additionally, our live imaging results indicate the LSD2/n-PAC associated condensation occurs in the absence of cell division, indicating an unlikelihood that the phenotype results from a dysfunction in chromosome decondensation after mitosis. These results suggest an LSD2/n-PAC induction of chromatin condensation independent of cell cycling. Based on the lack of mitotic markers and the absence of a requirement for cell division for the induction of the condensed chromatin phenotype in LSD2/n-PAC cells, we determined that the phenotype is induced during interphase of the cell cycle.

Interphase occupies approximately 90% of the cell cycle, while mitosis occupies the remainder of the cycle. Interphase consists of two Gap stages (G1 and G2), which border the S phase. S phase is characterized by replication of the genome in preparation for nuclear division. To further characterize the chromatin and cell cycle stage of LSD2/n-PAC condensed cells, we used immunostaining to determine if the “prophase-like” cells had undergone DNA replication. Using an antibody that stains very specifically for the centromere specific histone variant,

CENP-A, we were able to determine if the centromeres of condensed chromosomes had been replicated. DNA replication that results in the generation of sister chromosomes is readily observable, because duplication of the centromere results in CENP-A staining as doublets, whereas unreplicated centromeres stain for CENP-A as single foci. Because centromere replication occurs late in S phase, after the majority of the genome has been duplicated, CENP-A staining allowed us to determine if the cell had completed S phase and, therefore, if genome replication had been completed (58). The CENP-A staining pattern in prophase-like condensed LSD2/n-PAC cells was strikingly different from untransfected prophase condensed cells (3-26A). We observed very few condensed cotransfected cells displaying CENPA doublets, whereas every untransfected cell with a prophase DAPI pattern had CENP-A doublets (Figure 3-26 B). Our analysis showed very clearly that replication of centromeres had not occurred in cotransfected cells despite similar chromosome condensation patterns to untransfected prophase cells.

LSD2 Specific Function is Required to Induce "Prophase-Like" Chromosome Condensation

We only observed the "prophase-like" condensed chromatin phenotype when LSD2 and n-PAC were cotransfected. However, we were still uncertain of the role of each protein in the induction of the phenotype. To address the requirement for LSD2 demethylase activity to induce condensation, we utilized the LSD2 mutants previously described. The LSD2-M1 and LSD2-M2 demethylation inactive mutants cotransfected with n-PAC did not display the condensed phenotype as observed with wild-type LSD2 and n-PAC. This indicated a requirement for LSD2 specific enzymatic activity for the induction of chromosome condensation, and points to a role for K4 H3 demethylation in the process. Another interesting observation with the LSD2 mutant cotransfections was the loss of interaction between LSD2-M1 and n-PAC. LSD2-M1 appeared

unable to interact with n-PAC, and failed to adopt the punctate pattern characteristic of the LSD2/n-PAC interaction. The interaction between n-PAC and LSD2-M2 appeared unaffected.

Based on the LSD2 mutant's inability to induce the condensation phenotype, we proposed a role for global mono- and di-methyl K4 H3 demethylation in the condensation process. We wondered if we could induce a similar phenotype by overexpressing n-PAC in the context of LSD2 independent global mono- and/or di-methyl K4 H3 demethylation.

A family of Jumonji C-domain containing proteins (including SMCX, SMCY, and PLU-1) was recently identified as lysine 4 H3 histone demethylases (43). SMCX was shown to specifically demethylate di- and tri-methyl K4H3, but not monomethyl K4 H3 (103). PLU-1 catalyzes the demethylation of mono-, di-, and trimethyl K4H3 (43).

We transfected either human GFP-SMCX or mouse HA-tagged PLU-1 into U2OS cells to confirm their *in vivo* demethylase activity and their residue and modification specificity. Indeed, SMCX and PLU-1 displayed global demethylation towards Lys 4 H3 with the expected specificities (data not shown). N-PAC was then cotransfected with either SMCX or PLU-1. Cells were immunostained and analyzed for the localization patterns of the cotransfected proteins, histone methylation status, and the chromatin condensation state of cotransfected cells.

SMCX and n-PAC had no observable interaction with one another. In cotransfected cells, n-PAC retained its characteristic punctate nuclear staining, while SMCX displayed a diffuse nuclear pattern (as observed in cells transfected with SMCX alone). Neither SMCX nor PLU-1 cotransfected with n-PAC induced a "prophase-like" condensation phenotype. Thus, a "non-specific", global demethylation of Lys 4 combined with n-PAC is insufficient to induce the phenotype observed with LSD2 and n-PAC. There are numerous possible explanations for this

result, however, these data clearly implicate LSD2 specific catalytic activity and its n-PAC interactions in the induction of chromosome condensation.

LSD2 Interactions With SMC proteins

In light of the condensation phenotype observed for LSD2/n-PAC transfected cells, we turned to a potential role for several LSD2 interacting proteins identified in our mass spec analysis of TAP LSD2. The SMC (structural maintenance of chromosomes) proteins are members of a well-conserved family of chromosomal ATPases. SMC2 and SMC4 are the core subunits of the condensin complex, while SMC1 and SMC3 form the core of the cohesin complex, which are involved in chromosome condensation and sister chromatid cohesion, respectively. According to our mass spec data, SMC1, 2, 3, and 4 interact with LSD2 (Table 3-1). The mass spec results were supported by immuoblotting our LSD2 TAP samples for SMC1 and SMC2 (data not shown). We were also able to pull down SMC2 by n-PAC immunoprecipitation, although we were unable to do so with SMC1 (Figure 3-15).

Based on these data, we proposed that the induction of chromatin condensation by LSD2/n-PAC could be the result of the association of LSD2 and n-PAC with SMC2/SMC4 and the condensin complex. We immunostained LSD2/n-PAC transfected cells, but were unable to observe any changes in the amount or localization of SMC2 in either condensed or non-condensed cotransfected cells (not shown).

We also prepared metaphase chromosome spreads of HeLa pOZ-n-PAC cells stained for n-PAC and SMC2. SMC2 displayed a uniform staining pattern along the length of each chromosome. Despite our Co-IP results showing an interaction between n-PAC and SMC2, we saw no clear association between SMC2 and n-PAC in metaphase chromosomes. Furthermore, chromosome regions specifically enriched for n-PAC showed no enrichment for SMC2.

From these experiments, we were unable to draw any clear association between LSD2/n-PAC and the induction of chromosome condensation by SMC2 and the condensin complex.

LSD2 Knockdown Induces Precocious Sister Chromatid Separation

We next turned to RNA knockdown as a means to investigate the biological function of LSD2 and to investigate a potential role in chromosome condensation. We used a pMSCV construct containing a short hairpin sequence targeting *Aof1* mRNA to knockdown LSD2. Using this construct, we were able to effectively knockdown ~80% of *Aof1* mRNA in HeLa cells, as shown by real-time RT-PCR (Figure 3-27A). Because we suspected a role for LSD2 in chromosome condensation, we generated metaphase condensed chromosome spreads using the LSD2 knockdown cells. Comparisons of chromosome spreads between control HeLa and LSD2 knockdowns revealed a striking phenotype. The chromosome spreads of the LSD2 knockdown cells showed pairs of sister chromatids already separated at their centromeres, whereas wild-type chromosomes maintained their metaphase attachment (Figure 3-27B).

During S-phase genomic replication, duplicated sister chromosomes are held together by the SMC1/SMC3 containing cohesin complex. The cohesin complex maintains sister chromosome attachment along the length of the chromosomes from replication through prophase of mitosis. During prophase, cohesin attachment along the arms of sister chromatids is lost. However, pericentric heterochromatin cohesin persists in order to maintain sister chromatid cohesion until anaphase initiation. At anaphase, cohesin complexes at the centromeres disassemble and sister chromatids are segregated into daughter cells (38). The maintenance of centromere cohesion until anaphase induction is critical for cell passage through anaphase checkpoints and for the equal segregation of chromosomes to daughter cells (34, 63, 65, 96). Our metaphase spreads with LSD2 knockdown cells clearly showed precocious sister chromatid separation, indicative of a disruption in the centromere and pericentric heterochromatin cohesion.

Precocious Sister Chromatid Separation Implicates LSD2 in Centromere Cohesion

The striking phenotype of our LSD2 knockdown cells led us to once again revisit our proteomic analysis of TAP LSD2. The identification of SMC1 and SMC3 in our mass spec analysis, coupled with premature sister chromatid segregation induced by LSD2 knockdown, pointed towards a role for LSD2 in centromere cohesion. More importantly, it led us to look at the centromere/pericentromere as a possible unifying feature of our seemingly disparate results, including the condensation phenotype, precocious segregation phenotype, and the proteins that we identified in association with LSD2 and n-PAC (i.e. condensins, cohesins, histone modifying proteins, etc). The maintenance of pericentric heterochromatin (and its characteristic epigenetic profile) is essential to the function of the cohesin complex during mitosis and is also associated with the initiation of chromosome condensation at the outset of mitosis (REFERNCE)

To examine a possible role for LSD2 in centromere function, we used NIH 3T3 mouse fibroblasts. Mouse cells have clusters of pericentric heterochromatin formed from different chromosomes, called chromocenters, which stain very prominently with DAPI and allow easy visualization of pericentric regions within the nucleus. It has been shown that in these chromocenters, the DAPI dense region corresponds to pericentric heterochromatin, which is encircled by the centromeres of the contributing chromosomes (REFERENCE). We began by tranfecting GFP-LSD2 into 3T3s and observed a diffuse nuclear localization, similar to that seen in previously examined cell lines (Figure 3-28A). Transfected n-PAC also displayed its characteristic punctate nuclear staining (Figure 3-28A). Neither LSD2 nor n-PAC localized to the DAPI dense regions of pericentric heterochromatin. Surprisingly, though, when LSD2 and n-PAC were cotransfected, there was a striking change in their localization in many of the cotransfected 3T3s. In approximately 10-25% of the LSD2/n-PAC cotransfected cells, LSD2 and n-PAC colocalized to pericentric heterochromatin (as determined by DAPI identification of

chomocenters) and were vastly enriched in those regions (Figure 3-28A & B). This result was never observed with either LSD2 or n-PAC alone. Additionally, we immunostained transfected 3T3s for HP1α, which is typically enriched at pericentomeric heterochromatin (Figure 3-29). Cells cotransfected with LSD2/n-PAC compared to untransfected cells had a noticeable decrease in overall HP1α staining, despite the fact that the DAPI staining of their heterochromatin appeared unaffected (Figure 3-30). In many of the cotransfected cells, there remained HP1α enrichment at heterochromatin, but the overall intensity of HP1α in these regions and throughout the cell was weakened. In other cotransfected cells, HP1α enrichment at heterochromatin appeared disrupted. We observed a normal amount of cell to cell variation in the overall intensity of HP1α staining in 3T3s, with many untransfected cells showing similarly weak staining to the LSD2/n-PAC cotransfectants. However, there was clearly a propensity for cotransfected cells to have stain at the low end of the spectrum for HP1α intensity.

Using NIS-Software, we calculated the mean staining intensity of HP1α immunostaining between groups of LSD2/n-PAC transfected and untransfected NIH3T3s. Using this method, we determined the overall HP1α staining to be reduced by 33% in LSD2/n-PAC cells ($p=0.001$), confirming a disruption of HP1α in LSD2/n-PAC transfectants, and further supporting a relationship between LSD2/n-PAC and heterochromatin (Table 3-2).

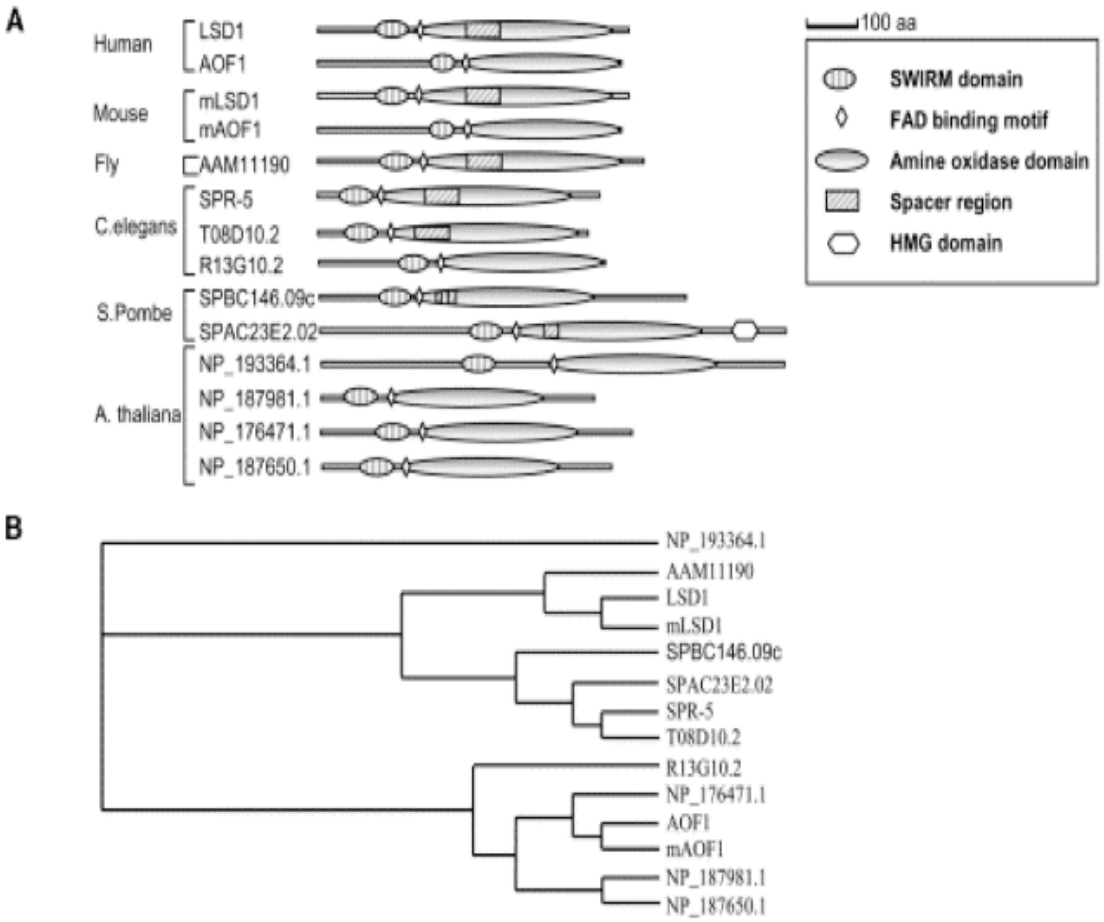

Figure 3-1. Nuclear amine oxidase family of enzymes. A) Nuclear amine oxidases are conserved from arabidopsis to human. Mammals contain 2 nuclear amine oxidase homologs, LSD1 and LSD2. All members of the family contain the SWIRM domain, and the amine oxidase domain with an FAD binding motif. B) Nuclear amine oxidase subfamily arrangement based on ClustalW-alignment of the amine oxidase domains. Two subfamilies, consisting of LSD1 homologs and LSD2 homologs differ primarily in the presence (LSD1 subfamily) or absence (LSD2 subfamily) of a spacer region in the amine oxidase domains. (YJ Shi et al)

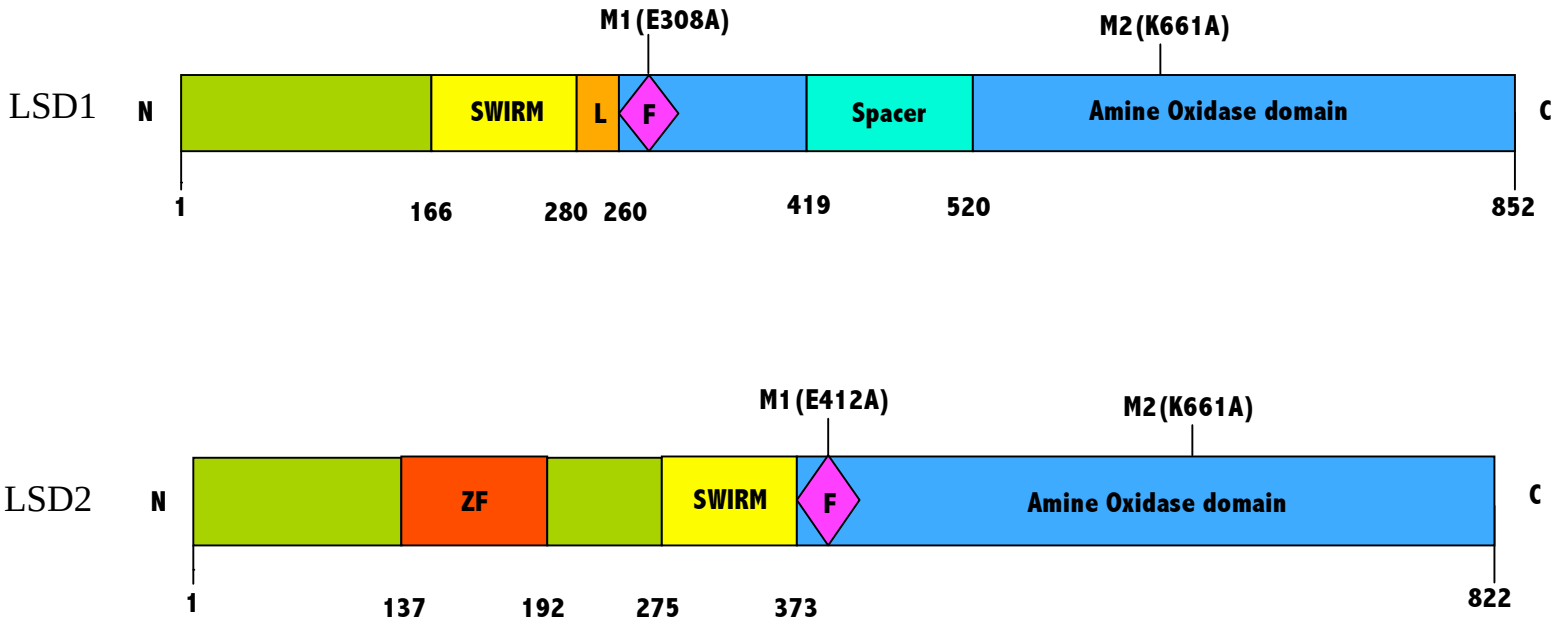

Figure 3-2. LSD1 and LSD2 domain comparison. Both LSD1 and LSD2 contain: an amine oxidase domain, which catalyzes the demethylation reaction; a conserved FAD-binding domain (F) binds the essential cofactor; and the SWIRM domain, a protein-protein interaction domain with a role in chromatin association. Only LSD1 contains the "spacer domain" within the amine oxidase domain. The spacer is involved in allosteric regulation of LSD1. LSD2 contains an N-terminal zinc-finger motif. M1 (Mutant 1) is a point mutation within the FAD-binding domain, converting a conserved glutamate to alanine, and abrogating FAD binding. M2 (Mutant 2) is a catalytic inactive point mutation in the amine oxidase domain. (M. Rutenberg)

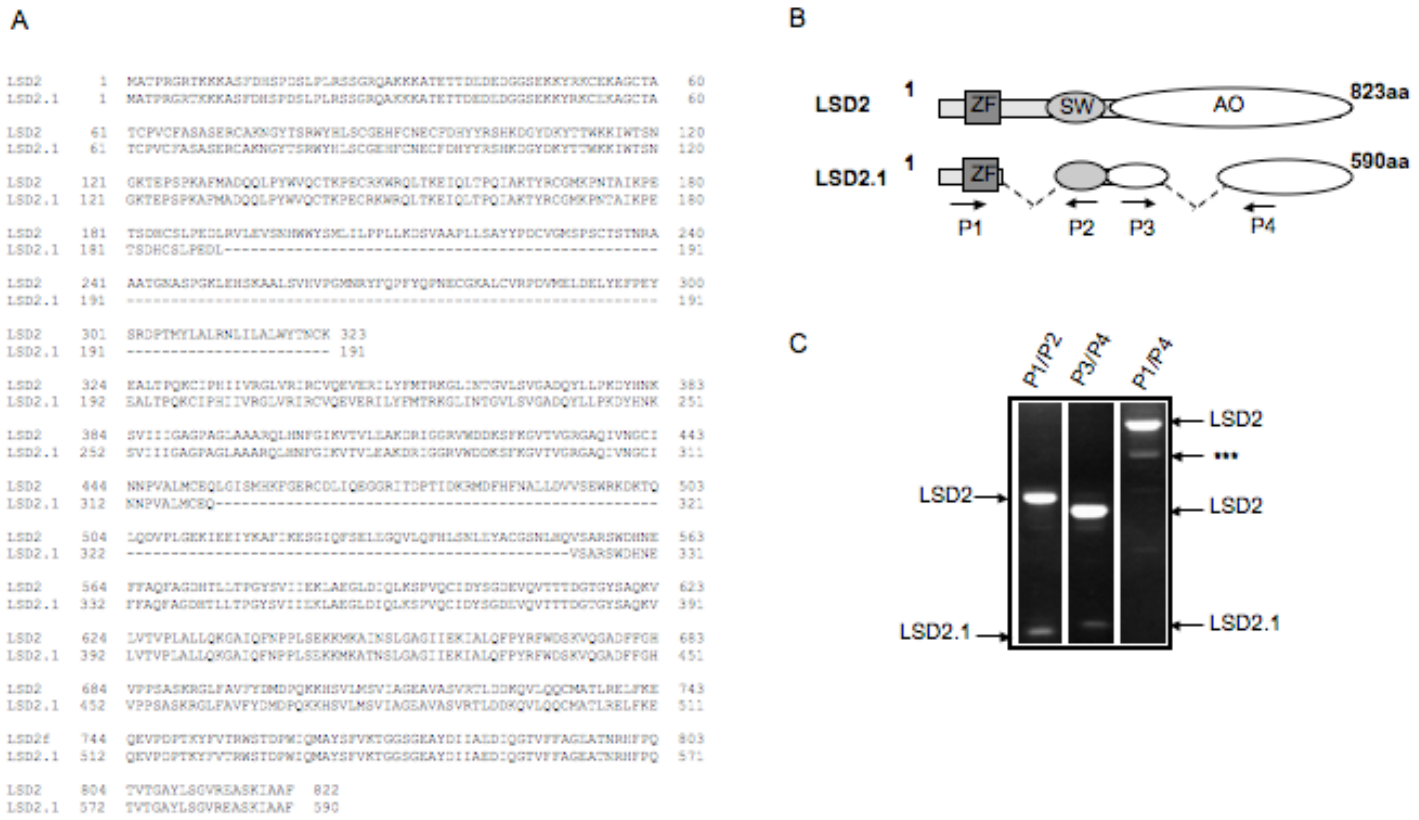

Figure 3-3. Full length LSD2 and splice variant LSD2.1 sequence and domain comparisons. Full length LSD2 was subcloned from a HeLa cDNA library and sequenced. LSD2.1 was identified in an EST library. A) Amino acid alignment of full length LSD2 and LSD2.1. B) Domain comparison of LSD2 and LSD2.1. LSD2.1 has deletions in the SWIRM domain and the amine oxidase domain. PCR primers used to distinguish between transcripts of LSD2 and LSD2.1 are denoted as P1, P2, P3, and P4. C) RT-PCR using primers flanking the deletion sites of LSD2.1, shows the amplification of both full length LSD2 and splice variant LSD2.1. Expected amplicon sizes are as follows: P1/P2: LSD2- 530bp, LSD2.1- 127bp; P2/P3: LSD2- 430bp, LSD2.1- 130bp. P1/P4: only amplifies LSD2- 1,240bp. *** non-specific band. (M. Rutenberg)

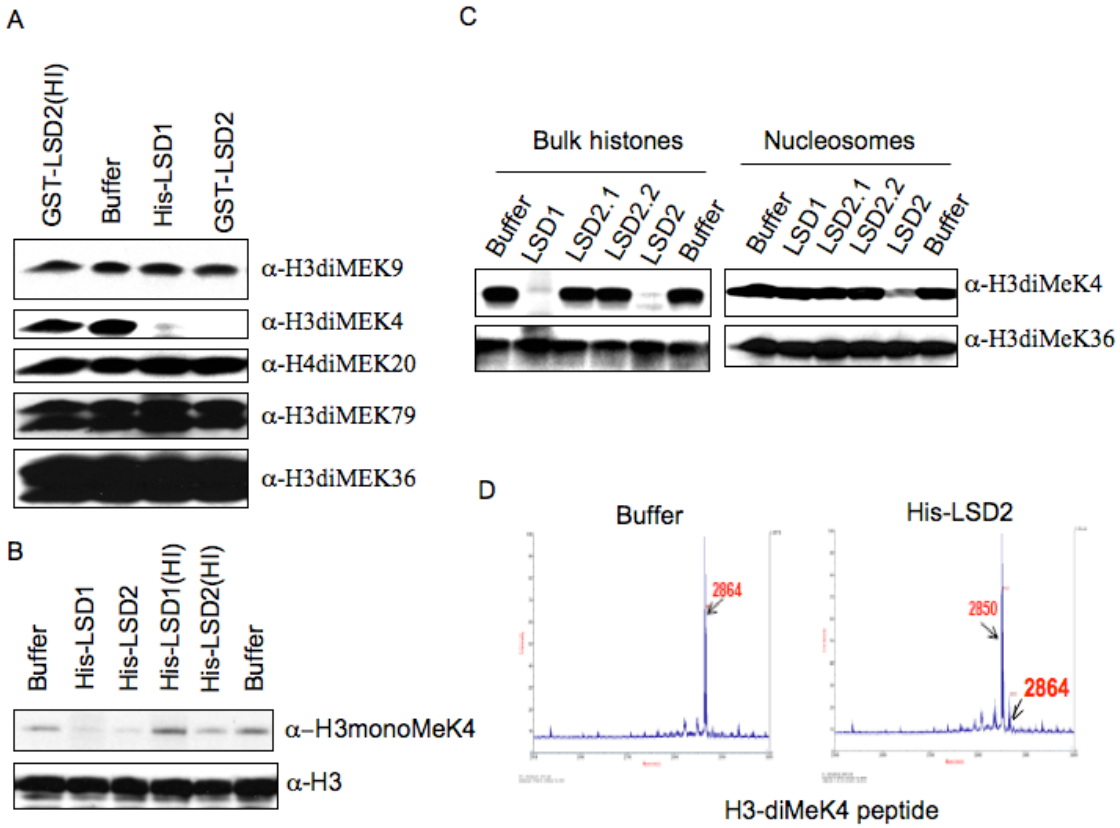

Figure 3-4. LSD2 demethylates mono- and di-methyl lysine 4 H3 *in vitro*. *In vitro* demethylase assays included recombinant enzymes, histone substrates, FAD+, Fomaldehyde Dehydrogenase, and ATP. A) Bulk histones used as substrate. LSD1 and LSD2 demethylation is specific for dimethyl lysine 4 H3, reducing the diMeK4H3 signal in those reactions. Heat inactivated enzyme (HI) and buffer alone shows no demethylation. B) LSD1 and LSD2 also demethylate monomethyl Lysine 4 H3 from bulk histones. C) Bulk histones (left column) or nucleosomes (right column) were incubated in demethylase buffer with recombinant enzymes and immunoblotted for methylation specfic residues. Recombinant LSD1 and LSD2 are both specific for demethylation of dimethyl K4 H3 on bulk histones. Only recombinant LSD2 is able to demethylate nucleosomal substrates. LSD1 requires protein cofactors for demethylating nucleosomes. D) Mass spec analysis of in vitro demethylation on dimethyl K4 H3 peptide substrates. Demethylase reactions with buffer only retain the molecular mass of the original H3 peptide (2864 daltons); while reactions with recombinant LSD2 have a shift in the mass peak of 16 daltons, equivalent to the loss of a single methyl group from the peptide. (YJ Shi, R. Fang, T. Leonor, and M. Rutenberg)

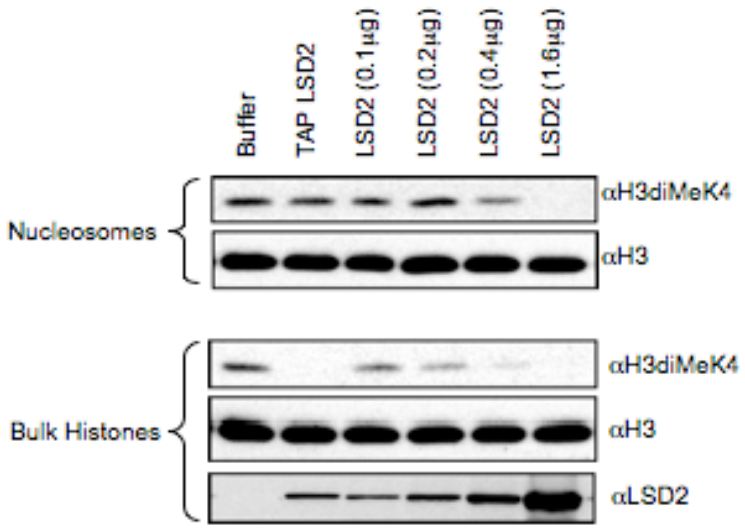

Figure 3-5. Dose dependent H3K4 demethylation by LSD2. In vitro demethylase assays using increasing levels of LSD2 shows a dose-dependent loss of H3diMeK4 signal on nucleosomes (top) and bulk histones (bottom). The same amount of TAP-LSD2 product has significantly more demethylase activity on bulk histones (lane 2, bottom) than nucleosomes (lane 2, top). (R. Fang)

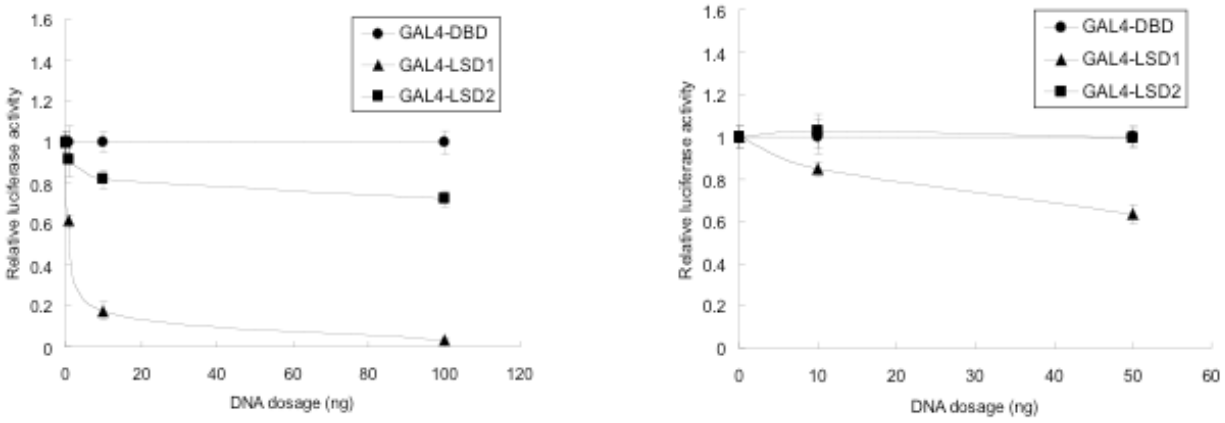

Figure 3-6. LSD1 and LSD2 luciferase assay for transcriptional activity. (left) Transiently tansfected TK promoter-luciferase construct with increasing amounts of Gal4-LSD1, Gal4-LSD2, or Gal4-DBD in U2OS cells. Relative luciferase activity was determined for each. LSD2 has very weak corepressor activity in comparison to LSD1. (right) HEK 293 cells stably transfected with TK-luciferase and transiently transfectedwith increasing amounts of Gal4-LSD1, Gal4-LSD2, or Gal4-DBD. Results are similar to A. Each transfection was done in duplicate. (F. Shimizu and M. Rutenberg)

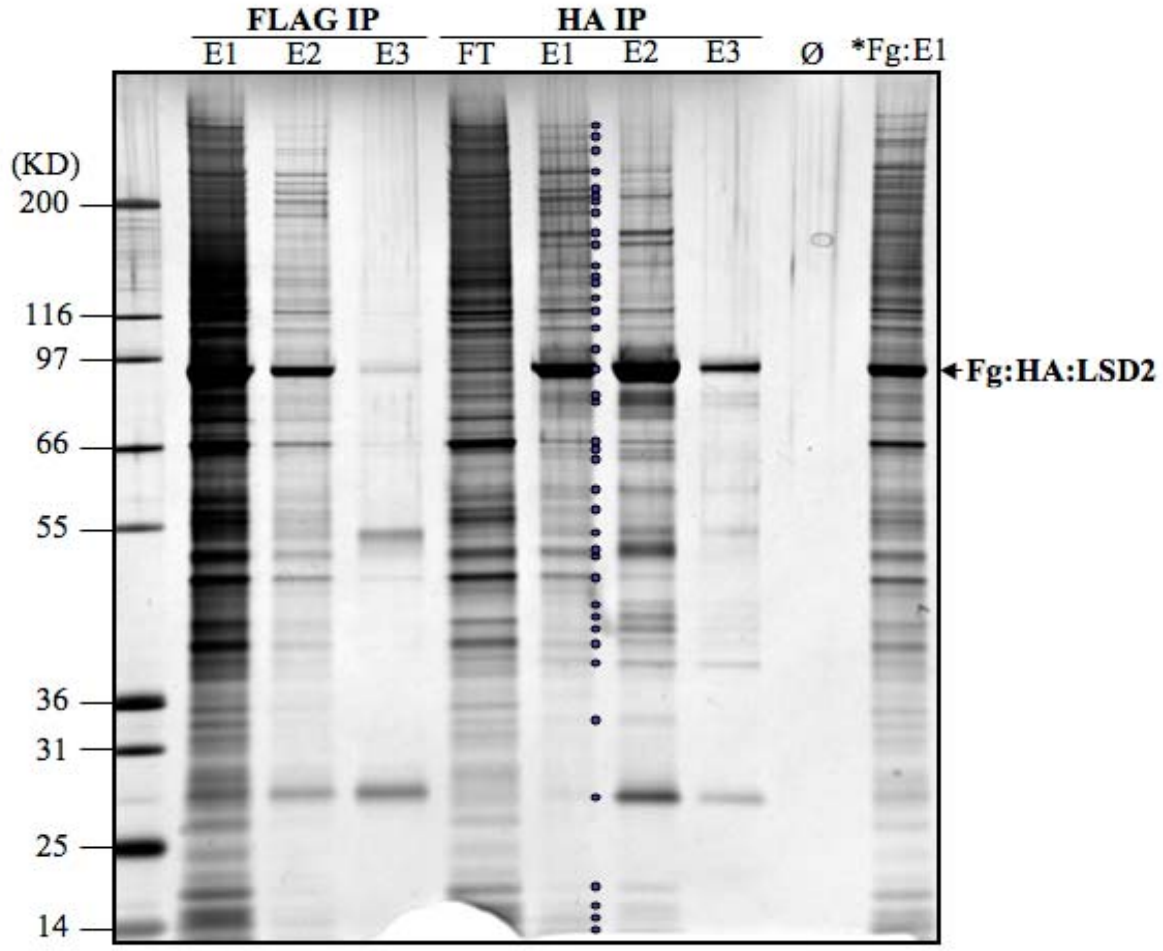

Figure 3-7. LSD2 tandem affinity purification products. 10ul of each elution fraction was separated on a 4-12% Nu-PAGE acrylamide gel and silver stained. A similar gel was loaded with larger amounts of HA-E1 and HA-E2 and stained with coommassie blue. Protein bands (represented by dots) were excised and submitted for tandem MS/MS analysis. The major band in each lane corresponds to the affinity purified Fg:HA-LSD2. *7.5ul instead of 10ul were loaded. (M. Rutenberg)

Mass Spec Results for LSD2 Tandem Affinity Purification	
Protein	**Peptides**
DNA Repair	
DNA-PKcs	>60
TRRAP	7
Topolla	16
RIF1	>40
MSH2	17
RAD50	13
MSH6	15
PARP1	11
Chromatin Remodeling	
BAP1	16
HCFC1	>60
TIP49A	13
TIP49B	20
Nuclear Matrix/Spindle	
SMC1	22
SMC2	15
SMC3	25
SMC4	11
GCN1L1	>100
RANBP2	22
MATR3	18
SA2	5
NUMA1	>60
Chromatin Modifying	
WHSC1L1 (NSD3)	
EHMT1	5
EHMT2	6
RBBP5	11
SMCA5	13
Snf2h	
Chromatin Associated	
n-PAC	
WDR5	5
histone H2A	3
histone H2B	7

Table 3-1. LSD2 affinity purification tandem mass spectrometry results. An incomplete list of the proteins identified in association with TAP LSD2 arranged into functional groups. (YJ Shi and M. Rutenberg)

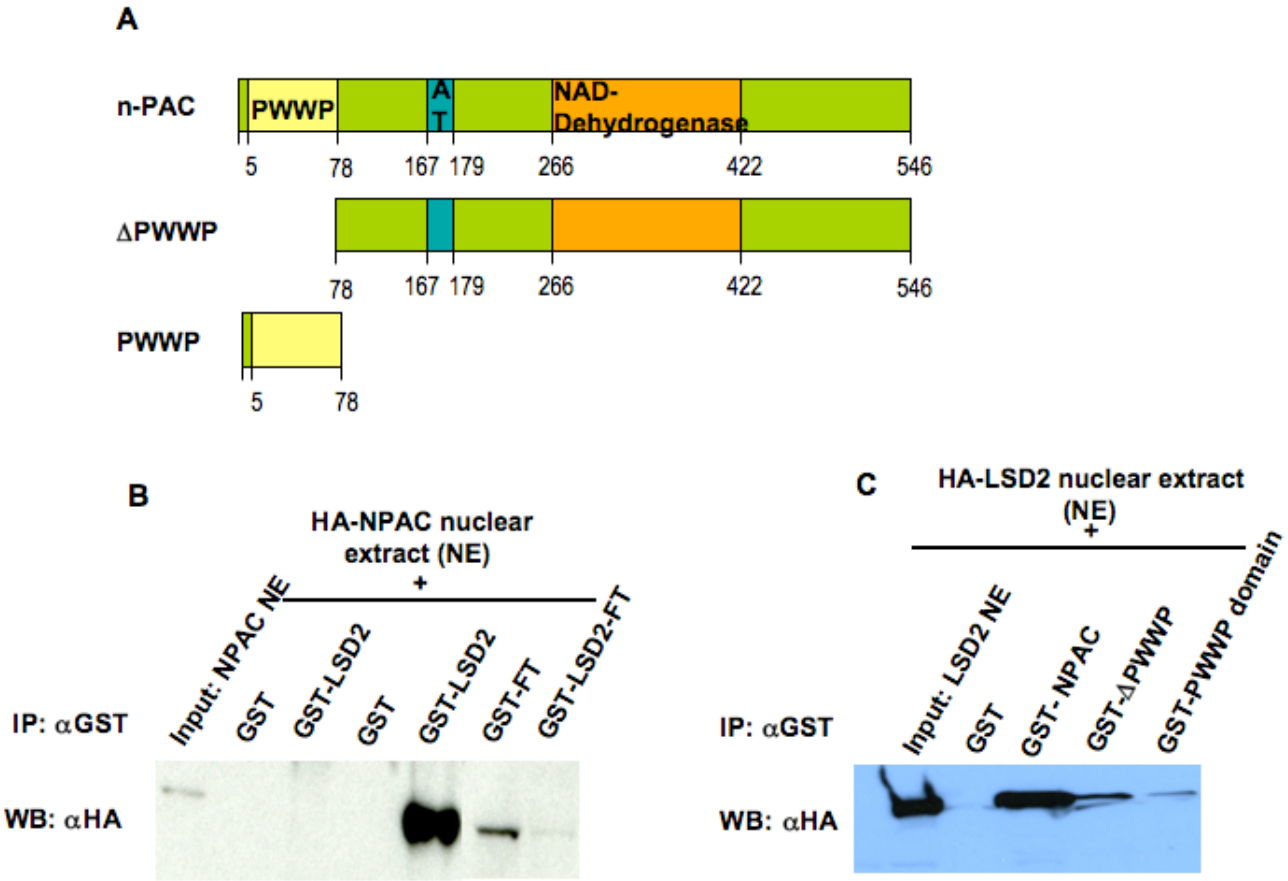

Figure 3-8. N-PAC domain structure and LSD2 interaction. A) Full length n-PAC contains an N-terminal PWWP domain, an AT hook zinc-finger (AT), and a carboxy-terminal NAD binding dehydrogenase domain. B) GST pulldown using nuclear extract from HA-n-PAC expressing HeLa cells incubated with GST-LSD2 or GST alone. GST-LSD2 pulls n-PAC, whereas GST does not. GST-LSD2 flow through (FT)) is depleted of npac compared to GST alone flow though (GST-FT). C) GST pulldown using nuclear extract from HA-LSD2 expressing HeLa cells incubated with full length GST-n-PAC. GST -n-PAC co-immunoprecipitates with HA-LSD2, while GST alone does not. (A- M. Rutenberg; B & C- P Mei)

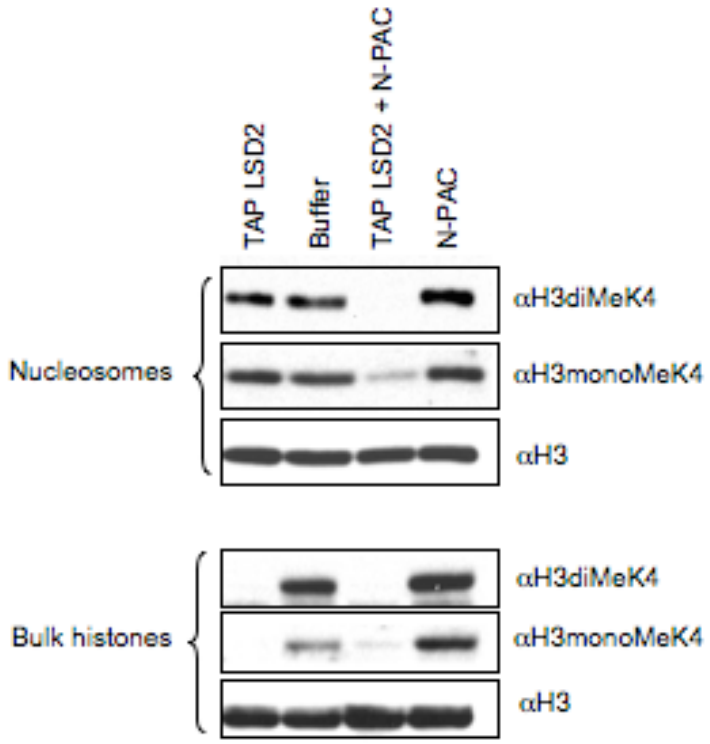

Figure 3-9. TAP LSD2 demethylates mono- and di-methyl K4 H3. Tandem affinity purified LSD2 was incubated in an *in vitro* demethylase assay with nucleosome substrates (top) or bulk histones (bottom) and immunoblotted for mono- and di-methyl K4 H3. Recombinant LSD2 strongly demethylates di-K4H3 on bulk histones and nucleosomes (lane 3, top and bottom). Despite using the same amount of TAP-LSD2 in every reaction, there is less demethylase activity on nucleosomes compared to bulk histones, (lane 1, top and bottom). TAP LSD2 demethylates bulk histones on mono- and di-K4H3, but the same amount of enzyme has much weaker activity on nucleosomes. The addition of recombinant n-PAC to TAP LSD2 vastly increases mono- and di-methyl K4H3 demethylase efficiency on nucleosomes (compare lanes 1 and 3, top). N-PAC alone has no intrinsic demethylase acitivity (lane 4). (R. Fang)

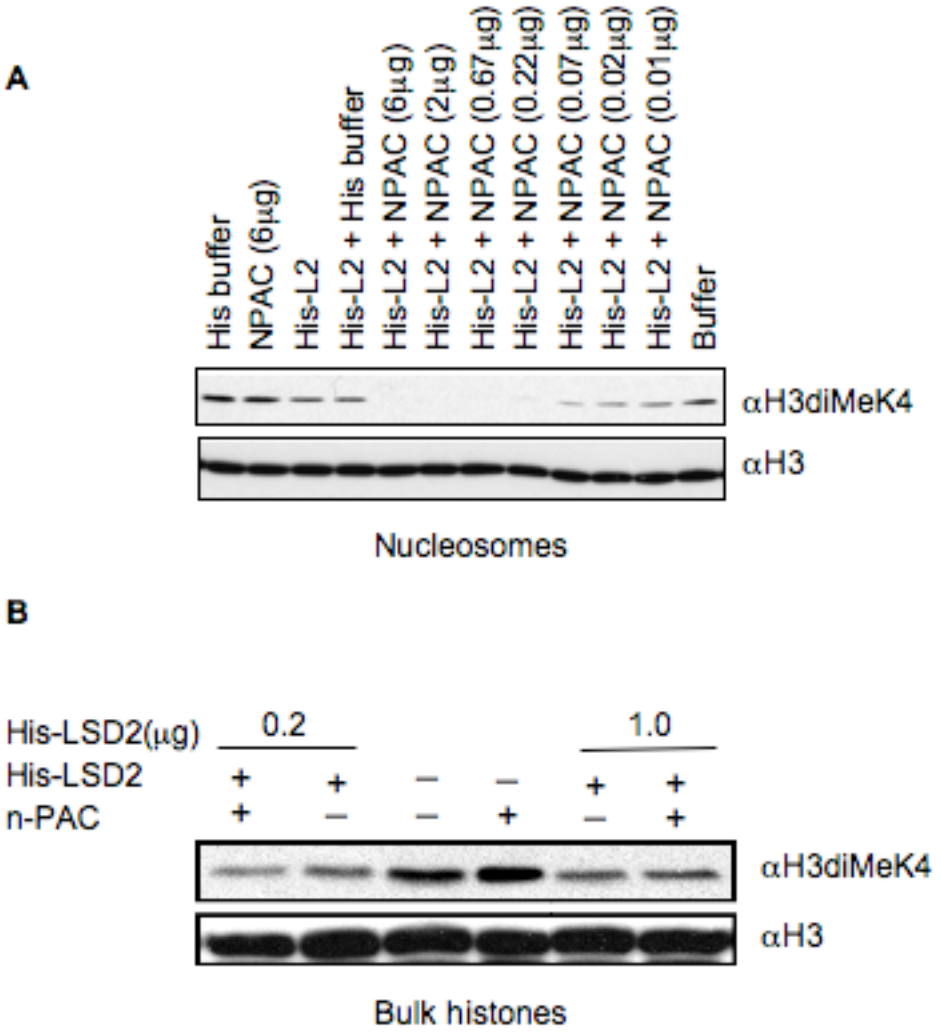

Figure 3-10. n-PAC enhances LSD2 demethylation of nucleosomes, but not bulk histones *in vitro*. A) *In vitro* demethylase assays using Recombinant His-LSD2 (His-L2) with or without recombinant n-PAC on nucleosomal substrates. With constant amounts of LSD2, demethylation of dimethyl K4 H3 increases with increasing amounts of n-PAC. N-PAC alone shows no demethylation activity. B) *In vitro* demethylase assays using Recombinant His-LSD2 with or without recombinant n-PAC on bulk histone substrates. Unlike with nucleosomal substrates, addition of n-PAC shows no enhancement of LSD2 demethylase activity on bulk histones. Total histone H3 was used as a loading control. (R. Fang)

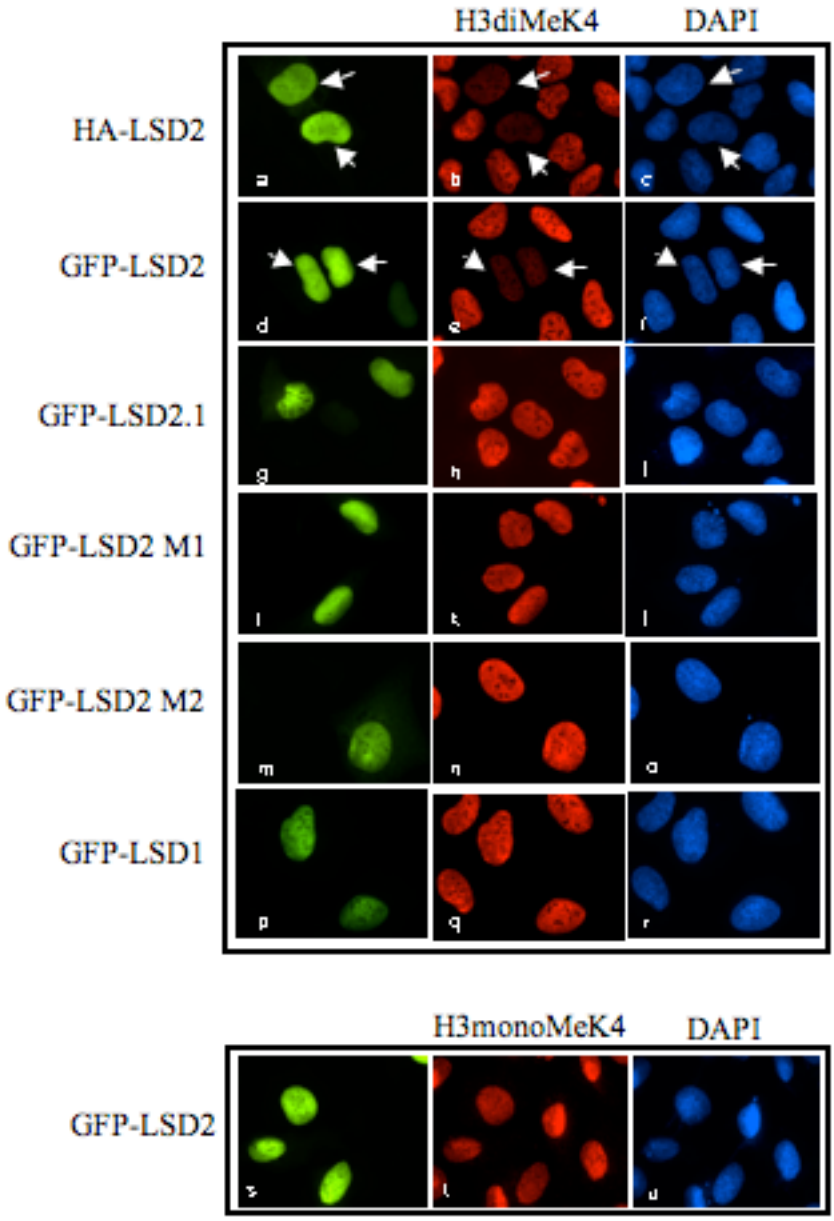

Figure 3-11. LSD2 nuclear localization and dimethyl K4 H3 demethylation activity *in vivo*. HA-LSD2 (a-c) and GFP-LSD2 (d-f) transfected into U2OS cells shows a global reduction in staining for dimethyl lys 4 H3 specific antibodies. Truncated splice variant LSD2.1 (g-i); FAD-binding mutant LSD2-M1 (j-l); and active site mutant LSD2-M2 (m-o) shows no diMeK4H3 demethylase activity. GFP-LSD1 (p-r) has no global demethylase activity in U2OS cells. GFP-LSD2 shows only weak demethylase activity in high expressing cells (s-u). (M. Rutenberg)

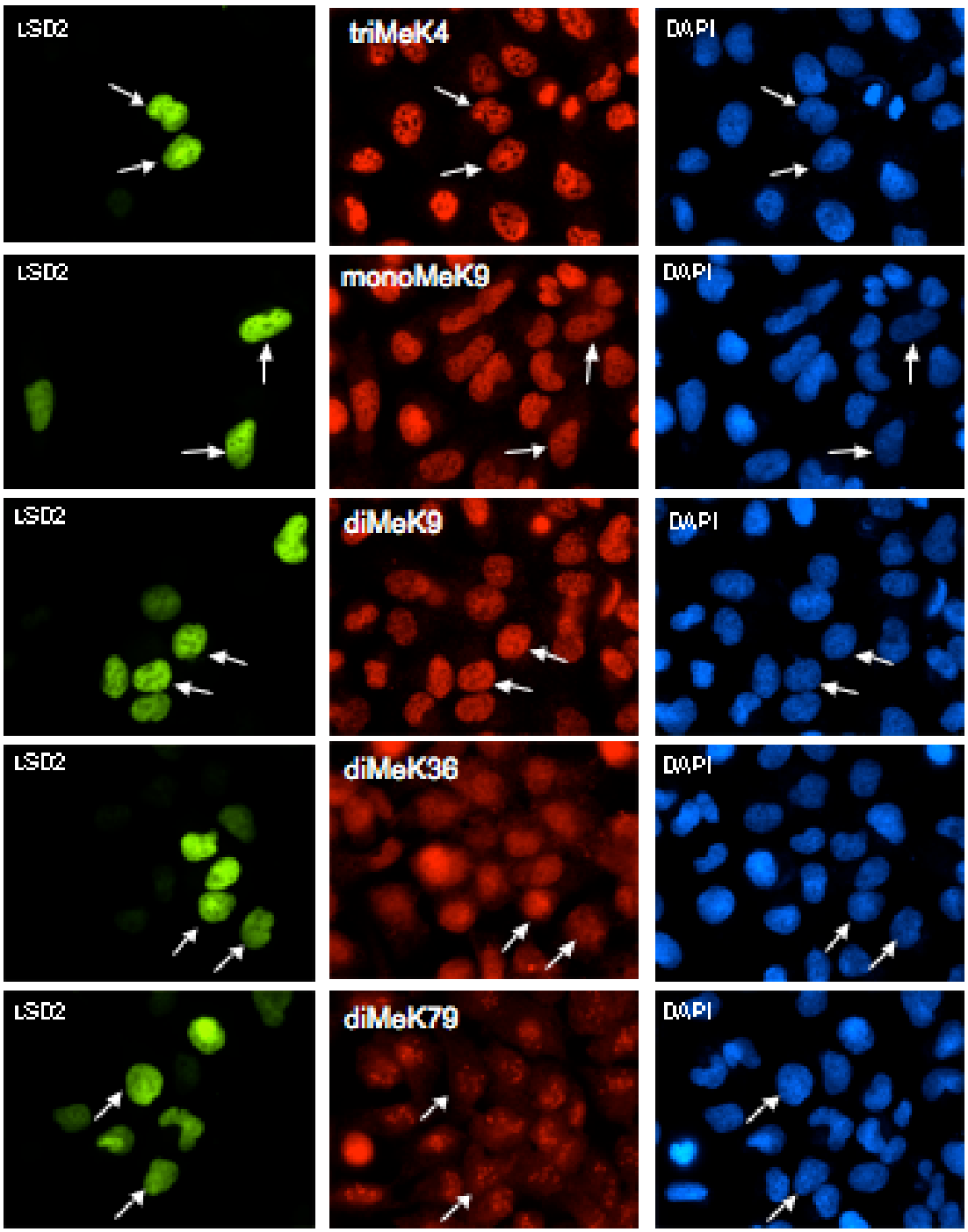

Figure 3-12. LSD2 is specific for lysine 4 H3 demethylation. Gfp-LSD2 transfected into U2OS cells and stained using antibodies specific for various histone modifications on H3. None of the modifications shown here were affected by LSD2 overexpresion. (M. Rutenberg)

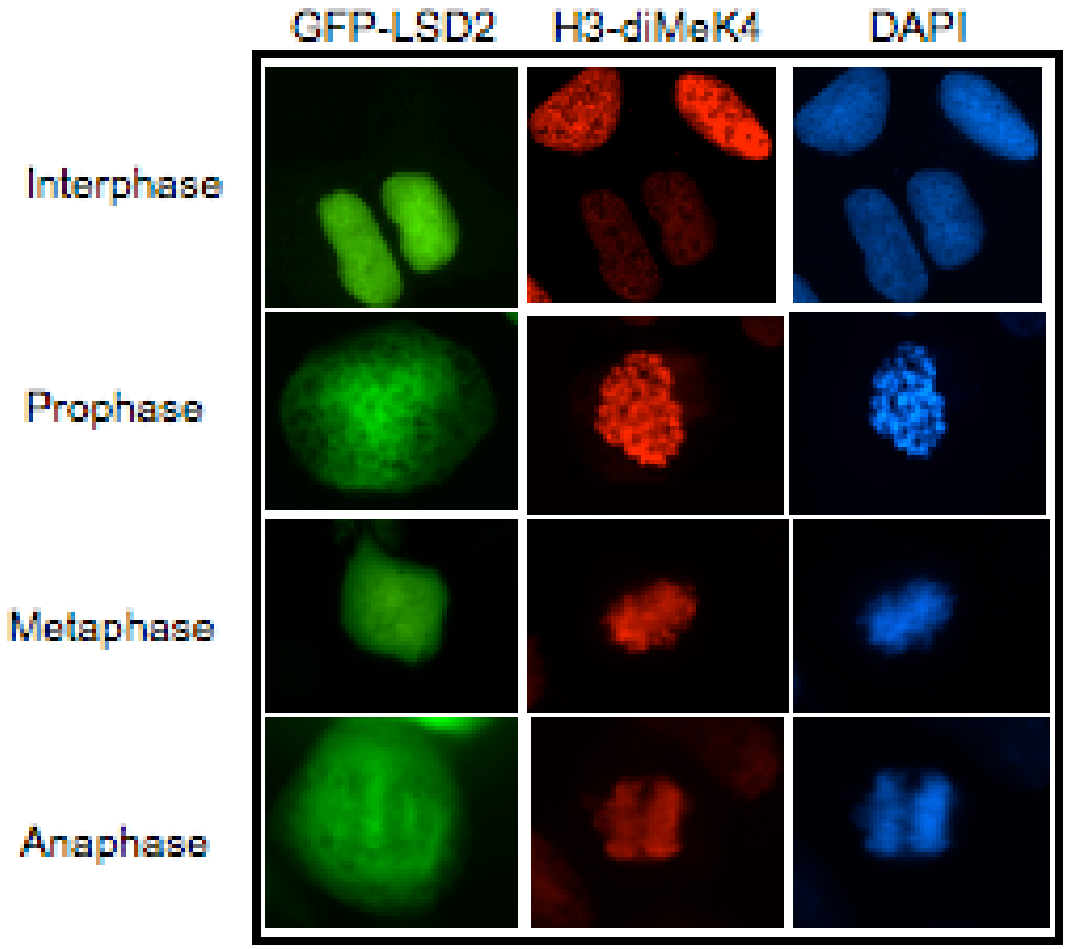

Figure 3-13. LSD2 is inactive on mitotic chromatin. GFP-LSD2 transfected cells at various stages of the cell cycle. LSD2 is diffuse throughout the nucleus in interphase cells and shows a reduction in H3diMeK4 staining. During all stages of mitosis (telophase not shown), LSD2 is excluded from regions of condensed chromatin and has no visible H3diMeK4 demethylase activity. (M. Rutenberg)

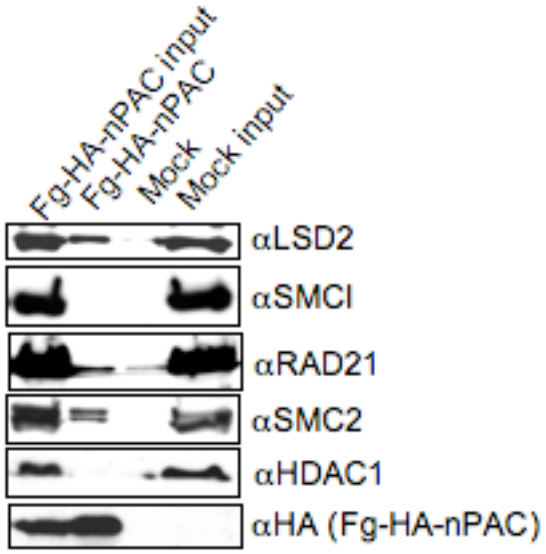

Figure 3-14. Fg-HA-nPAC reciprocal immunoprecipitation. HA-beads were used to immunoprecipitate tagged n-PAC, followed by immunoblotting for LSD2, SMC1 (cohesin complex), Rad21(cohesin), SMC2 (condensin), and HDAC1. LSD2, Rad21, SMC2 were all enriched by n-PAC immunoprecipitation. (R. Fang)

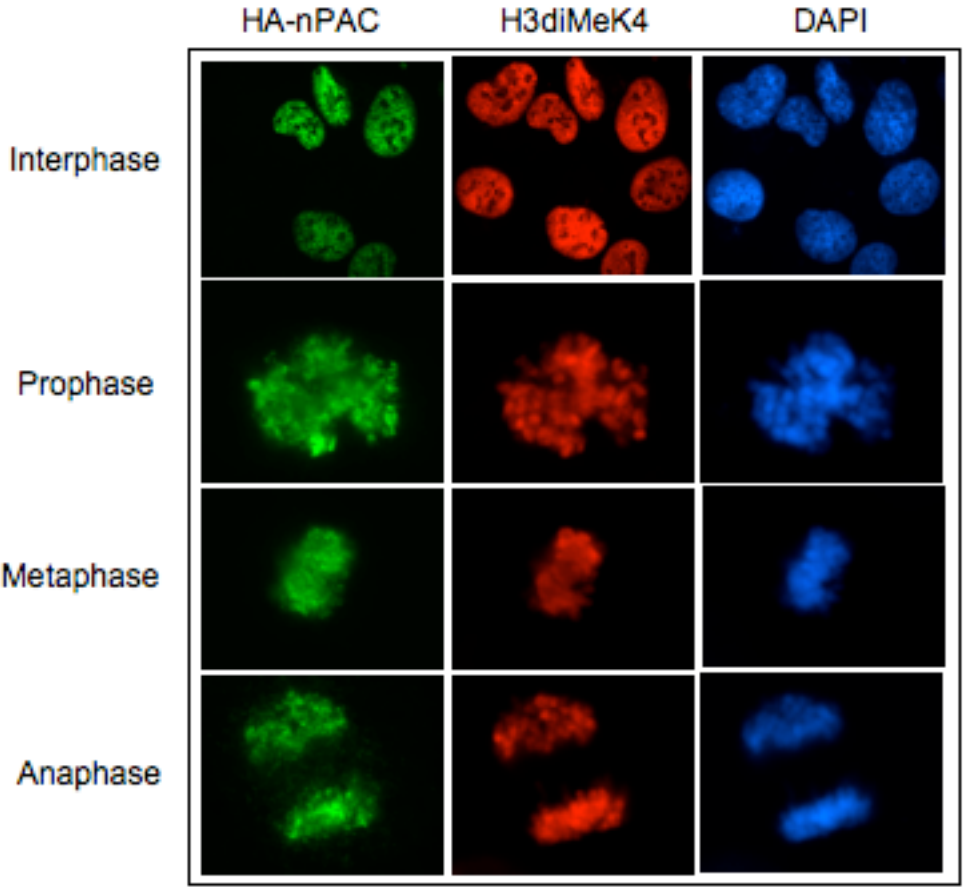

Figure 3-15. n-PAC nuclear localization and chromatin staining pattern. U2OS cells transfected with Fg-HA-nPAC and immunostained with α-HA and α-dimethylK4 H3 antibodies. N-PAC in staining during interphase is punctate throughout the nucleus. During all stages of mitosis (telophase not shown), n-PAC closely associates with the chromatin, visualized here by H3diMeK4 and DAPI staining. N-PAC transfected has no effect on the H3diMek4 signal. (M. Rutenberg)

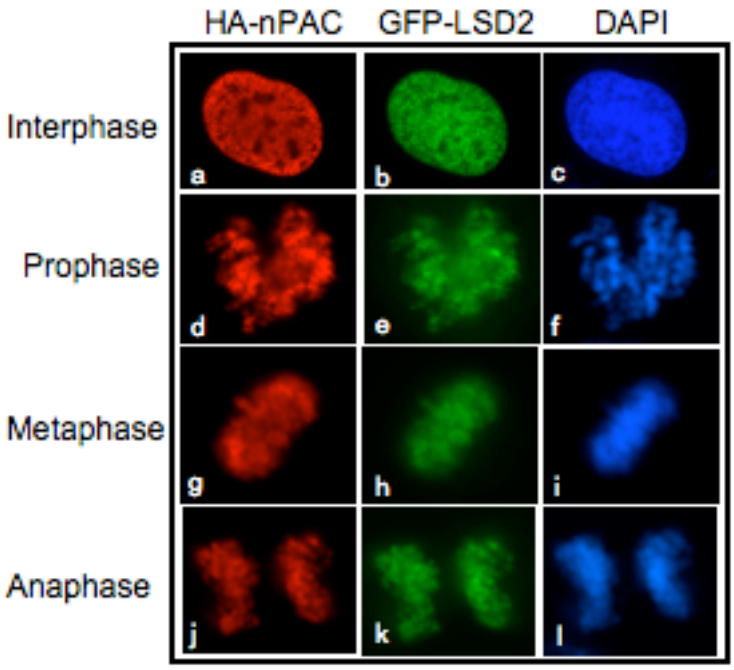

Figure 3-16. LSD2 undergoes a localization change in the presence of n-PAC. Gfp-LSD2 cotransfected with Fg-HA-nPAC in U2OS cells. LSD2 adopts the n-PAC punctate nuclear staining pattern in interphase cells (a-c). In the presence of n-PAC, LSD2 associates with mitotic chromatin and completely overlaps n-PAC staining (d-l). This contrasts with the lack of mitotic chromatin association of LSD2 transfected alone (see figure 3-14). (M. Rutenberg)

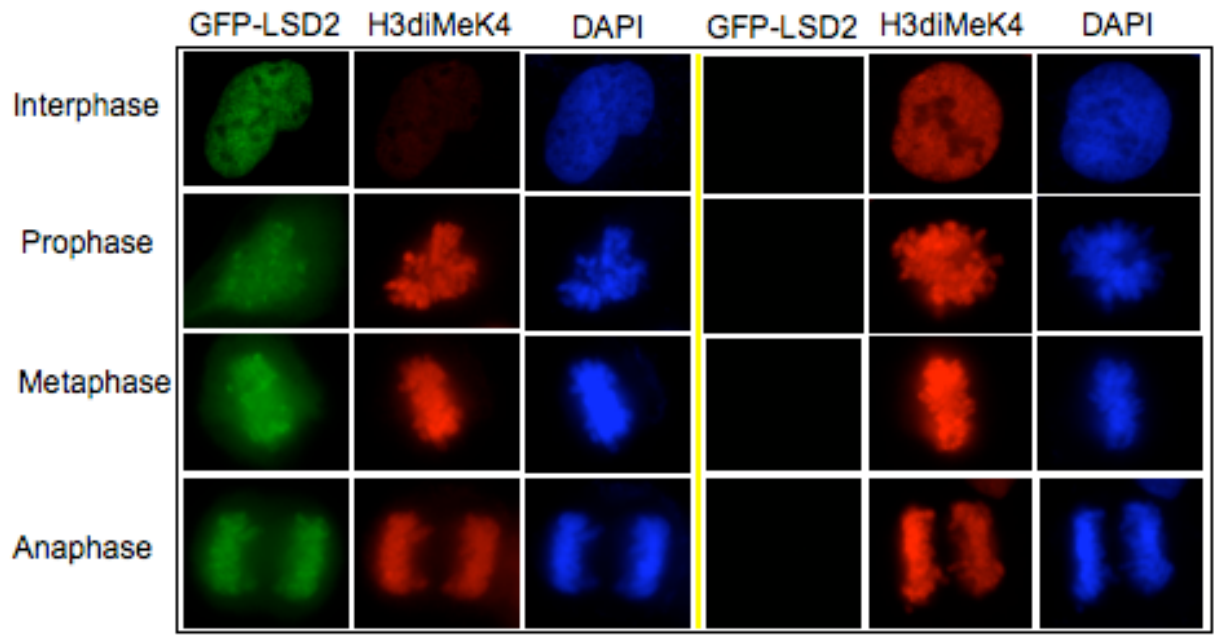

Figure 3-17. Despite LSD2 recruitment by n-PAC to mitotic chromatin, there is no H3K4 demethylation in dividing cells. U2OS cells cotransfected with LSD2 and n-PAC at various stages of mitosis. Despite LSD2 recruitment to mitotic chromatin, there is no loss of H3K4 demethylation in the cotransfected mitotic cells (left side) compared to untransfected cells (right side). Exposure times were held constant for each channel. (M. Rutenberg)

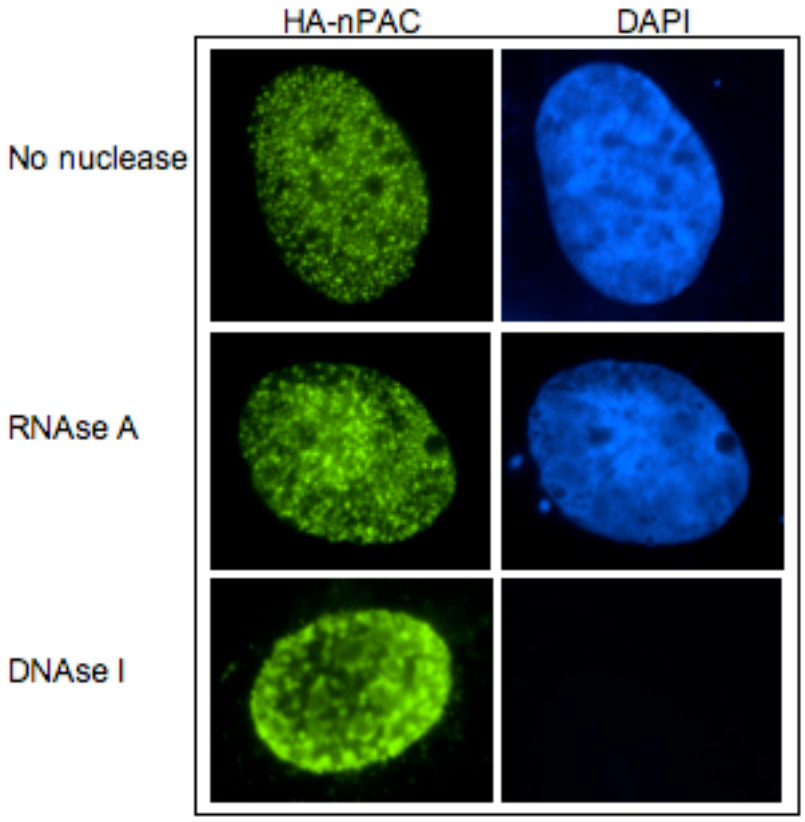

Figure 3-18. n-PAC interacts with chromatin and the nuclear matrix. Fg-HA-nPAC transfected U2OS cells were treated with nuclease, extracted with 0.5M NaCl, and immunostained with α-HA antibodies. No nuclease treated and RNase A treated extracted nuclei retain normal n-PAC punctate nuclear staining. In DNAse I treated extracted nuclei, most n-PAC is solubilized and extracted. The n-PAC retained after DNAse treatment could be matrix associated. (M. Rutenberg)

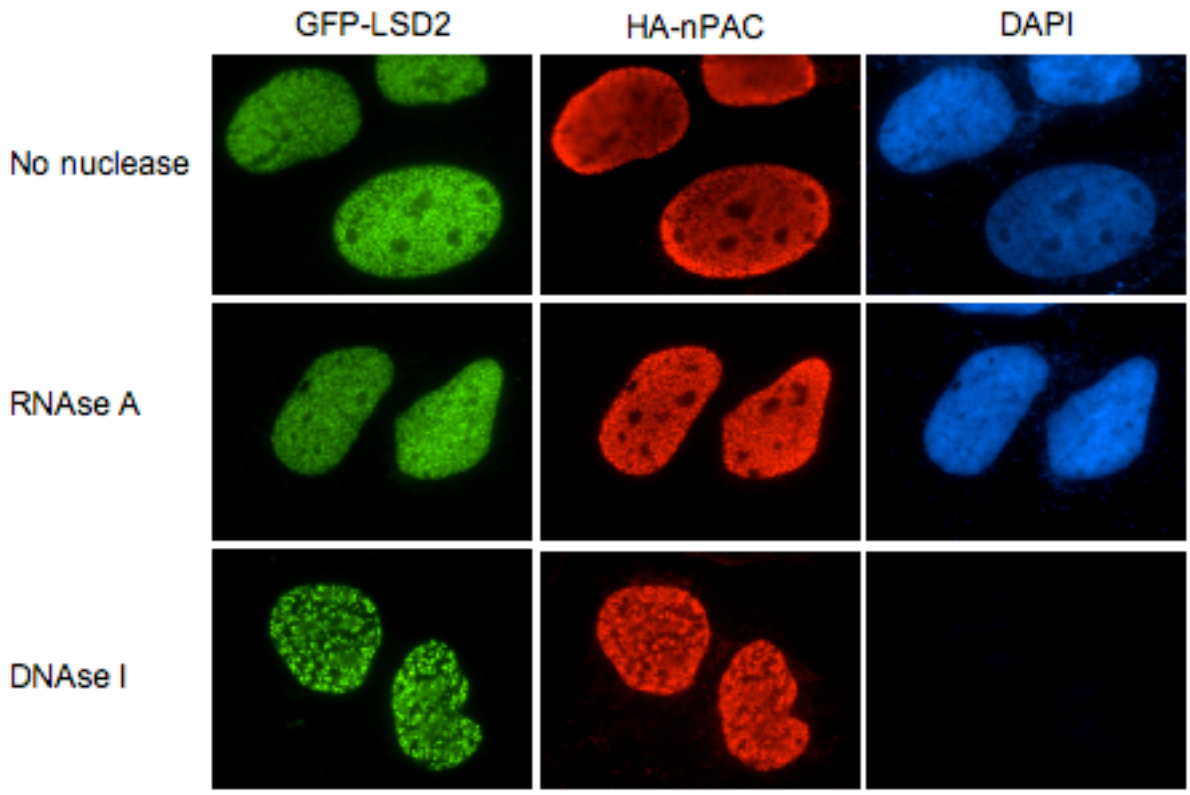

Figure 3-19. LSD2 is recruited to the chromatin and bound by nPAC. Gfp-LSD2 and Fg-HA-nPAC transfected cells were treated with nuclease, salt extracted, and immunostained with α-HA antibodies. No nuclease treated and RNase A treated extracted nuclei retain normal n-PAC and LSD2 punctate nuclear staining. In DNAse I treated extracted nuclei, most n-PAC and LSD2 is solubilized and extracted. The n-PAC and LSD2 retained after DNAse treatment could be matrix associated. (M. Rutenberg)

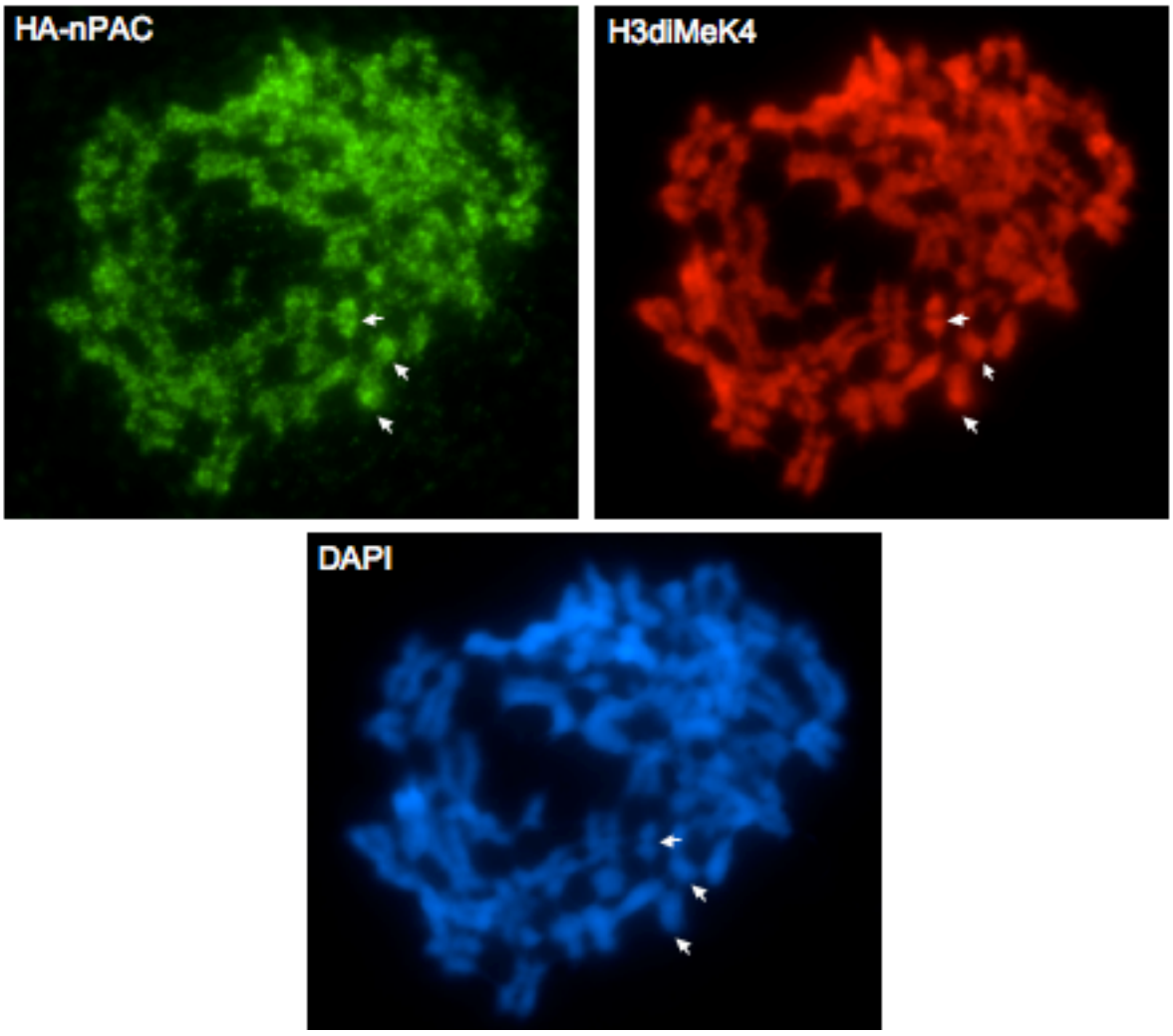

Figure 3-20. n-PAC binds mitotic chromosomes. HeLa cells stably expressing Fg-HA-nPAC were treated with colcemid and metaphase spreads were made. They were immunostained for HA and dimethyl K4H3. DNA is stained with DAPI. N-PAC has a speckled pattern of staining along many chromosomes that differs from chromosome to chromosome, but is symmetric for sister chromatids. Dimethyl K4H3 stains along the entire length of chromosomes, however there are regions off enrichment. N-PAC appears to be enriched in regions of intense diMeK4 H3 staining (white arrows). (M. Rutenberg)

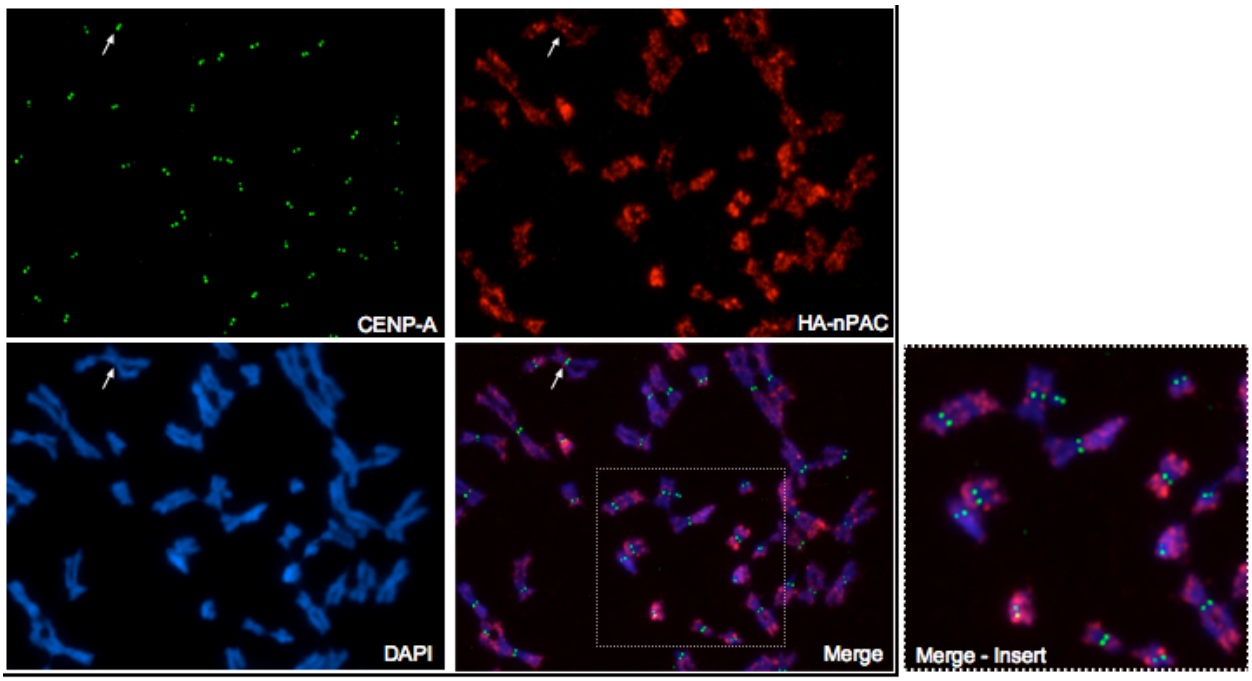

Figure 3-21. N-PAC stains sister chromatids in a symmetric pattern, but is absent from mitotic centromeres. Metaphase spreads were made using HeLa cells stably expressing Fg-HA-nPAC. They were immunostained using α-HA and α-CENP-A antibodies. While n-PAC does not appear to bind at most centromeres, there is a notable exception, where n-PAC appears to be flanking the CENP-A binding region of the centromere (white arrow). The sporadic n-PAC binding along the chromosomes is very evident here as well as the symmetry of n-PAC staining shared between sister chromatids. The area in the merged frame (denoted by a white square) is enlarged to the right to better visualize n-PAC and CENP-A localization. (M. Rutenberg)

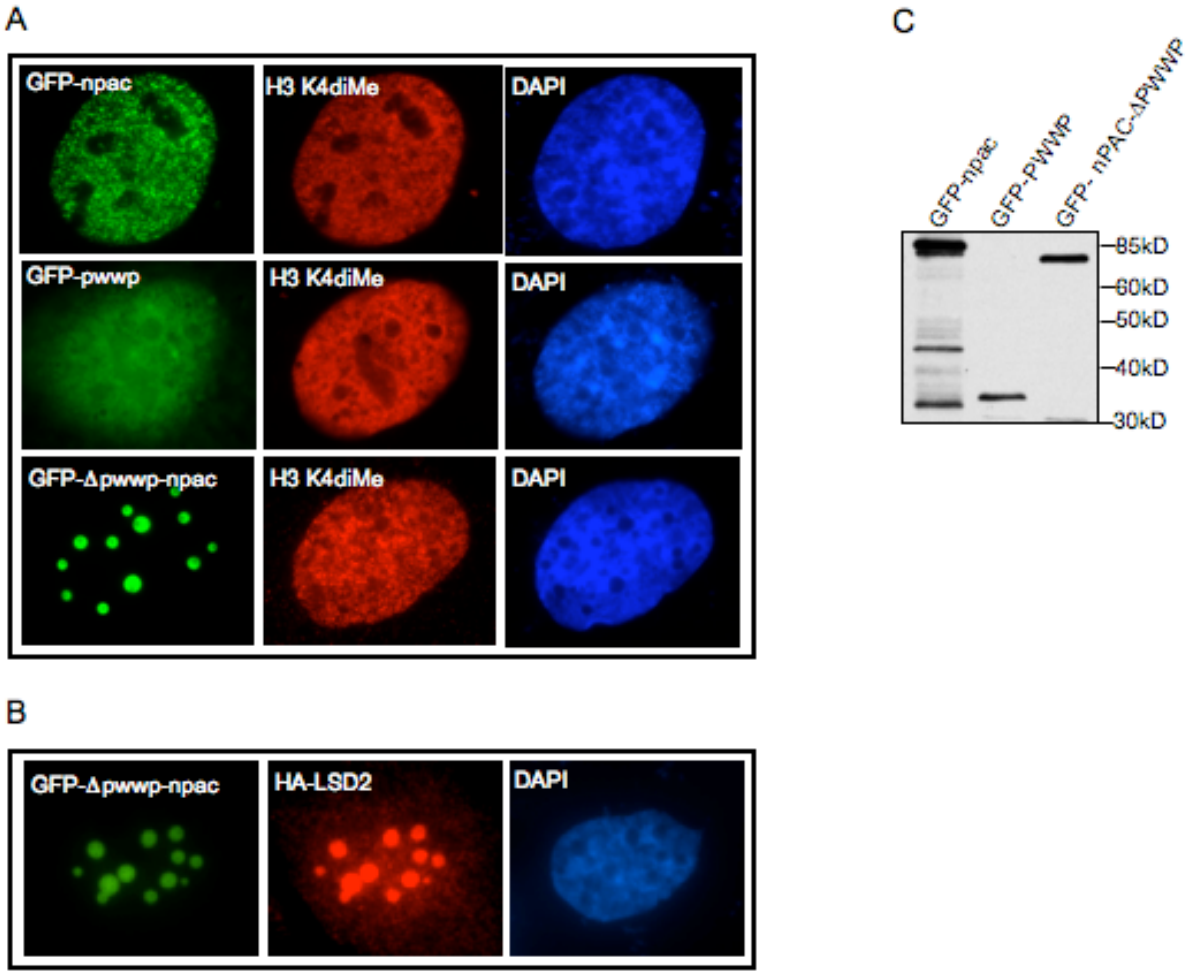

Figure 3-22. n-PAC N-terminal domain targets chromatin; the C-terminus interacts with LSD2. A) GFP-fused n-PAC deletion mutants were were transiently transfected into U2OS cells and immunostained for dimethyl K4 H3. Top- full length GFP-npac has normal punctate nuclear staining pattern. Middle- GFP-pwwp has diffuse nuclear staining. Bottom- GFP-Δpwwp-nPAC forms nuclear foci in regions devoid of chromatin. B) GFP-Δpwwp-nPAC cotransfected with HA-LSD2. GFP-Δpwwp-nPAC forms dense nuclear foci, however retains its capacity for LSD2 interaction, and recruits LSD2 to foci. C) GFP-nPAC fusion constructs expressed in U2OS cells. Full length n-PAC is 60kD. (M. Rutenberg)

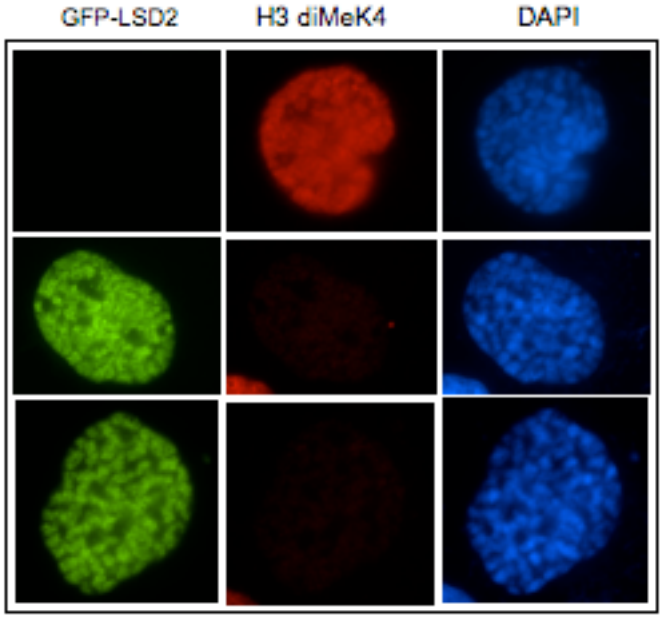

Figure 3-23. LSD2 cotransfected with n-PAC induces “prophase-like” condensed chromatin. U2OS cells were transfected with GFP-LSD2 and Fg-HA-nPAC and immunostained for dimethyl K4 H3. top- Untransfected cell with prophase pattern of condensed chromatin retains intense dimethyl K4 H3 staining. middle & bottom- examples of LSD2/n-PAC cotransfected cells with prophase pattern of condensed chromatin. LSD2 colocalizes with DAPI due to n-PAC recruitment to chromatin. Dimethyl K4 H3 staining is almost completely lost in the cotransfected cells. (M. Rutenberg)

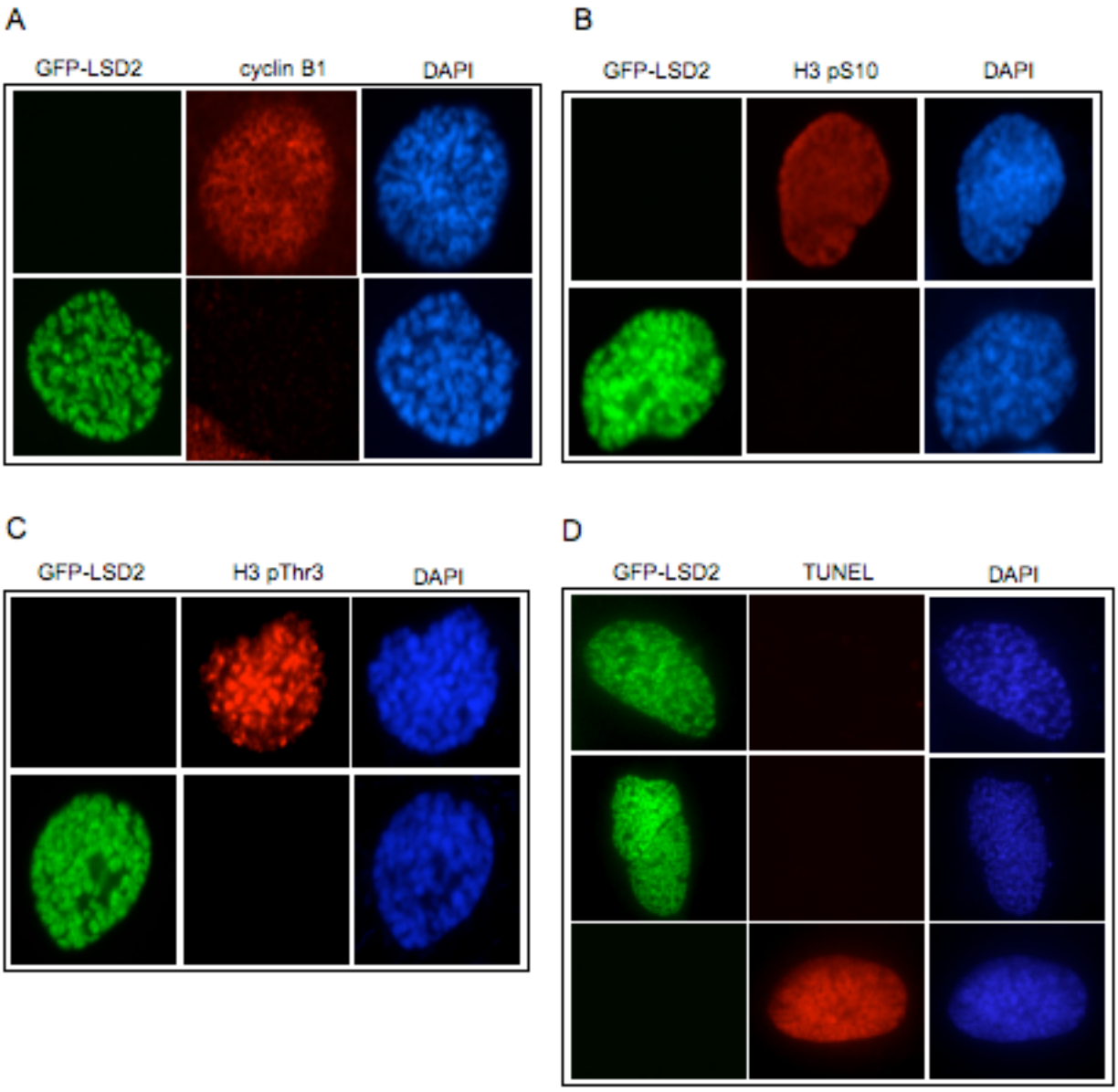

Figure 3-24. LSD2 and n-PAC cotransfected cells have “prophase-like” chromatin condensation in the absence of mitotic markers or apoptosis. Reprasentative images of untransfected or LSD2 and n-PAC cotransfected U2OS cells were immunostained for mitotic markers or TUNEL stained for apotosis. A) Untransfected prophase cells show intense nuclear cyclinB1 staining (top), while LSD2/n-PAC cells with similar condensation patterns are devoid of cyclinB1 (bottom). B) Untransfected prophase cells stain positively for the mitotic marker phosphorylated Serine 10 on H3 (H3 pS10), while LSD2/n-PAC cells with similar DAPI patterns lack H3 pS10. C) Untransfected prophase cells are positive for phospho-Threonine 3 on H3 (H3 pThr3), while cotransfected “prophase-like” are negative. D) TUNEL staining of LSD2/n-PAC cells for apoptosis are negative (top & middle). Postive control cells treated with DNAse I stain brightly for TUNEL (bottom). (M. Rutenberg)

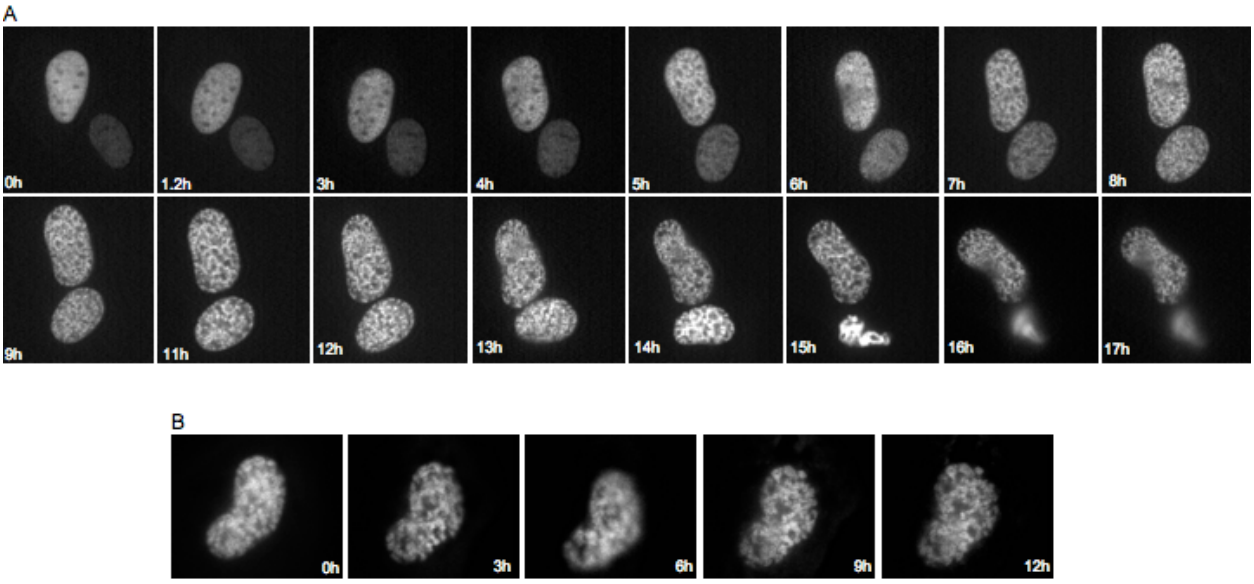

Figure 3-25. LSD2 and n-PAC induce a progressive and refractory chromosome condensation. U2OS cells were tranfected with GFP-LSD2 and Fg-HA-nPAC. Time-lapse imaging recorded the GFP-LSD2 staining patterns during growth in an environmental chamber. A) LSD2 staining began in a diffuse nuclear pattern and briefly adopted a punctate pattern before undergoing a more complete chromatin condensation, which persisted for over 8 hours. The lower cell in this image retained its condensed nuclear pattern until undergoing cell death. B) An LSD2/n-PAC cotransfected cell displaying "prophase-like" condensed chromatin for 12 hours. Typical prophase condensation would be on the order of minutes. Each time stamp is according to the time after recording began. Imaging began 16 hours after transfection (0h). (M. Rutenberg)

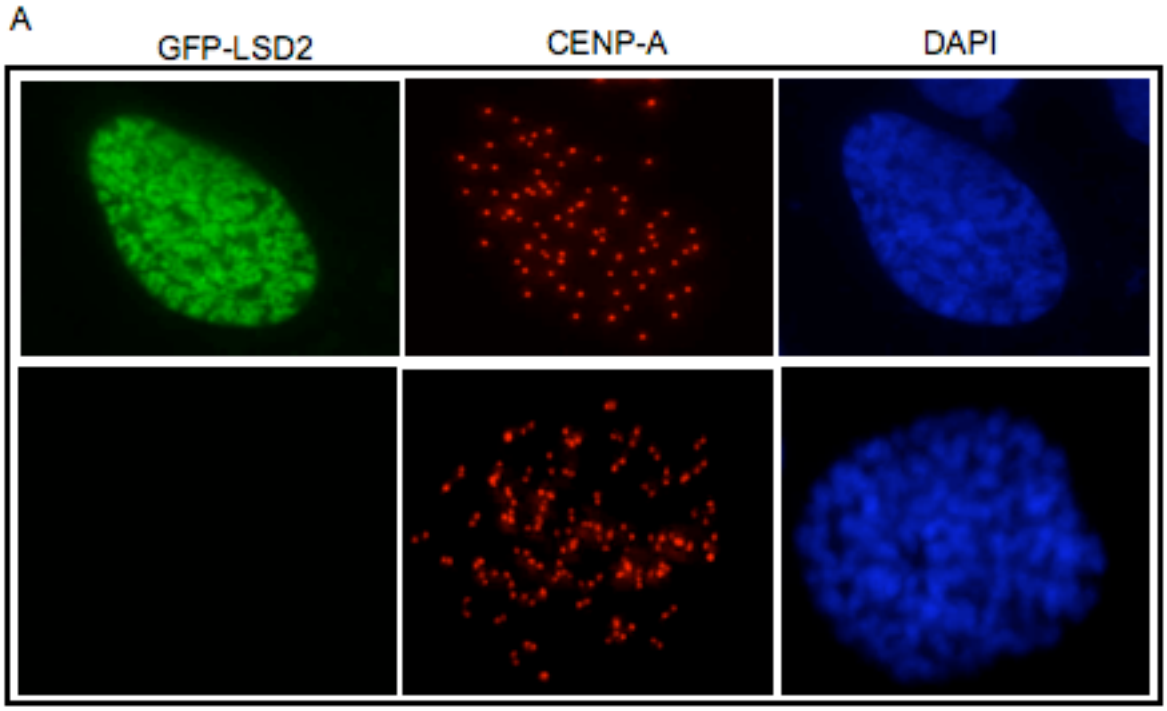

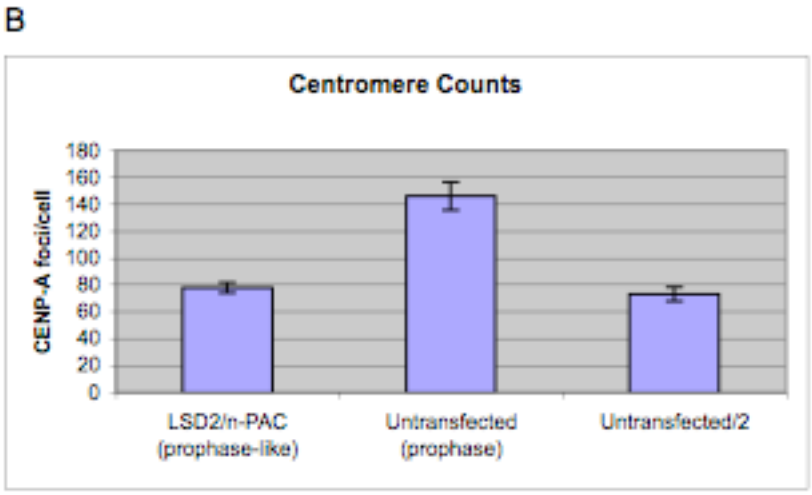

Figure 3-26. LSD2 and n-PAC cotransfected cells undergo chromatin condensation in the absence of DNA replication. GFP-LSD2/nPAC were cotransfected into U2OS cells and immunostained for the centromere marker, CENP-A. A) Representative images of LSD2/n-PAC cell with condensed "prophase-like" chromatin and unduplicated CENP-A (centromere) foci (top). Untransfected cells showing "prophase" chromatin condensation have CENP-A doublets, indicating replicated centromeres and DNA. B) The total number of CENP-A foci was counted in LSD2/n-PAC cotransfected cells and untransfected cells with condensed chromatin. Untransfected prophase cells have 4n CENP-A foci indicative of centromere/DNA replicatoion, whereas LSD2/n-PAC "prophase-like" cells have 2n CENP-A foci. U2OS cells are hypertriploid. N=8 for each category. (M. Rutenberg)

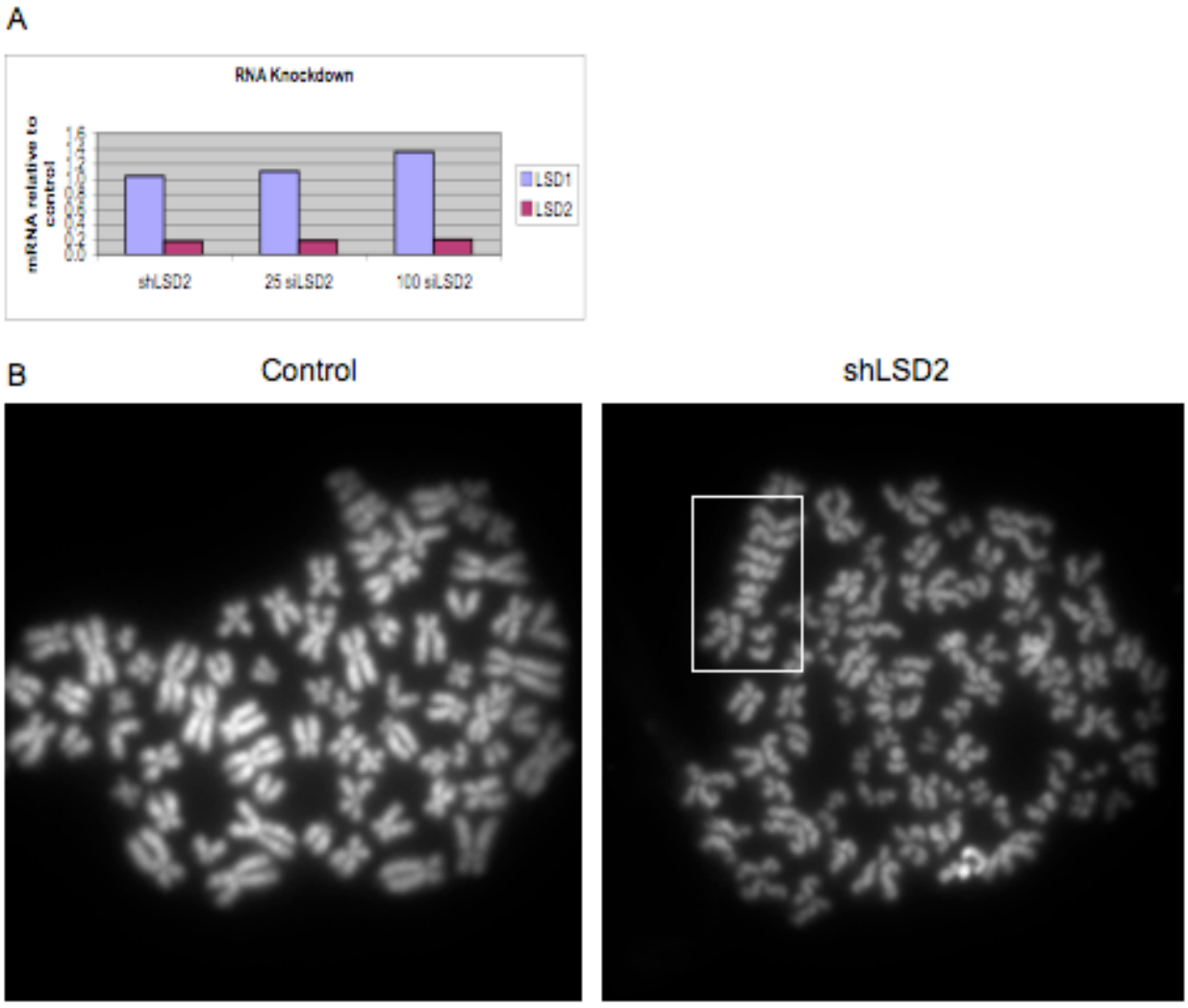

Figure 3-27. LSD2 knockdown induces precocious sister chromatid separation. A) HeLa cells were transfected with pMSCV-shLSD2 or siRNAs targeting LSD2 (25pmoles or 100pmoles). Expression levels were normalized to β-actin and the mRNA levels were compared for to either shGFP (for shLSD2) or scramled siRNA (for siLSD2). Each construct showed ~80% knockdown of LSD2. LSD1 expression was measured to ensure specific knockdown of LSD2. B) HeLa cells were transfected with either a knockdown control plasmid (shEGFP) (left) or a pMSCV-shLSD2 knockdown plasmid (right). Metaphase chromosomes spreads were made. The contol chromosomes show cohesion between sister chromatids at the centromere constriction, while many of the LSD2 knockdown sister chromatids have already lost attachment. The white box indicates several sister chromosomes with clear loss of cohesion. (A- M. Rutenberg; B- S. Liu)

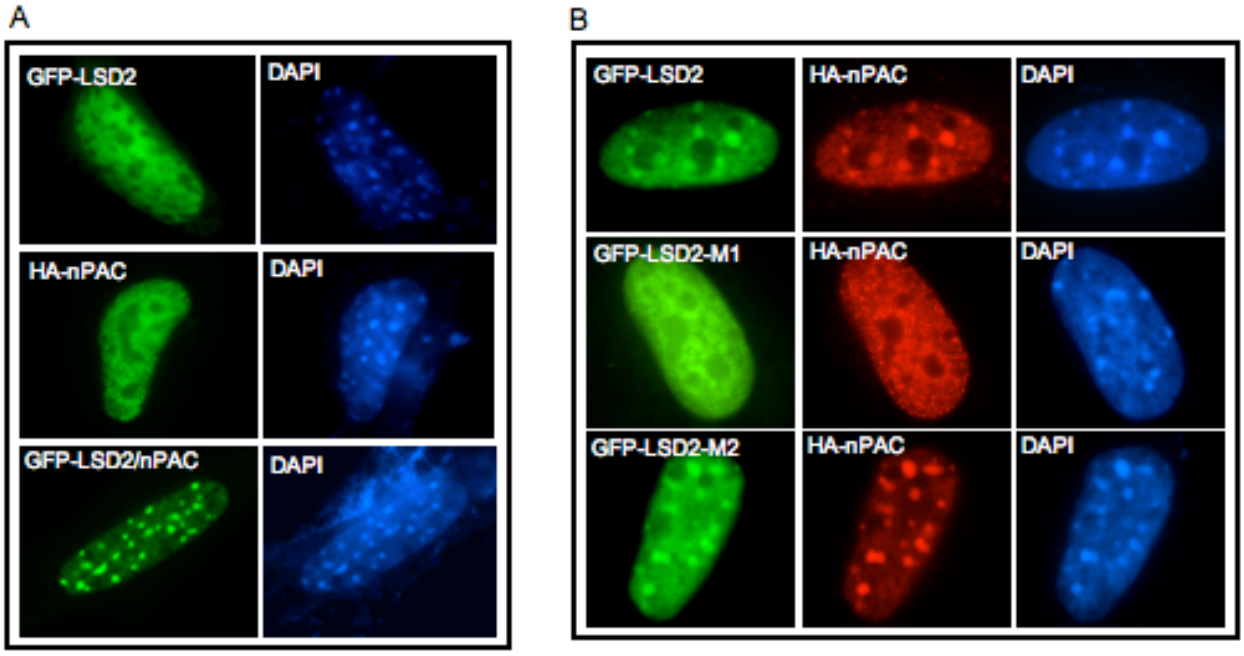

Figure 3-28. LSD2 and n-PAC are enriched at pericentric heterochromatin in NIH3T3 cells. A) top- GFP-LSD2 shows diffuse nuclear staining. middle- Fg-HA-nPAC shows a typical punctate nuclear staining pattern. bottom- Only when LSD2 and n-PAC are cotransfected do they localize to the DAPI dense regions of pericentric heterochromatin. B) LSD2 wild-type or mutants were cotranfected with n-PAC into NIH3T3 cells. top- wild-type LSD2 and n-PAC colocalize with DAPI dense pericentric heterochromatin. middle- LSD2-M1 and n-PAC are not enriched at pericentric heterochromatin. bottom- LSD2-M2 and n-PAC colocalize to pericentric regions. (M. Rutenberg)

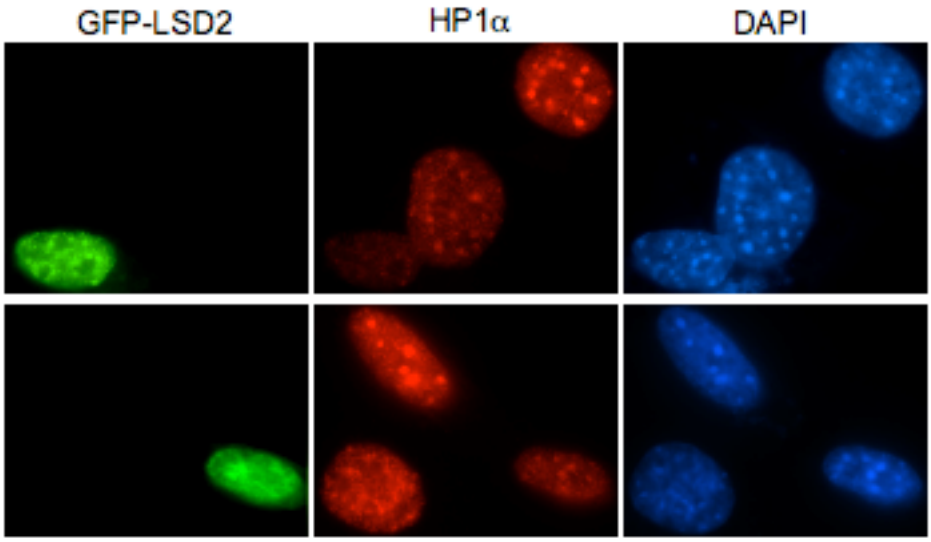

Figure 3-29. LSD2 and n-PAC cause a global decrease in HP1α. NIH3T3s were transfected with GFP-LSD2 and Fg-HA-nPAC, and immunostained for HP1α. Cotransfected cells have a decrease in overall HP1α, despite having clear DAPI dense regions of heterochromatin. (M. Rutenberg)

Cell/Field	LSD2	HP1a	DAPI	HP1a/DAPI	LSD2	HP1a	DAPI	HP1a/DAPI	HP1a(L2-nP)/HP1a(untr) relative to DAPI
1	1399	683	1504	0.454	148	1484	1760	0.843	0.539
2	1265	498	1818	0.274	135	882	2118	0.416	0.658
3	1672	556	1290	0.431	236	1561	1607	0.971	0.444
4	1702	841	1724	0.488	163	1649	1720	0.959	0.509
5	1376	705	2055	0.343	130	1506	2551	0.590	0.581
6	1668	542	2470	0.219	122	1257	2821	0.446	0.492
7	1103	748	1385	0.540	220	1281	1501	0.853	0.633
8	1735	719	1675	0.429	117	1820	1637	1.112	0.386
9	1782	289	1237	0.234	201	514	1142	0.450	0.519
10	1508	791	1126	0.702	355	498	1134	0.439	1.600
11	1172	819	1162	0.705	153	783	1258	0.622	1.132
12	1464	1424	1688	0.844	328	863	1451	0.595	1.418
13	1563	408	1040	0.392	149	882	966	0.913	0.430
14	901	460	1302	0.353	111	1023	1208	0.847	0.417
15	1135	552	1806	0.306	147	1604	1884	0.851	0.359
Average	**1430**	**669**	**1552**	**0.448**	**181**	**1174**	**1651**	**0.708**	**0.674**
St. Dev.				**0.183**				**0.230**	
p-value									**0.002**

Table 3-2. HP1α is reduced in LSD2/n-PAC transfected NIH 3T3s. NIS software was used to quantify the average relative fluorescence of HP1α and DAPI staining between LSD2/n-PAC cotransfected cells and untransfected cells. The columns show the relative intensity units measured for LSD2, HP1α, and DAPI, and are separated into LSD2/n-PAC transfected cells (left side) and untransfected cells (right side). The intensity of HP1α staining was calculated relative to DAPI for each cell (HP1a/DAPI). The intensity of HP1α in transfected cells was calculated as 67% of untransfected cells. Using a two-tailed t-test, a p-value of 0.002 was calculated. (M. Rutenberg)

CHAPTER 4
DISCUSSION

The idenification of LSD1 as the first bona fide histone demethylase shook the foundation of epigenetics. Prior to its discovery, the idea of histone methylation as a permanent epigenetic mark was gaining favor. LSD1 demethylase activity revealed the reversibility of histone methylation and uncovered a system by which the complex combinations of histone methylation could be translated into a dynamic system of genome regulation.

Because much of the focus on histone methylation has been on its role in transcription regulation, so has been the study of LSD1 and histone demethylation. Here, we have attempted to characterize the activity and function of the LSD1 homolog, LSD2. While initial protein domain analyses comparing LSD1 and LSD2 show conservation of their SWIRM domains and their C-terminal, FAD-dependent amine oxidase domains, they also reveal major structural differences between the two proteins. The tower domain of LSD1, which is noticeably absent from LSD2, is required for LSD1 enzymatic activity and mediates allosteric regulation. Additionally, the N-terminal zinc-finger present in LSD2 is absent in LSD1.

Despite the structural differences, we show that LSD2 shares the same substrate specificity as LSD1. Using *in vitro* and *in vivo* demethylase assays, we confirmed LSD2 demethylase activity on mono- and di-methyl lysine 4 H3. Using LSD2 point mutants disrupting either FAD-binding or the amine oxidase domain, we confirmed the requirement for LSD2 catalysis for *in vivo* demethylation. Based on these findings, we expected LSD2 to mediate a similar gene repression function as LSD1. However, using a luciferase reporter system for transcriptional activity, we found very little or no role for LSD2 in gene regulation, in contrast to strong repression mediated by LSD1. While this does not completely rule out the possibility that LSD2

regulates transcription, it does suggest a simple mode of lysine 4 demethylation as a means of repression is unlikely for LSD2.

Further differences between LSD1 and LSD2 were observed following tandem affinity purification of LSD2. Unlike LSD1, which co-purifies with an array of transcriptional coregulators (e.g. CtBP, CoREST, HDAC1/2), LSD2 TAP mass spectrometry sequence analysis displayed a very different protein profile. Instead of transcription regulators, our MS/MS analysis suggested that LSD2 associated with DNA damage repair/chromatin remodeling complexes and mitotic chromatin associated machinery, among other broad classes of chromatin-associated proteins. Our proteomic analysis revealed LSD2 association with several members of the NuA4/INO80 chromatin remodeling complex, including: BAP1, TIP49A, TIP49B, and others. We also identified the structural maintenance of chromosomes family members SMC1 and SMC3 (cohesin), and SMC2 and SMC4 (condensin). These findings indicate that LSD2 might mediate an unexpected function for histone demethylation beyond gene regulation.

In addition to a notable absence of transcriptional regulators, the LSD2 TAP MS/MS analysis revealed a previously uncharacterized protein of considerable interest. The n-PAC protein contains an N-terminal PWWP domain, a DNA-binding zinc-finger, and a C-terminal NAD dependent dehydrogenase domain. The PWWP domain is a DNA/chromatin binding domain that is also present in the DNA methyltransferases, DNMT3a and DNMT3b. Interestingly, the PWWP in the DNMTs has been shown to specifically target them to pericentric heterochromatin (16). We suspected the PWWP domain could mediate a similar interaction between n-PAC associated proteins and chromatin. We were also struck by the n-PAC dehydrogenase domain, and its relation to CtBP. CtBP is an NAD-binding dehydrogenase domain containing corepressor that is found in LSD1 corepressor complexes. We hypothesized

that CtBP and n-PAC dehydrogenase activities might play similar roles in association with their respective nuclear amine oxidases. One proposed role of their dehydrogenase domains is the elimination of hydrogen peroxide produced as a toxic by-product of amine oxidase demethylation. Hydrogen peroxide is produced by the reduction of molecular oxygen in the regeneration of FAD from reduced FADH following a cycle of demethylation. While the proposed role for CtBP and n-PAC in the elimination of hydrogen peroxide is not proven, we do know that CtBP and its NAD binding is required for its corepressor activity (60, 117). In addition to the mass spec data suggesting an n-PAC/LSD2 interaction, we confirmed their interaction using an *in vitro* binding assay and reciprocal immunoprecipitation.

Using recombinant n-PAC, we did, in fact, show an important role for n-PAC in LSD2 enzymatic activity. *In vitro*, n-PAC dramatically enhanced the mono- and di-MeK4 demethylation activity of recombinant LSD2 and LSD2 TAP products on nucleosomes. This enhancement was only observed for nucleosomal substrates, providing insight into a potential biological role for the n-PAC/LSD2 interaction. We propose that n-PAC mediates the recruitment and orientation of LSD2 on nucleosomes for demethylation. It is also possible, though, that n-PAC mediates a direct enzymatic reaction on either nucleosomes or LSD2.

Further analysis of n-PAC showed that it associates closely with chromatin, and we showed the requirement of its PWWP domain for mediating that association. We showed *in vivo* that in the absence of n-PAC, LSD2 interacts weakly with chromatin. The LSD2 staining pattern in the absence of n-PAC shows diffuse nuclear staining. In the presence of n-PAC, however, LSD2 adopts a striking change in localization, adopting the characteristic n-PAC punctate nuclear staining pattern. In the presence of n-PAC, LSD2 is recruited to specfic chromatin regions, where it efficiently binds interphase and mitotic chromatin. We show that while

elimination of the n-PAC PWWP domain abrogates its specific chromatin localization pattern, this domain is not required to maintain the interaction with LSD2. We also show the n-PAC/LSD2 interaction dramatically enhances LSD2 demethylase acitivty on mono- and di-methyl K4 H3 *in vivo*, consistent with our *in vitro* data.

While we were unable to determine specific genomic targets for n-PAC binding, metaphase chromosome analysis showed an interesting feature of n-PAC chromosome binding. Exogenous n-PAC has a very sporadic binding pattern along the chromosome arms and displays very different binding patterns between chromosomes. Importantly, though, sister chromatids showed very symmetric n-PAC staining. Because sister chromatids are genetically and epigenetically identical, whatever the target of n-PAC binding, it would be conserved between sisters, while binding targets could vary widely across different chromosomes. These data suggest a targeted binding of n-PAC (and therefore LSD2) rather than a non-specific, stochastic DNA/chromatin association. Interestingly, we also observed an enrichment of n-PAC binding on mitotic chromosomes in regions enriched for dimethyl K4 H3 staining.

Our *in vivo* overexpression of LSD2 and n-PAC displayed a striking phenotype that could give insight into a physiological role for LSD2 demethylation. As noted, coexpression of LSD2 and n-PAC induces a localization change in LSD2 and increases demethylase activity. We also observed an unusually high number of cotransfected cells with a characteristic prophase-like condensed chromatin phenotype, which was not observed in either LSD2 or n-PAC transfections alone. In contrast to untransfected prophase cells, however, LSD2/n-PAC transfectants lacked the standard markers for prophase or mitosis, including nuclear cyclin B1, phospho-serine 10 on histone H3, and phospho-threonine 3 on H3. Cotransfected cells were TUNEL negative, eliminating the likelihood of apoptosis as the source of the condesed chromatin phenotype.

In order to observe the cell cycling of LSD2/n-PAC cotransfectants, we conducted live imaging studies. We observed the prophase condensation in LSD2/n-PAC cotransfectants results from a progressive and protracted condensation state. The condensation can persist for many hours (>12) before the cells eventually die. Live imaging also revealed that the LSD2/n-PAC induced condensation does not occur as a disruption in decondensation at the exit of mitosis, as transfected cells underwent condensation in the absence of nuclear and cell division. Analysis of CENP-A staining in LSD2/n-PAC cells revealed the condensation occurs in the absence of duplicated centromeres, and therefore prior to the completion of S phase. The sum of these observations points to G1 or early S-phase as the stage for LSD2/n-PAC induced chromatin condensation.

Using LSD2 catalytic inactive point mutants, we showed that LSD2 demethylase acitivity is required for the induction of LSD2/n-PAC mediated chromatin condensation. This suggests that histone demethylation is involved in chromatin condensation, however, we cannot rule out the possibility that LSD2 catalytic activity is required to mediate demethylation reactions on non-histone substrates. We wondered if LSD2 specific demethylase activity is required or if non-specific lysine 4 H3 demethylation could induce a similar condensed chromatin phenotype. In order to address this, we used the recently identified Jumonji C domain containing lysine 4 H3 histone demethylases, SMCX and PLU-1. SMCX and PLU-1 mediate demethylation on di- and tri-methyl K4, or mono-, di-, and tri-methyl K4 H3 demethylation, respectively. Neither SMCX nor PLU-1 coexpressed with n-PAC were able to induce the chromatin condensation as observed with LSD2/n-PAC. Numerous conclusions can be inferred from these results, including: 1) LSD2-specific targeted histone demethylation is required and other dem(39)ethylases don't serve a redundant function; 2) The required specificity of histone demethylation is not intrinsic to

LSD2, but is determined by its interaction with n-PAC, which is exclusive to LSD2 and absent from SMCX and PLU-1, and 3) LSD2 demethylates a non-histone substrate that is responsible for the condensation phenotype. Regardless, these results indicate a specific activity mediated by the interaction of LSD2 and n-PAC that results in chromatin condensation.

Our mass spec analysis identified several proteins involved in chromatin condensation, which are particularly interesting given our findings. The structural maintenance of chromosome (SMC) proteins, SMC2 and SMC4 are the core subunits of the condensin I and II complexes and were identified by proteomic analysis of TAP LSD2. SMC2 and SMC4 associate with three other non-SMC proteins in each of the condensin complexes, and are required for proper chromatin compaction and mitotic chromosome stability (27, 39). We suspected that LSD2/n-PAC might induce chromosome condensation by recruitment of condensin. However, despite confirmation of n-PAC and SMC2 interaction by co-IP, using we were unable to establish any functional support for a role in condensin in LSD2/n-PAC induced chromatin condensation.

We then turned to RNA knockdown in order to further pursue the biological function of LSD2. Based on our overexpression data and the assumption that LSD2 is involved in condensin mediated chromatin compaction, we expected to see a disruption in condensation in LSD2 knockdowns. In lower organisms it has been shown that a variety of phenotypes result from disruption of condensin, including disruption of establishment/maintenance of condensation, loss of sister chromatid resolution, and disruption of the structure of the centromere and pericentric heterochromatin (75, 89). Interestingly, while LSD2 knockdown metaphase chromosome spreads had no obvious disruption in condensation, they did display a high incidence of precocious sister chromatid segregation. This phenotype is frequently an indication of a disruption of pericentric heterochromatin.

Pericentric heterochromatin is responsible for mediating many of the critical events involved in chromosome segregation during mitosis, including kinetechore formation for attachment of chromosomes to the mitotic spindle, sister chromatid cohesion, and providing the initiation site of chromosomal condensation at the outset of prophase (28, 56, 90). In particular, the pericentric heterochromatin is the initiation site for serine 10 H3 phosphorylation during mitotic condensation, from where it spreads along the lengths of the chromosomes. Condensin is also known to associate with these pericentric sites of serine 10 phosphorylation.

The cohesin complex (SMC1 and SMC3) is also functions at the pericentric heterochromatin. Cohesin mediates sister chromatid attachment following replication during S phase. It remains attached along the lengths of the sister chromatids until metaphase, at which point cohesin is removed from the chromosome arms and only remains attached at the pericentric heterochromatin. This heterochromatin attachment of sister chromatids is critical for chromosome alignment and proper segregation at the metaphase plate.

The epigenetic profile of pericentric heterochromatin is essential for its specialized functions. It is characterized by H3 and H4 hypoacetylation, hypomethylation of lysine 4 H3, and hypermethylation of di- and tri-methyl of lysine 9 H3. The pericentric heterochromatin flanks the centromere on both sides and is marked by a sharp transition from the epigenetic signature of the centromere, which is enriched for lysine 4 H3 methylation, and hypomethylated on lysine 9 H3. The centromere is also marked by the presence of the centromere specific histone H3 variant CENP-A.

The pericentric heterochromatin is also characterized by the enrichment of HP1α, a heterochromatin associated protein that binds to methylated H3K9 and is required for the proper

recruitment of the cohesin complex. Loss of lysine 9 methylation, or HP1 itself, disupts cohesin loading and results in sister chromatid instability and precocious sister chromatid segregation.

The total of our results from these studies strongly suggest a disruption in the function of the pericentric heterochromatin. We propose that overexpression of LSD2 and n-PAC induces a genome-wide heterochromatinization. This could occur by n-PAC recruitment of LSD2 and other heterochromatin associated proteins to chromatin. LSD2 demethylation of H3K4 could be a critical step in the induction of heterochromatinization. Interestingly, our TAP purification of LSD2 identified EHMT1 and EHMT2, two set domain containing H3K9 methyltransferases. It is possible that these enzymes could coordinate the methylation of K9H3 with LSD2 demethylation of K4H3 to generate the epigenetic profile of heterochromatin. In this scenario, the physiological function of LSD2 and n-PAC would be confined to pericentric heterochromatin, our overexpression system forces a more widespread effect.

Our LSD2 knockdown data also supports the hypothesis that LSD2 and n-PAC mediate the formation/maintenance of heterochromatin. Loss of LSD2 function could lead to the loss of maintenance of the characteristic epigenetic profile of this region. The balance between K4H3 demethylation and K9H3 methylation is essential for heterochromatin function in sister chromatid cohesion. LSD2/n-PAC could mediate the maintenance of K4 hypomethylation, either throughout the cell cycle, or possibly, during DNA replication in which induction of K4H3 hypomethylation must be faithfully reproduced in newly replicated heterochromatin (Figure 4-1). Our data showing chromatin condensation in LSD2/n-PAC overexpressing cells prior to the completion of S-phase supports the idea that LSD2/n-PAC are active during this stage of the cell cycle.

There exists a dynamic balance between the distinct domains of centromeric chromatin. Overexpression of the K9H3 methyltransferase, Su(var)3-9, or HP1 result in the spread of heterochromatin into adjacent regions of euchromatin and potentially into centromeric chromatin. In contrast, overexpression of CENP-A causes spreading of the centromere chromatin into flanking heterochromatin. LSD2 and n-PAC could serve a specific function in maintaining the unique hypomethylated profile of this heterochromatic region, preventing incursion by either proximal centromere chromatin or distal euchromatin. The localization of LSD2/n-PAC to the DAPI dense regions of pericentric heterochromatin in mouse 3T3 cells provides support for their localization to these regions.

We propose that the function of LSD2 and n-PAC represents a novel role for histone demethylation in the formation/maintenance of heterochromatin. Because of the importance of this region during the cell cycle, and especially for the faithful transmission of chromosomes to daughter cells during mitosis, LSD2 activity should be tightly regulated. Perhaps n-PAC is a major player in the regulation of LSD2 physiologically, in which case it is likely that n-PAC is active in a cell cycle specific manner. It is possible that n-PAC is regulated by expression changes during the cell cycle or post-translational regulation. However, there are almost certainly other factors involved in the regulation of LSD2 and its dynamic histone demethylation.

LIST OF REFERENCES

1. **Ahmad, K., and S. Henikoff.** 2002. Epigenetic consequences of nucleosome dynamics. Cell **111:**281-4.

2. **Allfrey, V. G., R. Faulkner, and A. E. Mirsky.** 1964. Acetylation and Methylation of Histones and Their Possible Role in the Regulation of Rna Synthesis. Proc Natl Acad Sci U S A **51:**786-94.

3. **Allshire, R. C., J. P. Javerzat, N. J. Redhead, and G. Cranston.** 1994. Position effect variegation at fission yeast centromeres. Cell **76:**157-69.

4. **Allshire, R. C., E. R. Nimmo, K. Ekwall, J. P. Javerzat, and G. Cranston.** 1995. Mutations derepressing silent centromeric domains in fission yeast disrupt chromosome segregation. Genes Dev **9:**218-33.

5. **Bannister, A. J., P. Zegerman, J. F. Partridge, E. A. Miska, J. O. Thomas, R. C. Allshire, and T. Kouzarides.** 2001. Selective recognition of methylated lysine 9 on histone H3 by the HP1 chromo domain. Nature **410:**120-4.

6. **Bernard, P., J. F. Maure, J. F. Partridge, S. Genier, J. P. Javerzat, and R. C. Allshire.** 2001. Requirement of heterochromatin for cohesion at centromeres. Science **294:**2539-42.

7. **Bernstein, B. E., E. L. Humphrey, R. L. Erlich, R. Schneider, P. Bouman, J. S. Liu, T. Kouzarides, and S. L. Schreiber.** 2002. Methylation of histone H3 Lys 4 in coding regions of active genes. Proc Natl Acad Sci U S A **99:**8695-700.

8. **Bernstein, B. E., M. Kamal, K. Lindblad-Toh, S. Bekiranov, D. K. Bailey, D. J. Huebert, S. McMahon, E. K. Karlsson, E. J. Kulbokas, 3rd, T. R. Gingeras, S. L. Schreiber, and E. S. Lander.** 2005. Genomic maps and comparative analysis of histone modifications in human and mouse. Cell **120:**169-81.

9. **Bienz, M.** 2006. The PHD finger, a nuclear protein-interaction domain. Trends Biochem Sci **31:**35-40.

10. **Briggs, S. D., T. Xiao, Z. W. Sun, J. A. Caldwell, J. Shabanowitz, D. F. Hunt, C. D. Allis, and B. D. Strahl.** 2002. Gene silencing: trans-histone regulatory pathway in chromatin. Nature **418:**498.

11. **Brownell, J. E., J. Zhou, T. Ranalli, R. Kobayashi, D. G. Edmondson, S. Y. Roth, and C. D. Allis.** 1996. Tetrahymena histone acetyltransferase A: a homolog to yeast Gcn5p linking histone acetylation to gene activation. Cell **84:**843-51.

12. **Buker, S. M., T. Iida, M. Buhler, J. Villen, S. P. Gygi, J. Nakayama, and D. Moazed.** 2007. Two different Argonaute complexes are required for siRNA generation and heterochromatin assembly in fission yeast. Nat Struct Mol Biol **14:**200-7.

13. **Cam, H. P., T. Sugiyama, E. S. Chen, X. Chen, P. C. FitzGerald, and S. I. Grewal.** 2005. Comprehensive analysis of heterochromatin- and RNAi-mediated epigenetic control of the fission yeast genome. Nat Genet **37:**809-19.

14. **Cao, R., L. Wang, H. Wang, L. Xia, H. Erdjument-Bromage, P. Tempst, R. S. Jones, and Y. Zhang.** 2002. Role of histone H3 lysine 27 methylation in Polycomb-group silencing. Science **298:**1039-43.

15. **Chen, D., H. Ma, H. Hong, S. S. Koh, S. M. Huang, B. T. Schurter, D. W. Aswad, and M. R. Stallcup.** 1999. Regulation of transcription by a protein methyltransferase. Science **284:**2174-7.

16. **Chen, T., N. Tsujimoto, and E. Li.** 2004. The PWWP domain of Dnmt3a and Dnmt3b is required for directing DNA methylation to the major satellite repeats at pericentric heterochromatin. Mol Cell Biol **24:**9048-58.

17. **Daniel, J. A., M. G. Pray-Grant, and P. A. Grant.** 2005. Effector proteins for methylated histones: an expanding family. Cell Cycle **4:**919-26.

18. **De Rubertis, F., D. Kadosh, S. Henchoz, D. Pauli, G. Reuter, K. Struhl, and P. Spierer.** 1996. The histone deacetylase RPD3 counteracts genomic silencing in Drosophila and yeast. Nature **384:**589-91.

19. **Dhalluin, C., J. E. Carlson, L. Zeng, C. He, A. K. Aggarwal, and M. M. Zhou.** 1999. Structure and ligand of a histone acetyltransferase bromodomain. Nature **399:**491-6.

20. **Di Stefano, L., J. Y. Ji, N. S. Moon, A. Herr, and N. Dyson.** 2007. Mutation of Drosophila Lsd1 disrupts H3-K4 methylation, resulting in tissue-specific defects during development. Curr Biol **17:**808-12.

21. **Eissenberg, J. C., T. C. James, D. M. Foster-Hartnett, T. Hartnett, V. Ngan, and S. C. Elgin.** 1990. Mutation in a heterochromatin-specific chromosomal protein is associated with suppression of position-effect variegation in Drosophila melanogaster. Proc Natl Acad Sci U S A **87:**9923-7.

22. **Ekwall, K., E. R. Nimmo, J. P. Javerzat, B. Borgstrom, R. Egel, G. Cranston, and R. Allshire.** 1996. Mutations in the fission yeast silencing factors clr4+ and rik1+ disrupt the localisation of the chromo domain protein Swi6p and impair centromere function. J Cell Sci **109 (Pt 11):**2637-48.

23. **Fischle, W., Y. Wang, S. A. Jacobs, Y. Kim, C. D. Allis, and S. Khorasanizadeh.** 2003. Molecular basis for the discrimination of repressive methyl-lysine marks in histone H3 by Polycomb and HP1 chromodomains. Genes Dev **17:**1870-81.

24. **Fuks, F., P. J. Hurd, R. Deplus, and T. Kouzarides.** 2003. The DNA methyltransferases associate with HP1 and the SUV39H1 histone methyltransferase. Nucleic Acids Res **31:**2305-12.

25. **Garcia-Bassets, I., Y. S. Kwon, F. Telese, G. G. Prefontaine, K. R. Hutt, C. S. Cheng, B. G. Ju, K. A. Ohgi, J. Wang, L. Escoubet-Lozach, D. W. Rose, C. K. Glass, X. D. Fu, and M. G. Rosenfeld.** 2007. Histone methylation-dependent mechanisms impose ligand dependency for gene activation by nuclear receptors. Cell **128:**505-18.

26. **Geiman, T. M., U. T. Sankpal, A. K. Robertson, Y. Chen, M. Mazumdar, J. T. Heale, J. A. Schmiesing, W. Kim, K. Yokomori, Y. Zhao, and K. D. Robertson.** 2004. Isolation and characterization of a novel DNA methyltransferase complex linking DNMT3B with components of the mitotic chromosome condensation machinery. Nucleic Acids Res **32:**2716-29.

27. **Gerlich, D., T. Hirota, B. Koch, J. M. Peters, and J. Ellenberg.** 2006. Condensin I stabilizes chromosomes mechanically through a dynamic interaction in live cells. Curr Biol **16:**333-44.

28. **Giet, R., and D. M. Glover.** 2001. Drosophila aurora B kinase is required for histone H3 phosphorylation and condensin recruitment during chromosome condensation and to organize the central spindle during cytokinesis. J Cell Biol **152:**669-82.

29. **Goldberg, A. D., C. D. Allis, and E. Bernstein.** 2007. Epigenetics: a landscape takes shape. Cell **128:**635-8.

30. **Gordon, M., D. G. Holt, A. Panigrahi, B. T. Wilhelm, H. Erdjument-Bromage, P. Tempst, J. Bahler, and B. R. Cairns.** 2007. Genome-wide dynamics of SAPHIRE, an essential complex for gene activation and chromatin boundaries. Mol Cell Biol **27:**4058-69.

31. **Grewal, S. I., M. J. Bonaduce, and A. J. Klar.** 1998. Histone deacetylase homologs regulate epigenetic inheritance of transcriptional silencing and chromosome segregation in fission yeast. Genetics **150:**563-76.

32. **Grewal, S. I., and A. J. Klar.** 1996. Chromosomal inheritance of epigenetic states in fission yeast during mitosis and meiosis. Cell **86:**95-101.

33. **Grewal, S. I., and D. Moazed.** 2003. Heterochromatin and epigenetic control of gene expression. Science **301:**798-802.

34. **Guacci, V., D. Koshland, and A. Strunnikov.** 1997. A direct link between sister chromatid cohesion and chromosome condensation revealed through the analysis of MCD1 in S. cerevisiae. Cell **91:**47-57.

35. **Gurley, L. R., J. A. D'Anna, S. S. Barham, L. L. Deaven, and R. A. Tobey.** 1978. Histone phosphorylation and chromatin structure during mitosis in Chinese hamster cells. Eur J Biochem **84:**1-15.

36. **Hakimi, M. A., D. A. Bochar, J. A. Schmiesing, Y. Dong, O. G. Barak, D. W. Speicher, K. Yokomori, and R. Shiekhattar.** 2002. A chromatin remodelling complex that loads cohesin onto human chromosomes. Nature **418:**994-8.

37. **Hakimi, M. A., Y. Dong, W. S. Lane, D. W. Speicher, and R. Shiekhattar.** 2003. A candidate X-linked mental retardation gene is a component of a new family of histone deacetylase-containing complexes. J Biol Chem **278:**7234-9.

38. **Hauf, S., and Y. Watanabe.** 2004. Kinetochore orientation in mitosis and meiosis. Cell **119:**317-27.

39. **Hirota, T., D. Gerlich, B. Koch, J. Ellenberg, and J. M. Peters.** 2004. Distinct functions of condensin I and II in mitotic chromosome assembly. J Cell Sci **117:**6435-45.

40. **Holliday, R.** 1994. Epigenetics: an overview. Dev Genet **15:**453-7.

41. **Horn, P. J., and C. L. Peterson.** 2006. Heterochromatin assembly: a new twist on an old model. Chromosome Res **14:**83-94.

42. **Humphrey, G. W., Y. Wang, V. R. Russanova, T. Hirai, J. Qin, Y. Nakatani, and B. H. Howard.** 2001. Stable histone deacetylase complexes distinguished by the presence of SANT domain proteins CoREST/kiaa0071 and Mta-L1. J Biol Chem **276:**6817-24.

43. **Iwase, S., F. Lan, P. Bayliss, L. de la Torre-Ubieta, M. Huarte, H. H. Qi, J. R. Whetstine, A. Bonni, T. M. Roberts, and Y. Shi.** 2007. The X-linked mental retardation gene SMCX/JARID1C defines a family of histone H3 lysine 4 demethylases. Cell **128:**1077-88.

44. **James, T. C., and S. C. Elgin.** 1986. Identification of a nonhistone chromosomal protein associated with heterochromatin in Drosophila melanogaster and its gene. Mol Cell Biol **6:**3862-72.

45. **Jenuwein, T.** 2006. The epigenetic magic of histone lysine methylation. Febs J **273:**3121-35.

46. **Jenuwein, T., and C. D. Allis.** 2001. Translating the histone code. Science **293:**1074-80.

47. **Kantidze, O. L., O. V. Iarovaia, and S. V. Razin.** 2006. Assembly of nuclear matrix-bound protein complexes involved in non-homologous end joining is induced by inhibition of DNA topoisomerase II. J Cell Physiol **207:**660-7.

48. **Karpen, G. H., and R. C. Allshire.** 1997. The case for epigenetic effects on centromere identity and function. Trends Genet **13:**489-96.

49. **Lachner, M., D. O'Carroll, S. Rea, K. Mechtler, and T. Jenuwein.** 2001. Methylation of histone H3 lysine 9 creates a binding site for HP1 proteins. Nature **410:**116-20.

50. **Lan, F., M. Zaratiegui, J. Villen, M. W. Vaughn, A. Verdel, M. Huarte, Y. Shi, S. P. Gygi, D. Moazed, R. A. Martienssen, and Y. Shi.** 2007. S. pombe LSD1 homologs regulate heterochromatin propagation and euchromatic gene transcription. Mol Cell **26:**89-101.

51. **Lee, M. G., C. Wynder, N. Cooch, and R. Shiekhattar.** 2005. An essential role for CoREST in nucleosomal histone 3 lysine 4 demethylation. Nature **437:**432-5.

52. **Liang, G., J. C. Lin, V. Wei, C. Yoo, J. C. Cheng, C. T. Nguyen, D. J. Weisenberger, G. Egger, D. Takai, F. A. Gonzales, and P. A. Jones.** 2004. Distinct localization of histone H3 acetylation and H3-K4 methylation to the transcription start sites in the human genome. Proc Natl Acad Sci U S A **101:**7357-62.

53. **Litt, M. D., M. Simpson, M. Gaszner, C. D. Allis, and G. Felsenfeld.** 2001. Correlation between histone lysine methylation and developmental changes at the chicken beta-globin locus. Science **293:**2453-5.

54. **Losada, A., and T. Hirano.** 2005. Dynamic molecular linkers of the genome: the first decade of SMC proteins. Genes Dev **19:**1269-87.

55. **Ma, H., C. T. Baumann, H. Li, B. D. Strahl, R. Rice, M. A. Jelinek, D. W. Aswad, C. D. Allis, G. L. Hager, and M. R. Stallcup.** 2001. Hormone-dependent, CARM1-directed, arginine-specific methylation of histone H3 on a steroid-regulated promoter. Curr Biol **11:**1981-5.

56. **Maddox, P. S., N. Portier, A. Desai, and K. Oegema.** 2006. Molecular analysis of mitotic chromosome condensation using a quantitative time-resolved fluorescence microscopy assay. Proc Natl Acad Sci U S A **103:**15097-102.

57. **Mahadevan, L. C., A. C. Willis, and M. J. Barratt.** 1991. Rapid histone H3 phosphorylation in response to growth factors, phorbol esters, okadaic acid, and protein synthesis inhibitors. Cell **65:**775-83.

58. **Maison, C., and G. Almouzni.** 2004. HP1 and the dynamics of heterochromatin maintenance. Nat Rev Mol Cell Biol **5:**296-304.

59. **McManus, K. J., V. L. Biron, R. Heit, D. A. Underhill, and M. J. Hendzel.** 2006. Dynamic changes in histone H3 lysine 9 methylations: identification of a mitosis-specific function for dynamic methylation in chromosome congression and segregation. J Biol Chem **281:**8888-97.

60. **Meloni, A. R., C. H. Lai, T. P. Yao, and J. R. Nevins.** 2005. A mechanism of COOH-terminal binding protein-mediated repression. Mol Cancer Res **3:**575-83.

61. **Mersfelder, E. L., and M. R. Parthun.** 2006. The tale beyond the tail: histone core domain modifications and the regulation of chromatin structure. Nucleic Acids Res **34:**2653-62.

62. **Metzger, E., M. Wissmann, N. Yin, J. M. Muller, R. Schneider, A. H. Peters, T. Gunther, R. Buettner, and R. Schule.** 2005. LSD1 demethylates repressive histone marks to promote androgen-receptor-dependent transcription. Nature **437:**436-9.

63. **Michaelis, C., R. Ciosk, and K. Nasmyth.** 1997. Cohesins: chromosomal proteins that prevent premature separation of sister chromatids. Cell **91:**35-45.

64. **Minc, E., J. C. Courvalin, and B. Buendia.** 2000. HP1gamma associates with euchromatin and heterochromatin in mammalian nuclei and chromosomes. Cytogenet Cell Genet **90:**279-84.

65. **Mito, Y., A. Sugimoto, and M. Yamamoto.** 2003. Distinct developmental function of two Caenorhabditis elegans homologs of the cohesin subunit Scc1/Rad21. Mol Biol Cell **14:**2399-409.

66. **Mizuguchi, G., T. Tsukiyama, J. Wisniewski, and C. Wu.** 1997. Role of nucleosome remodeling factor NURF in transcriptional activation of chromatin. Mol Cell **1:**141-50.

67. **Murray, K.** 1964. The Occurrence of Epsilon-N-Methyl Lysine in Histones. Biochemistry **3:**10-5.

68. **Nicolas, E., M. G. Lee, M. A. Hakimi, H. P. Cam, S. I. Grewal, and R. Shiekhattar.** 2006. Fission yeast homologs of human histone H3 lysine 4 demethylase regulate a common set of genes with diverse functions. J Biol Chem **281:**35983-8.

69. **Nielsen, A. L., M. Oulad-Abdelghani, J. A. Ortiz, E. Remboutsika, P. Chambon, and R. Losson.** 2001. Heterochromatin formation in mammalian cells: interaction between histones and HP1 proteins. Mol Cell **7:**729-39.

70. **Nimmo, E. R., G. Cranston, and R. C. Allshire.** 1994. Telomere-associated chromosome breakage in fission yeast results in variegated expression of adjacent genes. Embo J **13:**3801-11.

71. **Noma, K., C. D. Allis, and S. I. Grewal.** 2001. Transitions in distinct histone H3 methylation patterns at the heterochromatin domain boundaries. Science **293:**1150-5.

72. **Nonaka, N., T. Kitajima, S. Yokobayashi, G. Xiao, M. Yamamoto, S. I. Grewal, and Y. Watanabe.** 2002. Recruitment of cohesin to heterochromatic regions by Swi6/HP1 in fission yeast. Nat Cell Biol **4:**89-93.

73. **Nowak, S. J., and V. G. Corces.** 2004. Phosphorylation of histone H3: a balancing act between chromosome condensation and transcriptional activation. Trends Genet **20:**214-20.

74. **Nowak, S. J., C. Y. Pai, and V. G. Corces.** 2003. Protein phosphatase 2A activity affects histone H3 phosphorylation and transcription in Drosophila melanogaster. Mol Cell Biol **23:**6129-38.

75. **Oliveira, R. A., P. A. Coelho, and C. E. Sunkel.** 2005. The condensin I subunit Barren/CAP-H is essential for the structural integrity of centromeric heterochromatin during mitosis. Mol Cell Biol **25:**8971-84.

76. **Pazin, M. J., and J. T. Kadonaga.** 1997. What's up and down with histone deacetylation and transcription? Cell **89:**325-8.

77. **Peters, A. H., D. O'Carroll, H. Scherthan, K. Mechtler, S. Sauer, C. Schofer, K. Weipoltshammer, M. Pagani, M. Lachner, A. Kohlmaier, S. Opravil, M. Doyle, M. Sibilia, and T. Jenuwein.** 2001. Loss of the Suv39h histone methyltransferases impairs mammalian heterochromatin and genome stability. Cell **107:**323-37.

78. **Peterson, C. L., and M. A. Laniel.** 2004. Histones and histone modifications. Curr Biol **14:**R546-51.

79. **Pines, J., and T. Hunter.** 1991. Human cyclins A and B1 are differentially located in the cell and undergo cell cycle-dependent nuclear transport. J Cell Biol **115:**1-17.

80. **Pokholok, D. K., C. T. Harbison, S. Levine, M. Cole, N. M. Hannett, T. I. Lee, G. W. Bell, K. Walker, P. A. Rolfe, E. Herbolsheimer, J. Zeitlinger, F. Lewitter, D. K. Gifford, and R. A. Young.** 2005. Genome-wide map of nucleosome acetylation and methylation in yeast. Cell **122:**517-27.

81. **Polioudaki, H., Y. Markaki, N. Kourmouli, G. Dialynas, P. A. Theodoropoulos, P. B. Singh, and S. D. Georgatos.** 2004. Mitotic phosphorylation of histone H3 at threonine 3. FEBS Lett **560:**39-44.

82. **Pray-Grant, M. G., J. A. Daniel, D. Schieltz, J. R. Yates, 3rd, and P. A. Grant.** 2005. Chd1 chromodomain links histone H3 methylation with SAGA- and SLIK-dependent acetylation. Nature **433:**434-8.

83. **Rea, S., F. Eisenhaber, D. O'Carroll, B. D. Strahl, Z. W. Sun, M. Schmid, S. Opravil, K. Mechtler, C. P. Ponting, C. D. Allis, and T. Jenuwein.** 2000. Regulation of chromatin structure by site-specific histone H3 methyltransferases. Nature **406:**593-9.

84. **Renauld, H., O. M. Aparicio, P. D. Zierath, B. L. Billington, S. K. Chhablani, and D. E. Gottschling.** 1993. Silent domains are assembled continuously from the telomere and are defined by promoter distance and strength, and by SIR3 dosage. Genes Dev **7:**1133-45.

85. **Rieder, C. L., and R. Cole.** 1999. Chromatid cohesion during mitosis: lessons from meiosis. J Cell Sci **112 (Pt 16):**2607-13.

86. **Rountree, M. R., K. E. Bachman, and S. B. Baylin.** 2000. DNMT1 binds HDAC2 and a new co-repressor, DMAP1, to form a complex at replication foci. Nat Genet **25:**269-77.

87. **Rudolph, T., M. Yonezawa, S. Lein, K. Heidrich, S. Kubicek, C. Schafer, S. Phalke, M. Walther, A. Schmidt, T. Jenuwein, and G. Reuter.** 2007. Heterochromatin formation in Drosophila is initiated through active removal of H3K4 methylation by the LSD1 homolog SU(VAR)3-3. Mol Cell **26:**103-15.

88. **Santos-Rosa, H., R. Schneider, A. J. Bannister, J. Sherriff, B. E. Bernstein, N. C. Emre, S. L. Schreiber, J. Mellor, and T. Kouzarides.** 2002. Active genes are tri-methylated at K4 of histone H3. Nature **419:**407-11.

89. **Savvidou, E., N. Cobbe, S. Steffensen, S. Cotterill, and M. M. Heck.** 2005. Drosophila CAP-D2 is required for condensin complex stability and resolution of sister chromatids. J Cell Sci **118:**2529-43.

90. **Schmiesing, J. A., H. C. Gregson, S. Zhou, and K. Yokomori.** 2000. A human condensin complex containing hCAP-C-hCAP-E and CNAP1, a homolog of Xenopus XCAP-D2, colocalizes with phosphorylated histone H3 during the early stage of mitotic chromosome condensation. Mol Cell Biol **20:**6996-7006.

91. **Schneider, R., A. J. Bannister, F. A. Myers, A. W. Thorne, C. Crane-Robinson, and T. Kouzarides.** 2004. Histone H3 lysine 4 methylation patterns in higher eukaryotic genes. Nat Cell Biol **6:**73-7.

92. **Shi, X., T. Hong, K. L. Walter, M. Ewalt, E. Michishita, T. Hung, D. Carney, P. Pena, F. Lan, M. R. Kaadige, N. Lacoste, C. Cayrou, F. Davrazou, A. Saha, B. R. Cairns, D. E. Ayer, T. G. Kutateladze, Y. Shi, J. Cote, K. F. Chua, and O. Gozani.** 2006. ING2 PHD domain links histone H3 lysine 4 methylation to active gene repression. Nature **442:**96-9.

93. **Shi, Y., F. Lan, C. Matson, P. Mulligan, J. R. Whetstine, P. A. Cole, R. A. Casero, and Y. Shi.** 2004. Histone demethylation mediated by the nuclear amine oxidase homolog LSD1. Cell **119:**941-53.

94. **Shi, Y., J. Sawada, G. Sui, B. Affar el, J. R. Whetstine, F. Lan, H. Ogawa, M. P. Luke, Y. Nakatani, and Y. Shi.** 2003. Coordinated histone modifications mediated by a CtBP co-repressor complex. Nature **422:**735-8.

95. **Shi, Y. J., C. Matson, F. Lan, S. Iwase, T. Baba, and Y. Shi.** 2005. Regulation of LSD1 histone demethylase activity by its associated factors. Mol Cell **19:**857-64.

96. **Sonoda, E., T. Matsusaka, C. Morrison, P. Vagnarelli, O. Hoshi, T. Ushiki, K. Nojima, T. Fukagawa, I. C. Waizenegger, J. M. Peters, W. C. Earnshaw, and S. Takeda.** 2001. Scc1/Rad21/Mcd1 is required for sister chromatid cohesion and kinetochore function in vertebrate cells. Dev Cell **1:**759-70.

97. **Stavropoulos, P., G. Blobel, and A. Hoelz.** 2006. Crystal structure and mechanism of human lysine-specific demethylase-1. Nat Struct Mol Biol **13:**626-32.

98. **Sterner, D. E., and S. L. Berger.** 2000. Acetylation of histones and transcription-related factors. Microbiol Mol Biol Rev **64:**435-59.

99. **Strahl, B. D., and C. D. Allis.** 2000. The language of covalent histone modifications. Nature **403:**41-5.

100. **Strahl, B. D., R. Ohba, R. G. Cook, and C. D. Allis.** 1999. Methylation of histone H3 at lysine 4 is highly conserved and correlates with transcriptionally active nuclei in Tetrahymena. Proc Natl Acad Sci U S A **96:**14967-72.

101. **Sullivan, B. A., and G. H. Karpen.** 2004. Centromeric chromatin exhibits a histone modification pattern that is distinct from both euchromatin and heterochromatin. Nat Struct Mol Biol **11:**1076-83.

102. **Sun, Z. W., and C. D. Allis.** 2002. Ubiquitination of histone H2B regulates H3 methylation and gene silencing in yeast. Nature **418:**104-8.

103. **Tahiliani, M., P. Mei, R. Fang, T. Leonor, M. Rutenberg, F. Shimizu, J. Li, A. Rao, and Y. Shi.** 2007. The histone H3K4 demethylase SMCX links REST target genes to X-linked mental retardation. Nature **447:**601-5.

104. **Taunton, J., C. A. Hassig, and S. L. Schreiber.** 1996. A mammalian histone deacetylase related to the yeast transcriptional regulator Rpd3p. Science **272:**408-11.

105. **Tong, J. K., C. A. Hassig, G. R. Schnitzler, R. E. Kingston, and S. L. Schreiber.** 1998. Chromatin deacetylation by an ATP-dependent nucleosome remodelling complex. Nature **395:**917-21.

106. **Trojer, P., and D. Reinberg.** 2006. Histone lysine demethylases and their impact on epigenetics. Cell **125:**213-7.

107. **Tschiersch, B., A. Hofmann, V. Krauss, R. Dorn, G. Korge, and G. Reuter.** 1994. The protein encoded by the Drosophila position-effect variegation suppressor gene Su(var)3-9 combines domains of antagonistic regulators of homeotic gene complexes. Embo J **13:**3822-31.

108. **Vakoc, C. R., S. A. Mandat, B. A. Olenchock, and G. A. Blobel.** 2005. Histone H3 lysine 9 methylation and HP1gamma are associated with transcription elongation through mammalian chromatin. Mol Cell **19:**381-91.

109. **Vakoc, C. R., M. M. Sachdeva, H. Wang, and G. A. Blobel.** 2006. Profile of histone lysine methylation across transcribed mammalian chromatin. Mol Cell Biol **26:**9185-95.

110. **Van Hooser, A., D. W. Goodrich, C. D. Allis, B. R. Brinkley, and M. A. Mancini.** 1998. Histone H3 phosphorylation is required for the initiation, but not maintenance, of mammalian chromosome condensation. J Cell Sci **111 (Pt 23):**3497-506.

111. **van Leeuwen, F., P. R. Gafken, and D. E. Gottschling.** 2002. Dot1p modulates silencing in yeast by methylation of the nucleosome core. Cell **109:**745-56.

112. **Wang, H., Z. Q. Huang, L. Xia, Q. Feng, H. Erdjument-Bromage, B. D. Strahl, S. D. Briggs, C. D. Allis, J. Wong, P. Tempst, and Y. Zhang.** 2001. Methylation of histone H4 at arginine 3 facilitating transcriptional activation by nuclear hormone receptor. Science **293:**853-7.

113. **Wang, J., K. Scully, X. Zhu, L. Cai, J. Zhang, G. G. Prefontaine, A. Krones, K. A. Ohgi, P. Zhu, I. Garcia-Bassets, F. Liu, H. Taylor, J. Lozach, F. L. Jayes, K. S. Korach, C. K. Glass, X. D. Fu, and M. G. Rosenfeld.** 2007. Opposing LSD1 complexes function in developmental gene activation and repression programmes. Nature **446:**882-7.

114. **Wei, Y., C. A. Mizzen, R. G. Cook, M. A. Gorovsky, and C. D. Allis.** 1998. Phosphorylation of histone H3 at serine 10 is correlated with chromosome condensation during mitosis and meiosis in Tetrahymena. Proc Natl Acad Sci U S A **95:**7480-4.

115. **Wysocka, J., T. Swigut, H. Xiao, T. A. Milne, S. Y. Kwon, J. Landry, M. Kauer, A. J. Tackett, B. T. Chait, P. Badenhorst, C. Wu, and C. D. Allis.** 2006. A PHD finger of NURF couples histone H3 lysine 4 trimethylation with chromatin remodelling. Nature **442:**86-90.

116. **Yang, M., C. B. Gocke, X. Luo, D. Borek, D. R. Tomchick, M. Machius, Z. Otwinowski, and H. Yu.** 2006. Structural basis for CoREST-dependent demethylation of nucleosomes by the human LSD1 histone demethylase. Mol Cell **23:**377-87.

117. **Zhang, Q., S. Y. Wang, A. C. Nottke, J. V. Rocheleau, D. W. Piston, and R. H. Goodman.** 2006. Redox sensor CtBP mediates hypoxia-induced tumor cell migration. Proc Natl Acad Sci U S A **103:**9029-33.

BIOGRAPHICAL SKETCH

Michael Rutenberg was born sometime in the 1970s to the loving parents, Howard and Judy Rutenberg, in Canton, Ohio. His older brother, Josh, has been the fortunate recipient of Michael's tutelage in snowboarding, mountain biking and general coolness. His younger brother, Adam, will never be able to beat him in basketball, baseball, soccer, or John Madden's NFL Football (for SEGA Genesis).

Michael is the product of the rigorous academic training provided by Williams Elementary School magnet program in Little Rock, Arkansas. His junior high school years were spent at Forest Heights, where he generally tried to avoid having his tennis shoes stolen by larger, stronger, meaner upperclassmen during bomb threats and fire alarms, where they were used to play football. While attending high school at University High School in Orlando, Michael ran a bold and courageous campaign for senior class president in an attempt unseat the evil and corrupt incumbent, Jerry "Jer-Bear" Buchert. Despite losing the campaign, Michael is still remembered for fighting the good fight and he is celebrated as a champion for the unheard voices of "the little people."

Michael graduated with a B.S. from the University of Florida in 1998.